SECRET

MARTIN MARIETTA ENERGY SYSTEMS LIBRARIES
3 4456 0360893 2

ORNL 1095
Progress Report
9w

LABORATORY RECORDS
1954

PHYSICS OF SOLIDS INSTITUTE

QUARTERLY PROGRESS REPORT

FOR PERIOD ENDING APRIL 30, 1951

CENTRAL RESEARCH LIBRARY
DOCUMENT COLLECTION
LIBRARY LOAN COPY
DO NOT TRANSFER TO ANOTHER PERSON
If you wish someone else to see this document, send in name with document and the library will arrange a loan.

OAK RIDGE NATIONAL LABORATORY
OPERATED BY
CARBIDE AND CARBON CHEMICALS DIVISION
UNION CARBIDE AND CARBON CORPORATION
UCC
POST OFFICE BOX P
OAK RIDGE, TENNESSEE

SECRET

[redacted]

ORNL-1095

This document consists of 124 pages.
Copy 9 of 134. Series A.

Contract No. W-7504, eng 26

METALLURGY DIVISION

J. H. Frye, Jr., Director

PHYSICS OF SOLIDS INSTITUTE

D. S. Billington, Acting Director

QUARTERLY PROGRESS REPORT
for Period Ending April 30, 1951

DECLASSIFIED

CLASSIFICATION CHANGED TO:
BY AUTHORITY OF: TID-1148
BY: O. Morrison 7/11/57

Edited by

D. S. Billington and J. T. Howe

DATE ISSUED: NOV 12 1951

OAK RIDGE NATIONAL LABORATORY
operated by
CARBIDE AND CARBON CHEMICALS COMPANY
A Division of Union Carbide and Carbon Corporation
Post Office Box P
Oak Ridge, Tennessee

RESTRICTED DATA

This document contains restricted data as defined in the Atomic Energy Act of 1946.

[redacted]

This document contai
the National Defens
Its transmission o
contents in any manner
person is prohibited and may result in severe
criminal penalties under applicable Federal
laws.

MARTIN MARIETTA ENERGY SYSTEMS LIBRARIES
3 4456 0360893 2

Internal Distribution

1	G. T. Felbeck (C&CCC)
2-3	Chemistry Library
4	Physics Library
5	Biology Library
6	Health Physics Division
7	Metallurgy Library
8-9	Training School Library
10-13	Central Files
14	C. E. Center
15	C. E. Larson
16	W. B. Humes (K-25)
17	W. D. Lavers (Y-12)
18	A. M. Weinberg
19	E. H. Taylor
20	E. J. Murphy
21	E. D. Shipley
22	D. S. Billington
23	F. C. VonderLage
24	R. C. Briant
25	J. A. Swartout
26	S. C. Lind
27	F. L. Steahly
28	A. H. Snell
29	A. Hollaender
30	M. T. Kelley
31	G. H. Clewett
32	K. Z. Morgan
33	J. S. Felton
34	A. S. Householder
35	C. S. Harrill
36	C. E. Winters
37	D. W. Cardwell
38	E. M. King
39	C. B. Ellis
40	J. T. Howe
41	C. P. Keim
42	L. K. Jetter
43	E. J. Boyle
44	W. D. Manly
45	C. D. Susano
46	W. W. Parkinson
47	R. J. Gray
48	B. S. Borie
49	D. E. Hamby
50	E. E. Stansbury
51	G. P. Smith
52	J. E. Cunningham
53	E. C. Miller
54	A. Brasunas
55	A. G. H. Andersen
56	J. O. Betterton, Jr.
57	R. B. Oliver
58	P. Patriarca
59	T. H. Blewitt
60	W. E. Taylor
61	J. H. Crawford, Jr.
62	A. F. Cohen
63	J. C. Wilson
64	O. Sisman
65	W. J. Sturn
66	M. T. Robinson
67	R. H. Kernohan
68	M. T. Metcalt
69	G. W. Keilhotz
70	R. S. Livingston
71	R. J. Jones (Y-12)
72	Purdue (K. Lark-Horovitz)
73	Phillips Petroleum, Idaho Falls (Attn: Library)
74-76	Idaho Operations

RESTRICTED DATA

This document contains restricted data as defined in the Atomic Energy Act of 1946.

CAUTION

This document contains information affecting the National Defense of the United States. Its transmission or the disclosure of its contents in any manner to any unauthorized person is prohibited and may result in severe criminal penalties under applicable Federal laws.

External Distribution

77-84	Argonne National Laboratory
85-87	Atomic Energy Commission, Washington
88-91	Brookhaven National Laboratory
92-95	Carbide and Carbon Chemicals Company (Y-12)
96-98	Knolls Atomic Power Laboratory
99-100	General Electric Company, Richland
101	Hanford Operations Office
102-105	Los Alamos
106-107	New York Operations Office
108	Patent Branch, Washington
109-123	Technical Information Service, Oak Ridge
124-127	University of California Radiation Laboratory
128	Massachusetts Institute of Technology (Kaufmann)
129	Battelle Memorial Institute
130-132	North American Aviation
133	Westinghouse Electric Corporation
134	Savannah River Operations Office, Wilmington

RESTRICTED DATA

This document contains restricted data as defined in the Atomic Energy Act of 1946.

CAUTION

This document contains information affecting the National Defense of the United States. Its transmission or the disclosure of its contents in any manner to any unauthorized person is prohibited and may result in severe criminal penalties under applicable Federal laws.

The Physics of Solids Institute quarterly progress report previously issued in this series is as follows:

ORNL-1025 Period Ending January 31, 1951

Progress prior to this period was reported in the Physics Division quarterly progress reports.

RESTRICTED DATA

This document contains restricted data as defined in the Atomic Energy Act of 1946.

CAUTION

This document contains information affecting the National Defense of the United States. Its transmission or the disclosure of its contents in any manner to any unauthorized person is prohibited and may result in severe criminal penalties under applicable Federal laws.

SECRET

TABLE OF CONTENTS

	Page No.
INTRODUCTION AND SUMMARY	1
1. BUILDING STATUS	8
Hot Cells	8
Cells 1, 2, and 3	8
Master-slave cells	8
2. CRYSTAL PHYSICS	9
In-Pile Relative Thermal-Conductivity Measurements on Structural Materials at High Temperatures	9
X-Ray Work	13
Stored Energy Associated with Vacant and Interstitial Lattice Sites	13
Metal Crystals	17
Y-12 Cyclotron Studies	22
Purdue Cyclotron Creep	26
3. SOLID-STATE REACTIONS	27
Variation of Ionization Energy with Bombardment in Cuprous Oxide	27
Annealing of Radiation Damage in Cuprous Oxide	33
Silicon Bombardment Experiments	35
Evidence for Hole Traps in Germanium Resulting from Fast-Neutron Bombardment	36
Cryostat for Pile Irradiations	39
4. RADIATION METALLURGY	42
Investigation of Homogeneous Deformation of Copper	42
Annealing of Radiation Hardening of Copper and Copper Alloys	45
Creep Under Irradiation	46
Radiation Effects in Supersaturated Solid Solutions	51
X-ray investigations	51
Metallographic investigations	52
Comparison of thermal aging with "irradiation aging"	52
Effects of dissolved beryllium	59
Investigations of other age-hardenable alloys	60

SECRET

5. ENGINEERING PROPERTIES 61
Lithium-Iron Cyclotron Bombardment 61
Liquid-Metal Loops 69
Physical Properties of Plastics 75
Plastics 75
Elastomers 75
Pile-Induced Radiation 82
Radiation Effects on Kovar 91
Thermal Conductivity of Uranium-Bearing Materials 102
Dead Weight Creep 105
Results 114
Irradiation of Graphite-Carbon Rods 114

6. LIQUID FUELS 115
Radiation Damage to Liquid Fuels 115

SECRET

LIST OF TABLES

		Page No.
Table 2.1	Change in Resistance and Resistivity of Polycrystalline Copper on Cold-Working	15
Table 2.2	Effect of Gamma Radiation on the Resistivity of Copper Single Crystals	20
Table 3.1	Effect of Bombardment on Experimental Ionization Energy of Cu_2O	31
Table 3.2	Change in Conductivity of P-Type Germanium on Bombardment	39
Table 4.1	Time Required for Cessation of Recovery of Hardness in Copper Alloys After Irradiation	46
Table 4.2	Effect of Overaging at Various Temperatures on Radiation-Induced Resistance Changes in Copper-Beryllium	59
Table 5.1	Composition of Elastomers	76
Table 5.2	Tensile Strength of Elastomers After Radiation Exposure	77
Table 5.3	Set at Break of Elastomers After Radiation Exposure	77
Table 5.4	Elongation of Elastomers After Radiation Exposure	78
Table 5.5	Compression Set of Elastomers After Radiation Exposure	78
Table 5.6	Specific Gravity of Elastomers After Radiation Exposure	79
Table 5.7	Change in Weight of Elastomers After Radiation Exposure	79
Table 5.8	Shore Durometer Hardness of Elastomers After Radiation Exposure	80
Table 5.9	Shore Elasticity of Elastomers After Radiation Exposure	80
Table 5.10	Volume Resistivity of Elastomers After Radiation Exposure	81
Table 5.11	Dielectric Strength of Elastomers After Radiation Exposure	81
Table 5.12	Analysis of Kovar Stock	92
Table 5.13	Classification of Kovar Specimens	92
Table 5.14	Length of Kovar Specimens	95
Table 5.15	Specific Volume of Kovar	98
Table 5.16	Hardness of Kovar	100
Table 5.17	Electrical Conductivity of Kovar at 20°C	101

SECRET

SECRET

LIST OF FIGURES

		Page No.
Fig. 2.1	Schematic Diagram for Measuring Changes in Thermal Conductivity of Metals and Alloys at High Temperatures	10
Fig. 2.2	Tensile Calorimeter (Cross-Section)	16
Fig. 2.3	Electron Diffraction Studies of a Copper Crystal	21
Fig. 2.4	Water-Cooled Fuel Target	25
Fig. 3.1	Cuprous Oxide Plate, Conductivity vs. Integrated Fast Neutron Flux	28
Fig. 3.2	Cuprous Oxide, Hall Coefficient vs. Reciprocal Temperature for Various Exposure Times	29
Fig. 3.3	Cuprous Oxide, Resistivity vs. Reciprocal Temperature for Various Exposure Times	30
Fig. 3.4	Experimental Ionization Energy vs. Exposure Time for Cu_2O	32
Fig. 3.5	Cuprous Oxide, Hall Coefficient vs. Reciprocal Temperature of Bombarded Cu_2O Annealed	34
Fig. 3.6	Low-Resistivity P-Type Ge, Conductivity vs. Bombardment	38
Fig. 3.7	P-Type Ge, Conductivity vs. Bombardment	40
Fig. 4.1	Method of Loading Single Crystal for Homogeneous Shear Experiment	43
Fig. 4.2	Stress-Strain Curve for Pure Copper Single Crystal Cu-T4 Deformed with Load Applied Parallel to Slip System	44
Fig. 4.3	In-Pile Cantilever Creep Test	48
Fig. 4.4	Cantilever Creep Test	49
Fig. 4.5	331 Line of Cu-Be Alloy	53
Fig. 4.6	Shift of 331 Line of Cu-Be Due to Irradiation	54
Fig. 4.7	Early Stages of Resistance Change of Solution-Quenched Cu-Be During Exposure to Reactor Radiations	55
Fig. 4.8	Comparison of Resistance Changes of Solution-Quenched Cu-Be During Thermal Aging and During Neutron Exposure	56
Fig. 4.9	Effect of Prior Cold Work on the Change of Resistance During Aging	58
Fig. 5.1	Old Capsule Assembly (Front View), Exploded	62
Fig. 5.2	Old Capsule Assembly (Rear View), Exploded	63
Fig. 5.3	Arrangement of Capsule and Associated Equipment	64

[redacted]

Fig. 5.4	Globeiron, Unirradiated Zone	68
Fig. 5.5	Globeiron, Zone to be Irradiated	68
Fig. 5.6	Globeiron, Unirradiated Zone	68
Fig. 5.7	Globeiron, Irradiated Zone	68
Fig. 5.8	New Capsule Assembly (Front View), Exploded and Assembled	70
Fig. 5.9	New Capsule Assembly (Rear View), Exploded and Assembled	71
Fig. 5.10	Pump and Flowmeter Test Loop	73
Fig. 5.11	In-Pile Lithium Loop	74
Fig. 5.12	Gamma Decay of Stainless Steels	83
Fig. 5.13	Gamma Decay of Stainless Steels	84
Fig. 5.14	Gamma Decay of Stainless Steels	85
Fig. 5.15	Gamma Decay of Steels	86
Fig. 5.16	Gamma Decay of Metals	87
Fig. 5.17	Gamma Decay of Metals	88
Fig. 5.18	Gamma Decay of Aluminum	89
Fig. 5.19	Gamma Decay of Concretes	90
Fig. 5.20	Specific Volume of Kovar vs. Neutron Irradiation	94
Fig. 5.21	Hardness of Kovar vs. Neutron Irradiation	96
Fig. 5.22a	Change in Hardness of Kovar vs. Neutron Irradiation	97
Fig. 5.22b	Change in Electrical Conductivity of Kovar vs. Neutron Irradiation	97
Fig. 5.23	Electrical Conductivity of Kovar vs. Neutron Irradiation	99
Fig. 5.24	Thermal Conductivity Sample	103
Fig. 5.25a	Fluxmeter	104
Fig. 5.25b	Heater Construction	104
Fig. 5.26	The Relative Thermal Resistivity of a UNH Impregnated Carbon Sample Irradiated in X-10	106
Fig. 5.27	Zr Creep Unit	107
Fig. 5.28	Circuit for LVDT	109
Fig. 5.29	Electrical Equivalent of an LVDT	110
Fig. 5.30	Vector Diagram of Transformer Shown in Fig. 5.29	111
Fig. 5.31	Vector Diagram for Balancing Extensometer with Reference LVDT	113
Fig. 5.32	Vector Diagram Showing the Voltage Recorded on the Micromax	113

INTRODUCTION AND SUMMARY

BUILDING STATUS

Hot Cells. Work on the hot cells has continued during the quarter. The Tell manipulators are in place in cells 1, 2, and 3, and wiring connections are being made preparatory to making final adjustments. Cell 3 can be used for hot work as soon as the manipulator is ready.

Cells 4, 5*a*, 5*b*, and 6 are also near completion. Two master-slave manipulators have been installed and are operating.

CRYSTAL PHYSICS

In-Pile Thermal-Conductivity Measurements of Structural Materials at High Temperatures. The problems incident to making conductivity measurements in the reactor are discussed, and the apparatus to be used is described in detail. It is thought that this thermal-conductivity apparatus may also be used for estimating the gamma heating produced in the sample and apparatus by irradiation.

Equipment is being constructed to measure in-pile changes in thermal or electrical conductivity of a number of metals and oxides while being irradiated in a ½-in. doughnut hole. Temperatures will vary from ambient to approximately 300°C.

X-Ray Work. The Hilger X-ray-diffraction unit was received at the end of the quarter. Features of this unit are discussed.

A small darkroom is being planned for film developing.

X-ray Laue pictures of special copper single crystals have been taken during the quarter using the Metallurgy Division X-ray-diffraction units. Orientations of these crystals were determined with respect to their axes.

Stored Energy Associated with Vacant and Interstitial Lattice Sites. It is thought that either high-energy particles or plastic deformation of metals will produce interstitial atoms, vacant lattice sites, and possibly other imperfections in metals at low temperatures.

A tensile calorimeter is being built to measure the energy released in a sample cold-worked at the temperature of liquid nitrogen. The calorimeter is pictured, and its operation is described.

Metal Crystals. Work is continuing on improvement of the technique for measuring the electrical resistivity of copper crystals. Potential probes are now sintered onto the samples, eliminating contact errors. Accuracy of temperature measurements will also be improved.

Resistance measurements made before and after exposure of copper crystals to a cobalt gamma source indicate that changes due to gamma bombardment are negligible.

Electron-diffraction studies of pile-bombarded copper crystals indicate that imperfections introduced by bombardment are of short range and that there is not a one-to-one correspondence between cold work and neutron irradiation.

A low-temperature cryostat employing a liquid-nitrogen bath has been designed and is under construction although it now appears unlikely that the hole in the LITR for which it was designed will be available for quite some time.

Y-12 Cyclotron Studies. Proton bombardment of annealed copper has produced a hardness increase of 20 DPH numbers on the Tukon tester. Only 1/16 in. of the leading edge of copper was irradiated. It is probable that this small area was overlooked previously, thus explaining the report last quarter of no hardness increase (ORNL-1025, p. 31).

Fuel and container material will be irradiated in the 86-in. cyclotron shortly. Corrosion, precipitation decomposition, etc. will be studied under conditions simulating the ANP reactor. The UF_4-NaF-KF system will be tested in an Inconel container at 1500°F initially.

In order to obtain power densities by proton bombardment in the liquid fuel comparable to those in the ARE, a water-cooled target is being designed for later tests. A design is also in progress for a liquid-metal-cooled target which will permit power densities comparable to those in the airplane reactor.

Creep-test work has continued during the quarter.

A copper single crystal was exposed in the 22-Mev cyclotron for 20 μa-hr at a proton energy of 1.3 Mev. Postirradiation studies are not complete.

Purdue Cyclotron Creep. Features of the extensometer design are listed. Bench tests have been run, and modifications are in process. The equipment is expected to be ready for creep measurements in the near future.

SOLID STATE REACTIONS

Variation of Ionization Energy with Bombardment in Cuprous Oxide. In-pile conductivity measurements indicate that for Cu_2O the initial portion of the conductivity vs. bombardment curve is approximately exponential. Experimental ionization energies of a Cu_2O plate were determined from both the Hall coefficient and resistivity measurements. Ionization energy appears to increase rapidly at the beginning of bombardment, level off to a maximum, and then decrease with further bombardment.

Annealing of Radiation Damage in Cuprous Oxide. Annealing of radiation damage is quite complicated. It is difficult to determine with sufficient accuracy the values of $\Delta\epsilon$ at various temperatures to permit a reliable comparison. Further experiments will be run on this problem.

Silicon Bombardment Experiments. Changes in electrical properties of silicon due to fast-neutron-flux bombardment have been measured for comparison with similar changes in germanium as previously measured. Analysis of data taken on a P-type silicon sample indicates that the change in carrier concentration per incident neutron, $dn_h/d(nvt)_{fast} = -5.0$. Similar analysis of an N-type silicon plate results in a value of -5.1 for $dn_e/d(nvt)_{fast}$. More extensive silicon bombardment experiments are planned.

Evidence of Hole Traps in Germanium Resulting from Fast-Neutron Bombardment. Experiment shows that the resistivity of low-resistivity P-type germanium increases with bombardment, which is the result expected if hole traps are introduced. The effect of temperature on the efficiency of hole traps was also investigated.

Cryostat for Pile Irradiations. The hole designated for cryostat installation has been changed from hole 50 to 52. The new location eliminates the problems of external shielding underneath the hole. The floor outside hole 50 has been removed, and proper bracing and shielding have been installed up to floor level.

RADIATION METALLURGY

Investigation of Homogeneous Deformation of Copper. An apparatus for homogeneous shearing of metal single crystals has been built and is being tested and refined. It will be used to investigate the effect of radiation on shear strength in single crystals.

Annealing of Radiation Hardening of Copper and Copper Alloys. Samples exposed in the X pile experienced an increase in hardness of about 20 DPH numbers. These samples are being annealed isothermally in a nitrate salt bath at 300°C. Some of the results are presented.

Creep Under Irradiation. Data taken on 347 stainless steel stressed to a maximum fiber stress of approximately 1700 psi at 1500°F indicate that irradiation reduces creep rate.

To determine the effect of bombardment on instrumentation, a microformer with a locked core was placed in a temperature-controlled oven in the reactor. Reactor operation at a series of power levels indicated that the microformer was flux-dependent in a nonlinear manner. Investigations are underway to determine the cause in the hopes that the trouble may be eliminated. One such investigation is being conducted on effects of neutron bombardment on length and magnetic permeability in an attempt to account for the changes noted.

Hollow cantilever specimens containing sodium or other corroding fluids have been run on the bench. In-pile tests will follow.

Means of incorporating a creep test specimen in the circulating metal loop in the LITR and MTR are being studied.

Radiation Effects in Supersaturated Solid Solutions. The investigation of radiation effects in copper-beryllium age-hardening alloy has continued. X-ray line-broadening studies indicate a contraction of the lattice caused by an increase in the amount of beryllium.

No irradiation-induced Gunier-Preston zones such as occur from thermal aging have been found to date. Experiments will be repeated using longer exposures.

Effects of irradiation on rate of precipitation are being studied. Change of resistance during irradiation and subsequent aging of irradiated specimens indicatesthe possibility of a similarity between "irradiation aging" and low-temperature thermal aging.

Apparatus for measuring the rate of precipitation at higher temperatures during irradiation is now being bench-tested. Single-crystal resistance specimens will be grown to exclude the effect of grain-boundary precipitate on subsequent aging and radiation aging.

These investigations are being extended to include other age-hardenable alloys. Aluminum-silicon and copper-titanium samples have been irradiated. Property changes noted have introduced the possibility that the irradiation effect may be characteristic of the solute element. Other alloys will be included in future studies.

ENGINEERING PROPERTIES

Lithium-Iron Cyclotron Bombardment. A study is being made of the iron-lithium system under conditions similar to those prevailing in a reactor. Iron capsules containing a liquid metal at 600 to 900°C were irradiated in the Berkeley 60-in. cyclotron.

Trouble has been experienced with high-temperature heaters in the magnetic field of the cyclotron.

One capsule was successfully irradiated at a temperature of 625°C in the irradiated zone. Total exposure was 25.5 μa-hr over an area of 0.608 by 0.250 in. An increase in grain size in the irradiated area was noted. Very little iron was dissolved by the lithium.

A second capsule was irradiated at approximately 900°C. Failure of the thermocouple on the front face and later rupture of the safety window stopped the run.

A third capsule was irradiated at too low an intensity to give an exposure comparable to that of a reactor.

Both capsule and heater are being redesigned for satisfactory operation at 900°C.

Chemical analyses of the capsule and lithium of the 625°C irradiation are given together with X-ray-diffraction measurements and photomicrographs.

Liquid-Metal Loop. The liquid-metal loop has been bench-tested and is expected to be installed in the X reactor in early July. The first loop will be run with lithium at 1000°F. Bremsstrahlung activity and activity introduced into the liquid metal by corrosion and recoil atoms from the container tube will be studied. Later, creep and stress-corrosion experiments are expected to be incorporated into the loop. A detailed description and pictures of the loop are given.

Physical Properties of Plastics. Report ORNL-928 describes the physical properties of pile-irradiated plastics. Similar studies will be made using beta and gamma bombardment. Other problems to be studied are effects of the presence of oxygen on the radiation damage to plastics, the effect of aging prior to irradiation, the damage contributed by thermal neutrons, and the effect of radiation intensity.

Physical properties of elastomers are being measured before and after irradiation. Description of the tests and results to date are given.

Pile-Induced Radiation. Decay curves are being run on a number of structural materials so that the radiation intensity to be encountered when equipment is removed from the reactor may be predicted more accurately.

Radiation Effects on Kovar. Irradiation of annealed and annealed-and-quenched Kovar specimens, with an nvt of 3.04×10^{20} n/cm^2, did not produce an observable change in length. Volume increase, if any, was less than 0.3%. The hardness and electrical conductivity of all specimens increased, but the changes were greater in the quenched ones. Both hardness and conductivity reached a maximum in the quenched specimens, and decreased on further irradiation.

Thermal Conductivity of Uranium-Bearing Materials. A fission-heating rate meter has been developed and inserted in the X reactor. It has proved very stable, having a relaxation time of 2 to 3 min. The device has shown that the fission heating is not proportional to the pile power as recorded by the pile operator. The fission-heating rate meter is being used in conjunction with the thermal-conductivity torpedo to determine more accurately the flux near the torpedo.

Measurements of thermal-conductivity changes in uranyl nitrate hexahydrate—impregnated carbon and graphite were continued. Results are given.

Dead Weight Creep. Gamma-heating calculations indicate that it will be necessary to redesign the torpedo for the zirconium creep rig. It was also necessary to rebuild the LVDT instrumentation. Performance of the equipment is given as a result of five bench runs. A load of 175 to 190 lb at 625°C on a 1/8-in.-diameter by 3-in.-long specimen after the initial set gave a creep rate of about 6 mils/day; after about a week the creep rate decreased to about 0.004 mil/day. Total elongation after 19 days was 0.125 in.

Irradiation of Graphite Carbon Rods. Physical measurements were made on 12 graphite carbon rods made by Battelle Memorial Institute using various methods. After a two-week irradiation in the fast-flux section of the X reactor measurements will be repeated. The same treatment will later be given bars containing UO_2 nodules in an effort to determine the optimum size of UO_2 nodule for minimum fission fragment damage.

LIQUID FUELS

Radiation Damage to Liquid Fuels. A group has recently been formed in the Physics of Solids Institute for the purpose of studying radiation damage to liquid fuels. Fuel containers will be bombarded in the X reactor, the LITR, the Y-12 cyclotron, and the Berkeley 60-in. cyclotron. Equipment is being bench-tested and is expected to go into the X reactor in June. Temperature and pressure measurements will be made during irradiation. Experiments should also begin in the LITR in the near future.

Liquid fuels have been bombarded in the 86-in. cyclotron at Y-12. Further discussion is given in Sec. 2 under "Y-12 Cyclotron Studies."

The Mass Spectrographic Analytical Chemistry and the Isotope Physics Spectrographic Groups at Y-12 are aiding in studies of materials evolved from fuels and methods of examining the irradiated fuels and capsules.

1. BUILDING STATUS

HOT CELLS

S. E. Dismuke

Cells 1, 2, and 3. Windows in cells 2 and 3 have been tested with water in them with the result that a few small holes in the Amercote opened and allowed the tank wall to rust. This has been corrected, and special precautions have been taken to prevent weak spots in the other cell windows.

Spotlights have been installed in all cells and are working. In cells 2 and 3 incandescent lights for general cell lighting are complete. In cell 3 temporary sodium-vapor lamps have been installed since there has been considerable delay in getting the complete Westinghouse units for which the cells were designed.

The Tell manipulators have been placed in the cells and should be operating in a few weeks.

Design for hydraulic operation of the inter-cell barrier door has been made to replace a hand-powered screw arrangement.

Cell 3 can be used as soon as the manipulator is ready. Cell 2 will be ready for use as soon as the sodium-vapor lamps are installed. Cell 1 will not be ready for use until the remote-controlled lathe is ready and installed; this should be some time in August.

Master-Slave Cells. Cells 4, 5*a*, 5*b*, and 6 are constructed of high-density concrete block held together with a lime-sand mortar so that alterations may be made easily without destroying the block. Access to the cells is made by moving the back wall, which is mounted on trucks that roll on tracks. The roof consists of 4 in. of steel plates with holes through which the master-slave manipulators operate. The master-slave manipulator, roof, and truck design were developed at Argonne National Laboratory.

The walls, windows, barrier transfer and storage, access holes, roof, and trucks have been essentially completed. Within another month the cell floors, lights, manipulator mountings, and painting should be completed and the cells ready for use.

2. CRYSTAL PHYSICS

IN-PILE RELATIVE THERMAL-CONDUCTIVITY MEASUREMENTS ON STRUCTURAL MATERIALS AT HIGH TEMPERATURES

A. Foner Cohen

Various schemes for measuring the effects of pile radiation on the thermal conductivity of structural alloys at high temperatures (about 820°C) have been under consideration. Among the many reasons for preferring in-pile thermal-conductivity experiments at high temperatures to before-after experiments are the facts that the difficulties in handling hot samples and the inaccuracy inherently to be expected of remote-control methods would be very pronounced at elevated temperatures, and that information on the behavior of the material under actual operating conditions is important. Since the changes in the alloys are expected to be rather small, a fairly accurate method should be used so that definite information will become available in a reasonable period of time.

The presently available facility in the X pile is a fuel channel hole. The maximum outside diameter of the entire apparatus must not exceed 1.25 in. In addition, it is desired that the temperature of the graphite in contact with the apparatus should not exceed 250°C. Fortunately, in a fuel channel a stream of air flows at approximately 120 ft/sec, thereby providing cooling to the outside of the experimental can. If the furnace and components of the experimental set-up are designed of small enough diameter, at equilibrium the highest temperature desired during the experiment can be obtained and the cooling will be sufficient to keep the graphite below 250°C. For these and other reasons, such as accuracy of measurements, a long cylindrical solid sample is desirable, with a furnace immediately surrounding it. The temperature gradient is then along the length of the sample. Figure 2.1 is a schematic diagram of the sample, furnace, supports, etc. set up for measuring changes in thermal conductivity at high temperatures.

For determining whether the thermal conductivity after a given irradiation period changes by an amount of, say, 2% from the original out-of-pile value,

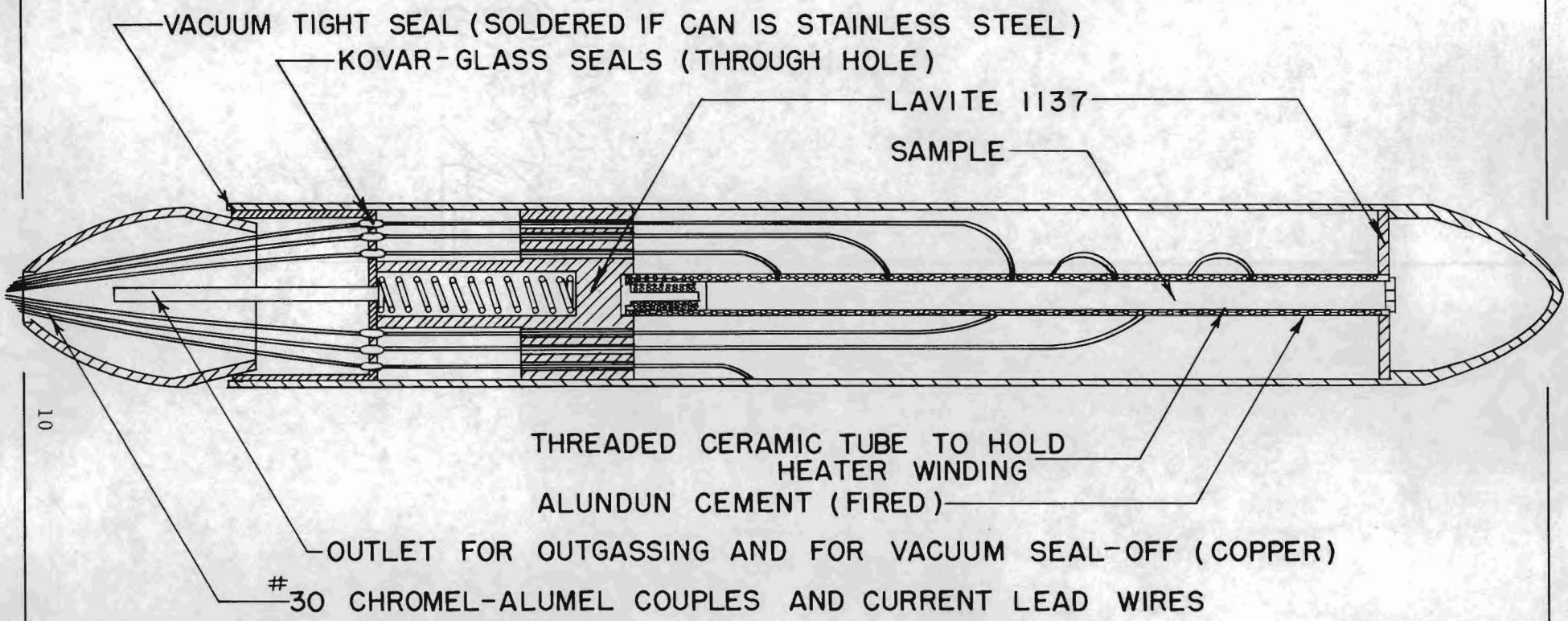

Fig. 2.1

UNCLASSIFIED

OAK RIDGE NATIONAL LABORATORY — Physics of Solids Institute				
SCHEMATIC DIAGRAM FOR MEASURING CHANGES IN THERMAL CONDUCTIVITY OF METALS AND ALLOYS AT HIGH TEMPERATURES				PSI-A-118
DRAWN BY: W.E.B.	FOR: A.F. COHEN	DATE: 5-17-51	SCALE:	DWG-11297

it is necessary that the out-of-pile reproducibility of the material itself be much better than 2% and, of course, that the measurements of temperature differentials be very accurate, which therefore sets the necessary accuracy of the associated instrumentation.

Since the measurements of interest are those which yield the change of thermal conductivity k as a function of irradiation, it is necessary to measure the property proportional to k in the radiation-free case under the same conditions as those when the sample is being irradiated. Assuming that the experiment is so arranged that a suitable temperature gradient exists along the length of the sample, then, at the operating temperature,

$$\frac{dq}{dt} = -kA\,\frac{(dT)}{dx}$$

initially, when irradiation is zero, and

$$\frac{dq}{dt} = -k_1 A\,\frac{(dT)_1}{dx}$$

at any specified radiation dosage. From these expressions,

$$\frac{k}{k_1} = \frac{(dT)_1}{(dT)}$$

or, at a given temperature, the change in thermal conductivity is inversely proportional to the change of the gradient between two specified points, at which locations thermocouples are welded. The gradient must be large enough so that within the accuracy of the measuring instruments, a small change in thermal conductivity can be detected. Since the same sample geometry, heaters, etc. are used before and during irradiation, any small corrections for a possible radial temperature gradient across the sample cancel. Chromel-Alumel thermocouples have been found to be satisfactory for measuring the high temperatures encountered. The thermocouples are attached to the specimen by use of a condenser-discharge welder built by the ORNL Instrument Department.

In some cases the can surrounding the apparatus to be put into the pile must be vacuum-tight, for example, in an investigation of molybdenum at approximately 800°C, at which temperature molybdenum is oxidized rapidly. A satisfactory vacuum-tight seal can be obtained using a stainless steel can soldered to a stainless steel lid, in which are sealed small Kovar-to-glass seals. A similar arrangement using 2S aluminum for the can and lid did not prove as satisfactory when the lid was heliarc-welded to the can. Other methods of making vacuum-tight seals requiring good electrical insulation for in-pile experiments are being tried. It may be possible to eliminate the Kovar seals entirely.

For immediate answers to engineering problems, the experiments now in progress out of and in the pile are to be run continuously at approximately 820°C after the alloy in question has been given the best metallurgically stabilizing heat treatment. It should be pointed out that in some alloys the heat treatment and subsequent heating to temperature and then cooling to room temperature affect the degree of reproducibility. The in-pile measurements will therefore be made for a long period at the high operating temperature. At present the materials being used for experiments are stainless steel 316 and Inconel.

An estimate of the gamma heating at operating temperature as a function of irradiation time for a given sample and apparatus may possibly also be determined with the apparatus shown in Fig. 2.1.

Experiments are being planned to determine the effect of radiation on sigma formation in alloys such as type 446 stainless steel.

Experimental equipment is being constructed to measure in-pile changes in thermal conductivity or electrical conductivity of other materials, including metals and metal oxides. These samples will be measured at temperatures very near room temperature or up to approximately 300°C. The facility to be used will be a doughnut hole, the outside diameter of the container to be no greater than ½ in. These experiments will be for exploratory purposes in some cases. They have the advantage that adequate temperatures for lower temperature experiments can be realized in such holes without tying up the more desirable experimental fuel channels.

X-RAY WORK

F. A. Sherrill

The Hilger X-ray diffraction unit has just arrived and will be installed in Laboratory 9 of the Physics of Solids Building. This unit has several advantages over others available:

1. It is designed to permit operation of four targets at the same time. The tube body is evacuated by a built-in pumping system to permit external rotation of the anode to obtain different targets. We now have an anode with target materials of copper, chromium, cobalt, and silver.

2. It has an electron focusing arrangement so that the focal width may be set over a desired range; this permits operation of each target at its maximum rating.

3. It can supply up to 160 ma total current at 60 kv, which is a much higher capacity than may be obtained with other available machines. The higher X-ray intensity is especially desirable in work with active materials since the intensity of the diffracted beam must be greater than the radiation given off by the sample itself.

The Hilger unit will also be used to supply power to a sealed-off General Electric diffraction tube in the hot cell, or to a special tube which may have to be developed at ORNL since no tube for this work seems to be commercially available.

Material and equipment have been ordered for construction of a small 4- by 8-ft dark room for developing X-ray film.

The Metallurgy Division X-ray diffraction unit in Building 2000 has been used during this quarter for making back-reflection Laue photographs of copper single crystals for the purpose of determining orientation.

STORED ENERGY ASSOCIATED WITH VACANT AND INTERSTITIAL LATTICE SITES

C. C. Webster T. H. Blewitt
J. G. Daunt (Consultant from Ohio State University)

Recent experiments have clearly indicated that some imperfections are mobile in metals at room temperature. The imperfections introduced at low

temperatures by both high-energy particles and plastic deformation move at appreciable rates at temperatures in the vicinity of 200°K. Investigations have shown that the electrical resistivity of metals worked at 86°K is reduced by allowing them to warm to temperatures above 200°K. Similar results have been found in the case of metals bombarded by high-energy particles.

It is reasonable to suppose that high-energy particles cause interstitial atoms and vacant lattice sites in metals. It is not yet clear that imperfections of other types are not formed by a thermal spike mechanism. It would be expected, however, owing to the relatively greater mobility of interstitials and vacancies over that of other types of imperfections, that the decreased resistivity is a result of the diffusion of these vacancies and interstitials. The diffusion of these imperfections to other types of imperfections such as dislocations, the clustering of the imperfections by the diffusion of like pairs, or the annihilation of them by the diffusion of unlike pairs would adequately explain the above results.

In the case of plastic deformation it is possible that many types of imperfections are formed. Studies of the effect of plastic deformation on the ionic conductivity of ionic crystals clearly show that vacancies are formed. Seitz has suggested that in the plastic deformation of metals vacancies are also formed. It was this theory that motivated the group at ORNL to determine the change in resistivity of polycrystalline copper on cold-working; the data are shown in Table 2.1. The similarity between these data and those obtained by the group at NAA from alpha-particle bombardment suggests that the change in resistivity resulting from plastic deformation is also a result of the mobility of vacancies and interstitials.

A determination of the energy released by the motion of interstitial and vacancy atoms will prove valuable in deciding what mechanism is occurring. While it would be more desirable to measure the release of stored energy in a particle-bombarded sample than in a cold-worked sample, effort is being directed toward the measurement of the stored energy of a cold-worked sample. Facilities for pile bombardments are not as yet available, but apparatus for making these measurements has been designed and construction is almost complete. A sketch of the apparatus is shown in Fig. 2.2. The experimental procedure will be that of measuring the specific heat of a rather massive sample (500 g) of copper in increments of about 2°K in the range 86 to 250°K by an adiabatic calorimeter. The samples will be pulled in tension in the

TABLE 2.1

Change in Resistance and Resistivity of Polycrystalline Copper on Cold-Working

	SAMPLE 1	SAMPLE 2	SAMPLE 3
Before cold-working at temperature of liquid nitrogen:			
Resistance (μohms)		4.3989 ± 0.004	4.8658
Resistivity (μohm-cm)		8.1917	0.18863
After cold-working at temperature of liquid nitrogen:			
Resistance (μohms)	16.529 ± 0.020	7.0369 ± 0.0094	7.3277 ± 0.0013
Resistivity (μohm-cm)		0.21458	0.20692
After cold-working at temperature of liquid nitrogen with a 16-hr anneal at -80°C:			
Resistance (μohms)			7.2193 ± 0.0212
Resistivity (μohm-cm)			0.20327
After cold-working at temperature of liquid nitrogen with a 16-hr anneal at 20°C:			
Resistance (μohms)	15.620 ± 0.015	6.8331 ± 0.009	7.1452
Resistivity (μohm-cm)		0.20825	0.20144
Elongation (%)	25.30	19.55	17.26

SUMMARY:

For sample 1, ΔR = 0.909 μohm resulting from anneal at room temperature.

For sample 2, $\Delta\rho$ = 0.02287 μohm-cm after cold-working and reduces to 0.01654 after room-temperature anneal.

For sample 3, $\Delta\rho$ = 0.01829 μohm-cm after cold-working and reduces to 0.01464 after dry ice anneal and to 0.01281 after room-temperature anneal.

Dwg. 11045
Not Classified

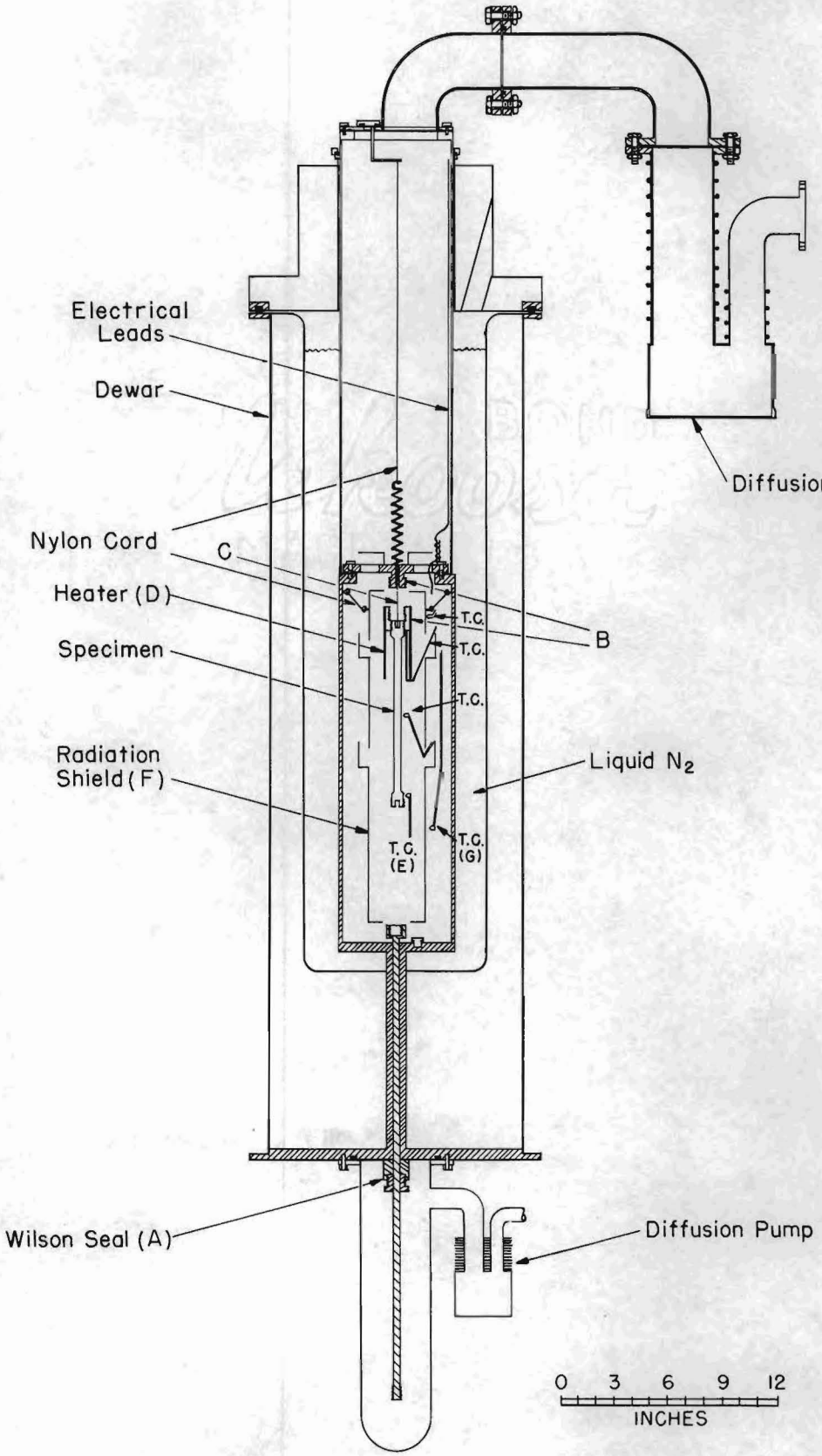

Fig. 2.2 – Tensile Calorimeter (Cross Section)

calorimeter at liquid-nitrogen temperatures. A Wilson seal *A* will be used to allow the tension to be applied in a vacuum chamber. The breech type grips *B* will then be released to thermally isolate the sample by means of the nylon cord *C*. A known amount of energy will be applied to the sample by the heater *D*, and the increase in temperature will be measured by thermocouple *E* after equilibrium has been reached. The adiabatic shield *F* will be maintained at the same temperature as the sample, as measured by the differential thermocouple *G* and a Speedomax-DAT control unit. A second run will subsequently be made to determine the normal specific heat in this temperature range, and the discrepancy between the two curves will thus be a measure of the energy released.

METAL CRYSTALS

T. H. Blewitt and R. R. Coltman

In a previous report[1] work has been described in which the effect of pile radiations on the density, electrical resistivity, and stress-strain curves of copper crystals were investigated. This work is being continued with the main effort directed toward improving the technique used to measure the electrical resistivity.

The previous technique employed had two disadvantages: (1) The potential probes, razor blades clamped into position with nylon clamps, had to be removed after each measurement, introducing an error since the physical dimensions of the sample could not be determined with the same accuracy as the resistance; (2) it was not possible to determine the temperature of the sample accurately. It was possible to overcome these difficulties to a degree and obtain results reproducible to ±0.05% by measuring the resistance at two temperatures and assuming that temperature dependence was unchanged. The assumption was thus made that the change in resistivity induced by the pile bombardment resulted from an increase in residual resistivity, with the Debye characteristic temperature, the mobility and the numbers of conduction electrons, and the physical dimensions of the sample being unchanged by the neutron bombardment. While this assumption seems valid if vacancies and interstitial atoms are the only imperfections introduced by the bombardment, there is some question whether these imperfections alone can explain the pronounced change in the

(1) T. H. Blewitt, R. R. Coltman, and F. A. Sherrill, "Study of the Effect of Radiation on Metal Crystals," *Physics of Solids Institute Quarterly Progress Report for Period Ending January 31, 1951*, ORNL-1025, p. 22 (July 17, 1951).

tensile properties. An improvement in technique which would permit an evalution of the increased resistivity at several temperatures would thus be of considerable value.

A technique has been developed to remove any errors introduced from the inaccuracy in the determination in the geometry of the samples. Potential probes are now sintered on the sample by the following procedure: The sample is first carefully cleaned with a dilute HNO_3 etching solution followed by a dilute solution of NH_4OH and is immediately placed in a vacuum furnace (10^{-4} mm Hg or better) mounted on a graphite block. The potential probes, 2-mil copper wires, are held in contact with the sample by the weight of the sample. A 1-hr soak at 1000°C is sufficient to sinter the probes and to anneal the sample. The sintered joint arising from such a treatment is stronger than the wire.

More than twenty samples have been prepared in this way. The resistivities of five of these have been measured at room temperature and at the temperature of liquid nitrogen. The results are surprisingly good when the inaccuracies induced from the temperature measurement are considered. It was found that the measurement could be repeated to within about 0.002 μohm at both room temperature and liquid-nitrogen temperature, or to about 0.01% of the room-temperature resistance. These samples have been bombarded for one month in the X pile, and the change in resistance will be determined. Vacuum anneals at temperatures in the vicinity of 250 to 400°C will then be made, and the subsequent changes in resistivity and tensile properties will be determined. These latter determinations should be interesting as it is known that the resistance of cold-worked polycrystalline samples recovers at lower annealing temperatures than those at which the hardness recovers. Results of a similar nature for radiation hardening would indicate that changes in resistivity may not be intimately connected with the changes in the tensile properties.

A change in technique is also being made to enable more accurate compensation for errors arising from inaccurate temperature measurements. (It is planned to compare the resistance of the samples with a standard resistance making good thermal contact with the sample.) Hence only comparative resistances need be determined. Alternate readings will thus be made of the standard and unknown samples at room temperature and at liquid-nitrogen temperature. In order to accomplish this, however, a double-pole double-throw

reversing switch must be made which is free of thermal emf's (less than 0.005 μvolt). A Wenner thermo-free reversing switch will be modified to accomplish this. Delivery of this item has delayed completion of this part of the program.

In order to determine the effects of gamma rays on radiation damage arising from the pile bombardment of copper crystals, two samples were irradiated in a cobalt gamma source of 15,000 r/min. The samples were irradiated for two weeks, which corresponds roughly to the gamma irradiation in both intensity and energy for a one-month bombardment in the X pile. The results of before and after resistance measurements are given in Table 2.2. It is apparent that the resistance changes are negligible from the gamma bombardment.

Tensile curves will also be run on these samples.

Electron diffraction studies have been completed on a copper crystal. Studies were made to determine the effects of pile bombardment (2×10^{18} nvt) on Kikuchi lines. The results are shown in Fig. 2.3, in which it will be noted that lines appear sharper after bombardment than before. Since the samples were re-etched after the bombardment, it is not clear that the increased sharpness is a result of the bombardment. It is reasonably clear, however, that the disorder introduced by the bombardment must be of very short range. Here also is evidence that there is not a 1-to-1 correspondence between cold-work and neutron irradiation. Experiments being performed on X-ray reflection coefficients should offer further evidence of the effect of fast neutrons on crystal perfection.

Single crystals of other metals are also being prepared for a study of the effects of pile bombardment on the tensile properties and the electrical resistance. Six zinc crystals have been prepared to date, and an equal number of bismuth crystals. These have the same shape as the copper crystals, namely, standard quarter-inch tensile specimens with a half-inch gage length. Efforts have been made to sinter leads on the sample without success; however, there is indication that this will be accomplished in the near future. Attempts made to grow aluminum crystals in the shape of tensile specimens have resulted in single crystals, but it is clear that some reaction occurred in all cases with the crucible material. Graphite and both fired and unfired lavite have been used for crucibles. It is possible that straight shank specimens may have to be made in alumina or quartz crucibles.

TABLE 2.2

Effect of Gamma Radiation on the Resistivity of Copper Single Crystals

SAMPLE NO	AREA/LENGTH (cm)	ROOM TEMPERATURE (°C)	AVG. RESISTIVITY AT ROOM TEMPERATURE (μohm-cm)	AVG. RESISTIVITY* AT 20°C (μohm-cm)	TEMPERATURE OF LIQUID NITROGEN (°C)	AVG. RESISTIVITY AT LIQUID-NITROGEN TEMPERATURE (μohm-cm)	AVG. RESISTIVITY** AT -196.0°C (μohm-cm)	Δρ AT 20°C	Δρ AT -196.0°C
19A	0.084438								
Before γ irradiation		18.27	1.6731_7	1.6846_2	-196.03	0.19692	0.19712		
		17.58	1.6685_8	1.6846_0	-196.01	0.19678	0.19685	-0.00002	-0.00027
		15.81	1.6569_3	1.6846_7				0.00005	
After γ irradiation		17.48	1.6679_6	1.6846_4	-195.91	0.19726	0.19666	0.00002	-0.00056
		18.19	1.6728_8	1.6848_6				0.00024	
		12.43	1.6347_3	1.6848_4				0.00022	
		18.21	1.6737_1	1.6855_6	-196.01	0.19642	0.19649	0.00094	-0.00063
21A	0.083904								
Before γ irradiation		18.59	1.6730_9	1.6824_2	195.99	0.19922	0.19915		
		20.86	1.6876_5	1.6819_4	196.02	0.19885	0.19898	-0.00048	-0.00017
		17.03	1.6628_1	1.6824_7	196.03	0.19926	0.19945	0.00005	0.00030
After γ irradiation		13.85	1.6418_1	1.6825_2	196.00	0.19941	0.19941	0.00010	0.00026
		8.28	1.6045_5	1.6821_4	196.11	0.19828	0.19902	-0.00028	-0.00013

*Temperature coefficient 12 to 20°C is 0.00662.

**Temperature coefficient -195 to 197°C is 0.0067.

[redacted]
Y-4273

BEFORE IRRADIATION

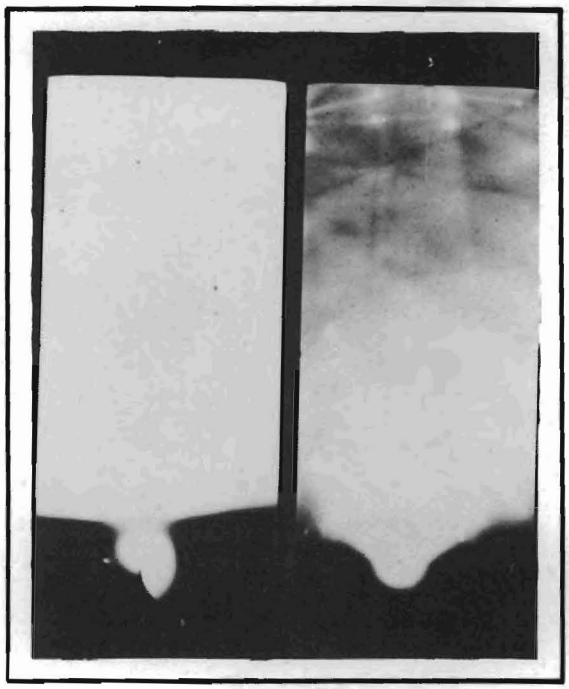

AFTER IRRADIATION

Fig. 2.3

ELECTRON DIFFRACTION STUDIES OF A COPPER CRYSTAL

In a previous report[2] the importance of conducting low-temperature bombardments in such a way that the samples can be removed and subsequent measurements made without warming was indicated. It appears that a precooled-gas type cryostat will be unsatisfactory for such bombardments, and a cryostat designed for this type of experiment is now under construction.

Such a cryostat would be quite easy to construct if a vertical pile hole were available, since a conventional metal Dewar flask could be lowered into the pile and replenished with liquid nitrogen at convenient intervals. The cryostat being constructed for use in a horizontal hole has a slight downward slope with a reservoir to provide a hydrostatic head. Some shielding difficulties must still be worked out. However, the hole in the Low Intensity Training Reactor assigned for this project has been reassigned to another group, and there is some question whether experiments of this type will be performed in the near future.

Y-12 CYCLOTRON STUDIES*

W. J. Sturm
M. J. Feldman, X-10
D. Binder
R. J. Jones
J. S. Luce
R. L. Knight
W. R. Smith

The investigation of the effect of protons on annealed copper has been continued. At first, as reported in the last quarterly report,[3] no increase in hardness was observed after proton irradiation of the copper samples. Subsequent samples with the same annealing history as previous samples have shown an increase in hardness on the very edge of the copper. Radiographs of the sample holder indicate that this was the only portion of the sample irradiated. One copper sample was irradiated with 25 μa-hr of 20-Mev protons. The hardness of the sample was measured on a Tukon hardness machine. At a distance of 1/16 in. from the leading edge of the copper sample, the hardness increased from the original annealed value to 20 numbers harder at the beam intercepting edge. Saturation hardness was not obtained on this sample since

(2) "Crystal Physics," ORNL-1025, *op. cit.*, p. 22.

* The Y-12 Cyclotron Group is under the supervision of R. S. Livingston, Director, Electromagnetic Division

(3) R. J. Jones, J. S. Luce, and M. J. Feldman, "86-in. Cyclotron Studies," ORNL-1025, *op. cit.*, p. 30.

a maximum did not occur in the hardness. A radiograph taken of the aluminum sample holder indicated a proton beam width of only 1/8 in. The wall of the aluminum sample holder intercepted 1/16 in. of the proton beam; thus only 1/16 in. of the leading edge of the copper sample was irradiated. It is probable that this small irradiated area was overlooked on samples previously reported, since a much wider beam pattern was expected.

Proposals have been made recently to irradiate, in the 86-in. cyclotron, fuel and container material of the ANP reactor. High power densities would thus be available for tests on corrosion, precipitation, decomposition, etc. under conditions simulating those in the reactor. Inconel is being used as container material as recommended by the ANP Group. A UF_4-NaF-KF fuel mixture will be used for the initial tests in the cyclotron in order to eliminate the beryllium hazard in case the fuel pin ruptures. A UF_4-BeF_2-NaK fuel mixture will be used following the first tests. The initial test will consist of an Inconel tube, approximately ¼ in. in diameter and 6 in. long, two-thirds of the volume filled with fuel and the remainder evacuated. The tubes will be heliarc-welded on one end and spot-welded across the other. Considerable difficulty has been encountered in welding these tubes because of the 0.006 in. wall thickness; however, it is possible with the present techniques to fabricate a limited number of fuel pins. A temperature of 1500°F will be maintained during irradiation by allowing the bombarding protons to heat the fuel pin. The pins will be supported at one end only to minimize heat losses by conduction, which should result in a more uniform temperature through the fuel pin; however, there is the disadvantage that only a small amount of heat can be dissipated. Calculations indicate that approximately 5 μa of protons at 26 Mev will maintain a 1500°F temperature equilibrium, assuming all the heat is dissipated by radiation. The volume of liquid irradiated will be approximately 1 cc; thus the average power density in the fuel at 5 μa and 26 Mev would be 105 watts/cc (25 watts would be lost in the Inconel).

In analyzing with respect to health hazards the activities that will result from the bombardment, all substances of half-lives of a minute or less were disregarded since, irrespective of the original intensity level, the activity will decay to a safe level an hour after the beam is turned off. Of the radioactivities with longer half-lives formed by (p,n) and $(p,2n)$ reactions, the chromium in the Inconel tubing is the only component that need be considered. Mn^{52}, 21 min, results from a $Cr^{52}(p,n)$ reaction; assuming 10-mil

tubing and a bombardment of several hours, the radiation level is roughly 50 millicuries per microampere. The other activities of importance result from the fission induced in the fuel. A few protons in ten thousand will cause a fission in the U-Na-K mixture.

Under the conditions of this preliminary experiment, the specific power dissipation in the fuel mixture is but 5% of that proposed for the ARE. However, various methods can be employed to increase the proton power dissipation density using the same geometry and the same 5-μa beam current of the preliminary experiment. By irradiating the entire volume of a tube of optimum dimensions, the dissipation can be increased to about 50% of the ARE proposed value, and the fuel element temperature can again be maintained at 1500°F by radiation cooling alone. Similarly, maintaining the same target temperature by radiation cooling, a bombardment with 5 μa of 40-Mev alpha particles at the Berkeley cyclotron, as is proposed by the NAA group, should yield specific power dissipations considerably in excess of ARE specifications, possibly approaching those of the aircraft reactor.

In order to obtain power densities by proton bombardment in liquid fuel comparable to the ARE, a water-cooled target is being designed, a sketch of which is shown in Fig. 2.4. The target consists of a fuel chamber and water channel machined from one piece of Inconel. A 0.010-in. window will allow the protons to penetrate into the fuel. A thick wall between the fuel and the water channel will allow a sufficient temperature drop to maintain the fuel at 1500°F and remove the heat from fuel by the water stream. Tests have been made to determine the necessary wall thickness between the fuel and water stream. A proton beam from a calutron was used to bombard a ½-in. stainless steel wall backed by a water channel similar to that of the target design for the cyclotron. The surface of the wall was bombarded with 3.2 kw over an area of 0.7 sq in., and an equilibrium temperature of 1200°F was maintained.

To obtain power densities by proton irradiation comparable to those in the airplane engine, it may be necessary to dissipate the heat generated in the fuel by means of liquid-metal cooling. A design of a liquid-metal-cooled target is in progress. The target will incorporate the same principle as the water-cooled target, the liquid metal being circulated by means of a thermal loop with heaters external to the cyclotron tank.

The work on the creep-test equipment has continued during the quarter. The handling equipment has been constructed and tested, and target design

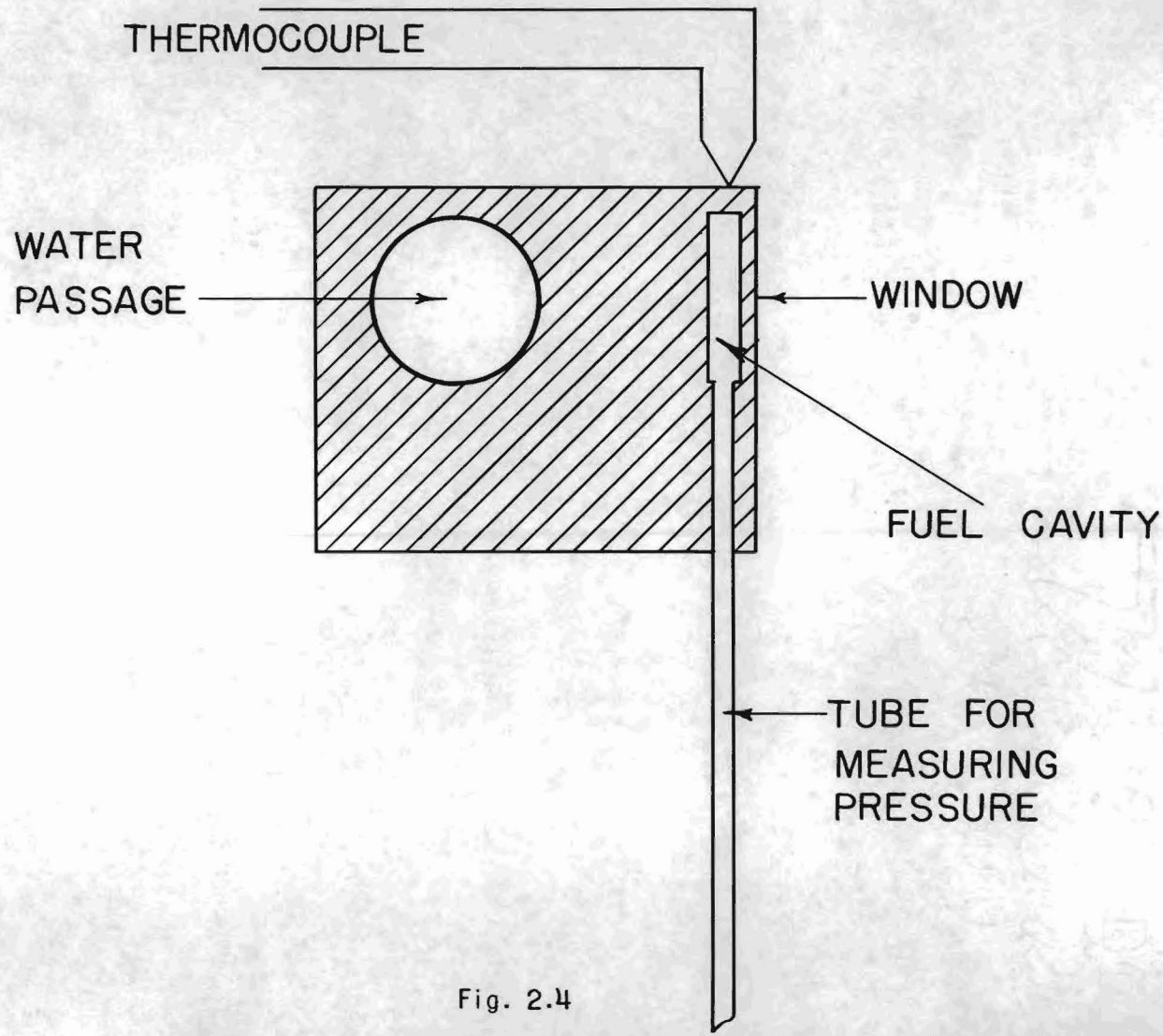

Fig. 2.4

OAK RIDGE NATIONAL LABORATORY - Physics of Solids Institute				
WATER-COOLED FUEL TARGET				PSI-A-128
DRAWN BY: WEB	FOR W. J. STURM	DATE 5-29-51	SCALE:	DWG.-11450

NOT CLASSIFIED

work is near completion. The construction of the target will probably be delayed somewhat by the urgency of fuel-pin tests.

Development of the deflection plates for the 22-in. cyclotron has continued, and a preliminary 4-hr irradiation has been made with this instrument on a copper single crystal. The crystal was covered with 0.002-in. aluminum foil to prevent contamination of the surface. One-half of the crystal was not irradiated in order that a control surface would be available. The crystal was irradiated for 20 μa-hr at a proton energy of 1.3 Mev. The studies of the effects of the irradiations, to be made by X rays, have not been completed.

PURDUE CYCLOTRON CREEP

K. Lark-Horovitz and B. R. Gossick
Purdue University

The creep apparatus has been completed. It permits precise vertical orientation of the specimen and provides a furnace with automatic temperature control. The extensometer now has a full-scale sensitivity of 2000 A and a linear range of 3.5 mm. Both creep and creep rate are recorded directly.

Practice creep measurements have been made to test the equipment. At present the microformers with bakelite coil forms are being replaced by microformers with ceramic forms. Although the bakelite forms appear to be satisfactory, the ceramic forms are expected to exhibit greater stability with temperature fluctuations. After this modification has been made, the equipment will be ready for creep measurements.

3. SOLID-STATE REACTIONS

VARIATION OF IONIZATION ENERGY* WITH BOMBARDMENT IN CUPROUS OXIDE

J. W. Cleland
J. H. Crawford, Jr.
J. C. Pigg
F. W. Young, Jr.

Studies on the behavior of the electrical properties of Cu_2O semiconductors under pile bombardment have been continued. In-pile conductivity measurements seem to indicate that the initial portion of the conductivity vs. bombardment curve for Cu_2O is approximately exponential. This is illustrated by a typical log conductivity vs. bombardment curve shown in Fig. 3.1. The carrier concentration is proportional to a Boltzmann factor which contains an ionization energy. Consequently, it might be expected that there is an initial linear increase of this ionization energy with bombardment. An experimental value for the ionization energy $\Delta\epsilon$ may be obtained from the slope of the log Hall coefficient vs. $1/T$ curve if $\Delta\epsilon$ is large compared to kT over the temperature range considered. The experimental value of $\Delta\epsilon$ may differ from the theoretical value by as much as a factor of 2 depending on conditions of impurity concentration and previous treatment.(1) Similar information may be obtained from the slope of the log resistivity vs. $1/T$ curve, but in this case the slope also reflects the exponential temperature dependence of mobility which has been shown to exist by Frohlich and Mott.(2)

In order to investigate this problem further a Cu_2O plate, suitably heat treated by annealing in air at 950°C for about 36 hr and quenching to room temperature, was given a series of short exposures in the pneumatic tube, and the Hall coefficient R and resistivity ρ were measured as a function of temperature after each exposure. These data are shown in Figs. 3.2 and 3.3, respectively. A "cooling" period of about one week was required after each exposure before the sample could be handled safely, but previous behavior of the resistivity in the pile during shutdown periods indicated little or no annealing during the cooling period.

*The usual nomenclature uses "activation energy" for this term. However, since the term "activation energy" is used universally to denote barrier height in rate process problems and since we are planning some kinetics studies, the term "ionization energy" (an even more descriptive term for carrier production) will be used to avoid ambiguity.

(1) N. F. Mott and R. W. Gurney, *Electronic Processes in Ionic Crystals*, p. 159, Oxford University Press, London, 1940.

(2) H. Fröhlich and N. F. Mott, "The Mean Free Path of Electrons in Polar Crystals," *Proc. Roy. Soc. London* A 171, 496 (1939).

Fig. 3.1

CUPROUS OXIDE PLATE
CONDUCTIVITY VS INTEGRATED FAST
NEUTRON FLUX
EXPOSURE TEMPERATURE 20° C

PSI-A-229
UNCLASSIFIED
DWG. 10507

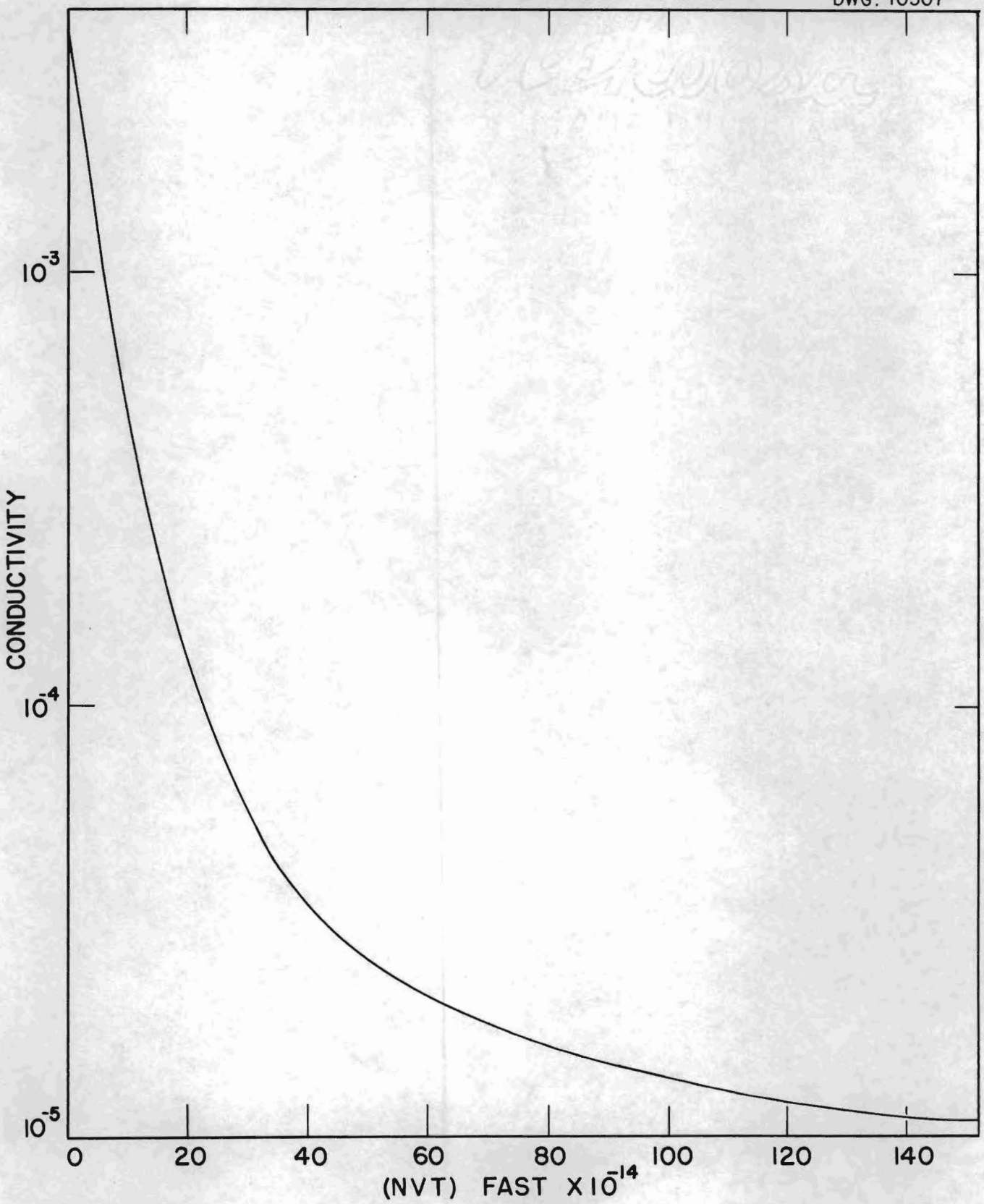

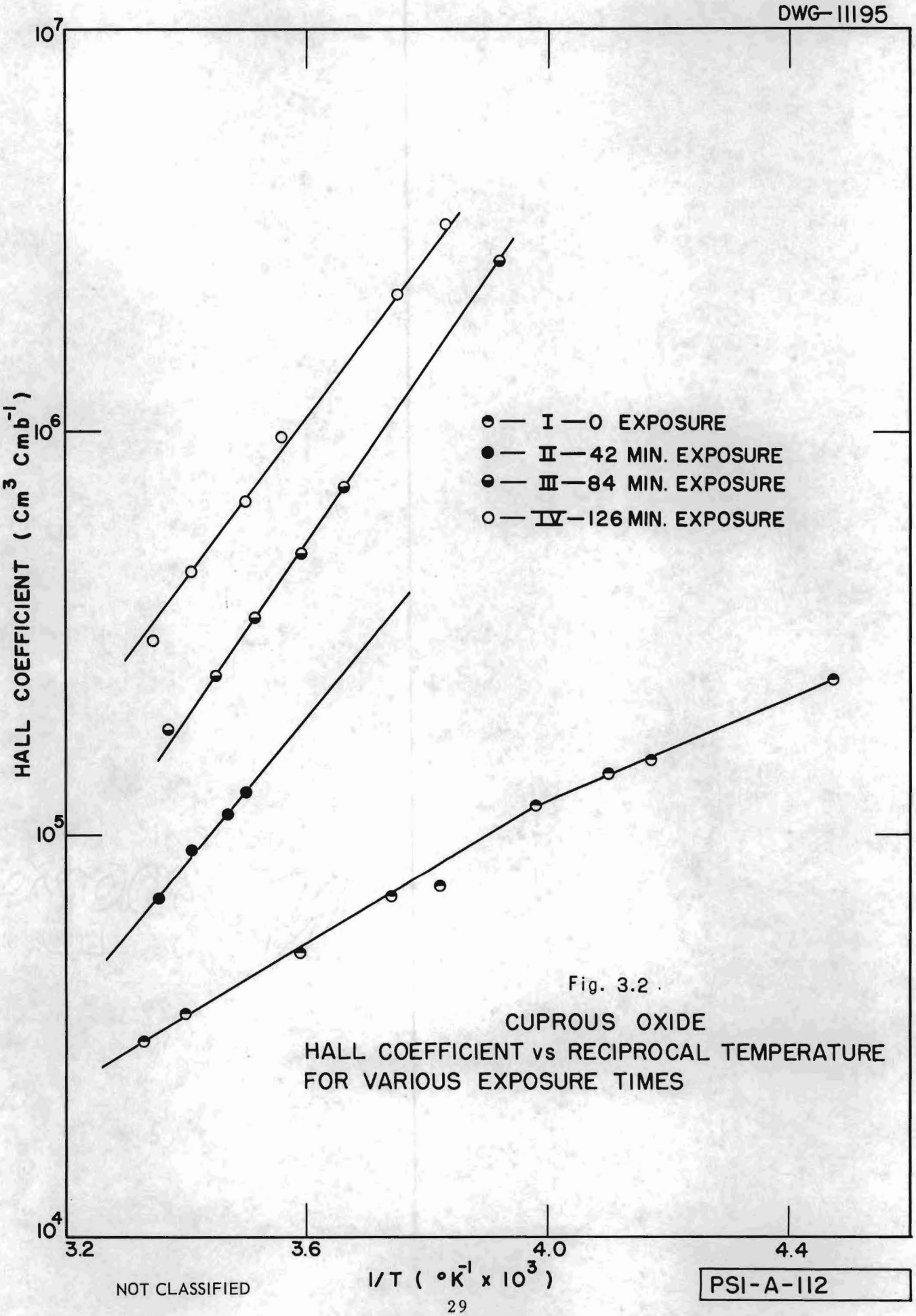

Fig. 3.2

CUPROUS OXIDE
HALL COEFFICIENT vs RECIPROCAL TEMPERATURE
FOR VARIOUS EXPOSURE TIMES

NOT CLASSIFIED

PSI-A-112

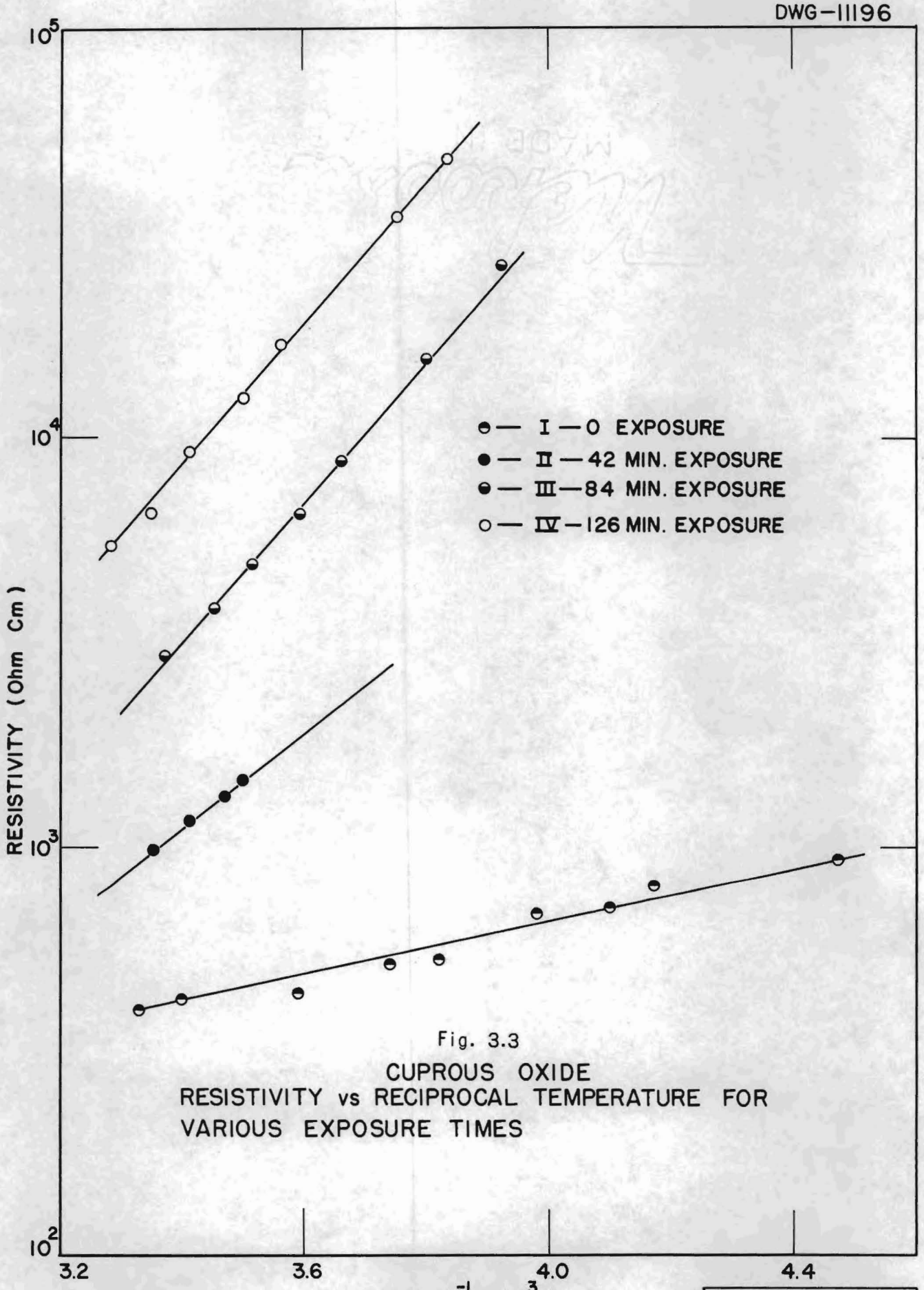

Fig. 3.3
CUPROUS OXIDE
RESISTIVITY vs RECIPROCAL TEMPERATURE FOR VARIOUS EXPOSURE TIMES

NOT CLASSIFIED

PSI-A-113

The experimental ionization energies were determined from the slopes of the log R vs. $1/T$ and log ρ vs. $1/T$ curves. These are listed in Table 3.1 for the various exposure periods. $\Delta\epsilon_R$ is the ionization energy determined from the slope of the log R vs. $1/T$ curve and $\Delta\epsilon_\rho$ is that determined from the log ρ vs. $1/T$ curve. These data are presented graphically in Fig. 3.4. $\Delta\epsilon$ appears to increase markedly during the first part of the exposure, and the rate of increase diminishes with further bombardment until a maximum value is reached. Further bombardment apparently causes a decrease in $\Delta\epsilon$. $\Delta\epsilon_\rho$ seems to reach this maximum later than $\Delta\epsilon_R$. Unfortunately, after the third exposure the resistance of the sample was so high that further measurements could not be made with any degree of accuracy with the present equipment. This experiment will be refined and repeated in more detail.

TABLE 3.1

Effect of Bombardment on Experimental Ionization Energy of Cu_2O

EXPOSURE TIME (min)	$\Delta\epsilon_R$ (ev)	$\Delta\epsilon_\rho$ (ev)
0	0.194	0.064
42	0.364	0.233
84	0.437	0.323
126	0.421	0.354

The difference between $\Delta\epsilon_R$ and $\Delta\epsilon_\rho$ (approximately 0.13 ev) is considerably larger than that used by Frohlich and Mott[2] (0.024 ev) to fit the data of Engelhard.[3] Our value is also larger than that of Angello[4] (approximately 0.06 ev). This difference may be due to different heat treatments used in sample preparation. However, differences of this sort are quite common in ionic semiconductor literature, indicating the very strong history dependence of the properties of these materials. It might also be mentioned that several other puzzling observations have been made in connection with ionization energy determinations. In particular, there are many cases in which the Hall coefficient curve shows a sudden decrease in slope toward low temperatures, and this change is not reflected in the resistivity curve (also see reference 3 for similar information on slope changes).

(3) E. Englehard, "Elektrisches und optishces Verhalten von Halbleitern IX," *Ann. Physik* 17, 501 (1933).

(4) S. J. Angello, "Hall Effect and Conductivity of Cuprous Oxide," *Phys. Rev.* 62, 371 (1942).

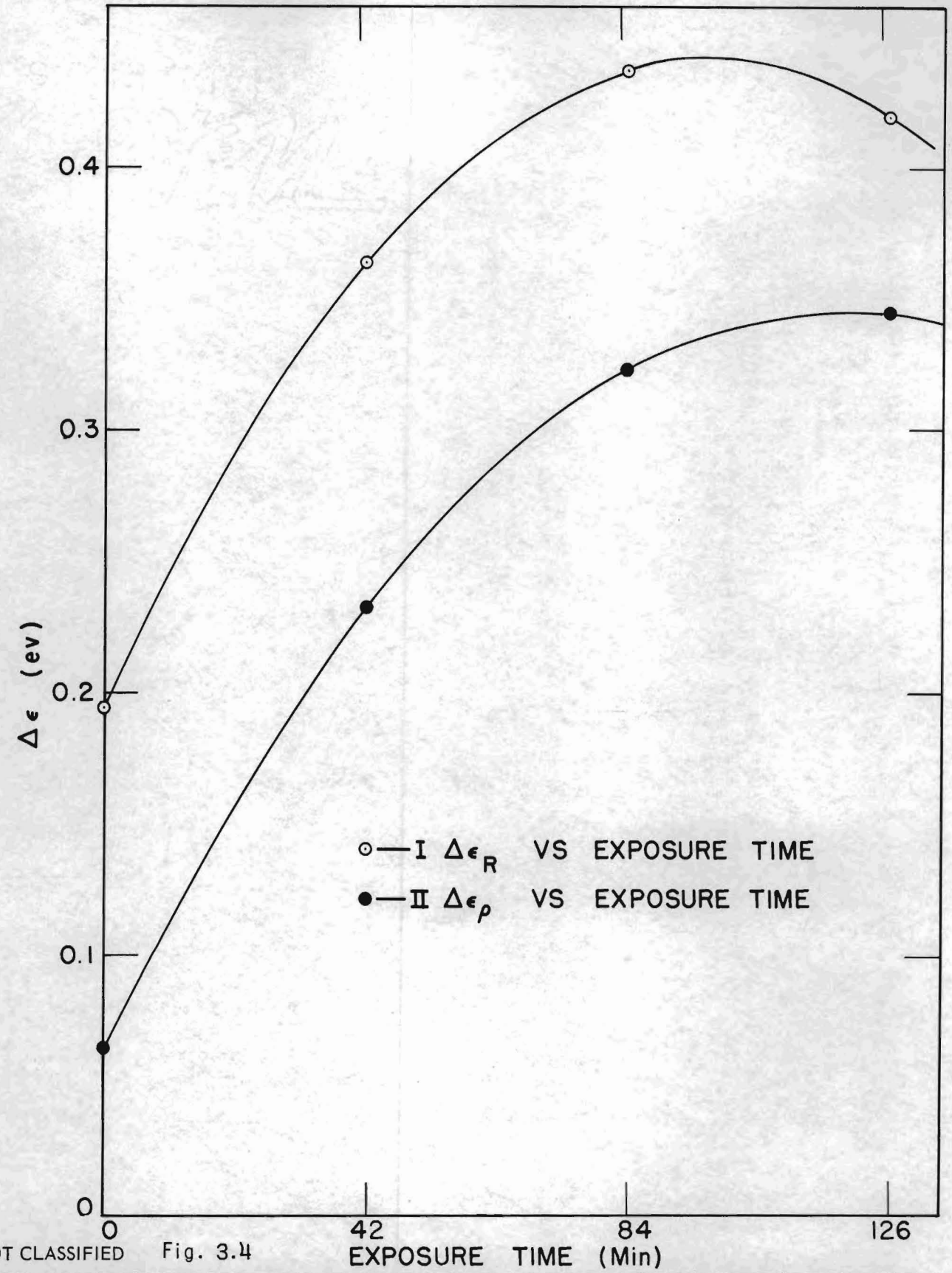

NOT CLASSIFIED Fig. 3.4

OAK RIDGE NATIONAL LABORATORY——— Physics of Solids Institute				
EXPERIMENTAL IONIZATION ENERGY VS. EXPOSURE TIME FOR Cu_2O				PSI-A-110
DRAWN BY: W.E. BUSBY	FOR: J.H. CRAWFORD	DATE: 5-4-51	SCALE	DWG-11193

ANNEALING OF RADIATION DAMAGE IN CUPROUS OXIDE

J. W. Cleland J. C. Pigg
J. H. Crawford, Jr. F. W. Young, Jr.

A simple annealing experiment was carried out on the sample used in the above study. Hall coefficient and resistivity measurements were taken while the sample was being heated (previously the sample temperature had not exceeded 30°C). After remaining at 130°C for about 20 min the sample was cooled to room temperature, and a second series of measurements was made while cooling to low temperatures. Finally, the sample was held at 120°C for 12 hr, and, after cooling, a third series of Hall coefficient and resistivity measurements was made. The Hall coefficients as a function of temperature for these operations are shown in Fig. 3.5. The resistivity curves (not shown) are quite similar to the Hall coefficient curves.

The initial measurement of the Hall coefficient as a function of temperature is shown in Curve I, Fig. 3.5. A decrease in ionization energy with increasing temperature was observed which may or may not be significant in connection with the annealing process. Curve II, taken after heating to 130°C, is displaced toward lower values of R, indicating an increase in carrier concentration. This is the expected behavior if the annealing were a simple, straightforward process. Curve III, however, taken after 12 hr at 120°C, lies about halfway between Curve I and Curve II. This indicates a decrease in carrier concentration over that existing when Curve II was taken. Consequently the annealing of damage in Cu_2O might be expected to be quite complicated.

There appear to be small changes in $\Delta\epsilon$ accompanying the heat treatment, but, owing to abrupt changes in slope toward low temperature in both Curves II and III, which may or may not be real, it is difficult to determine the values of $\Delta\epsilon$ sufficiently accurately to permit a significant comparison. This experiment will be repeated in the near future.

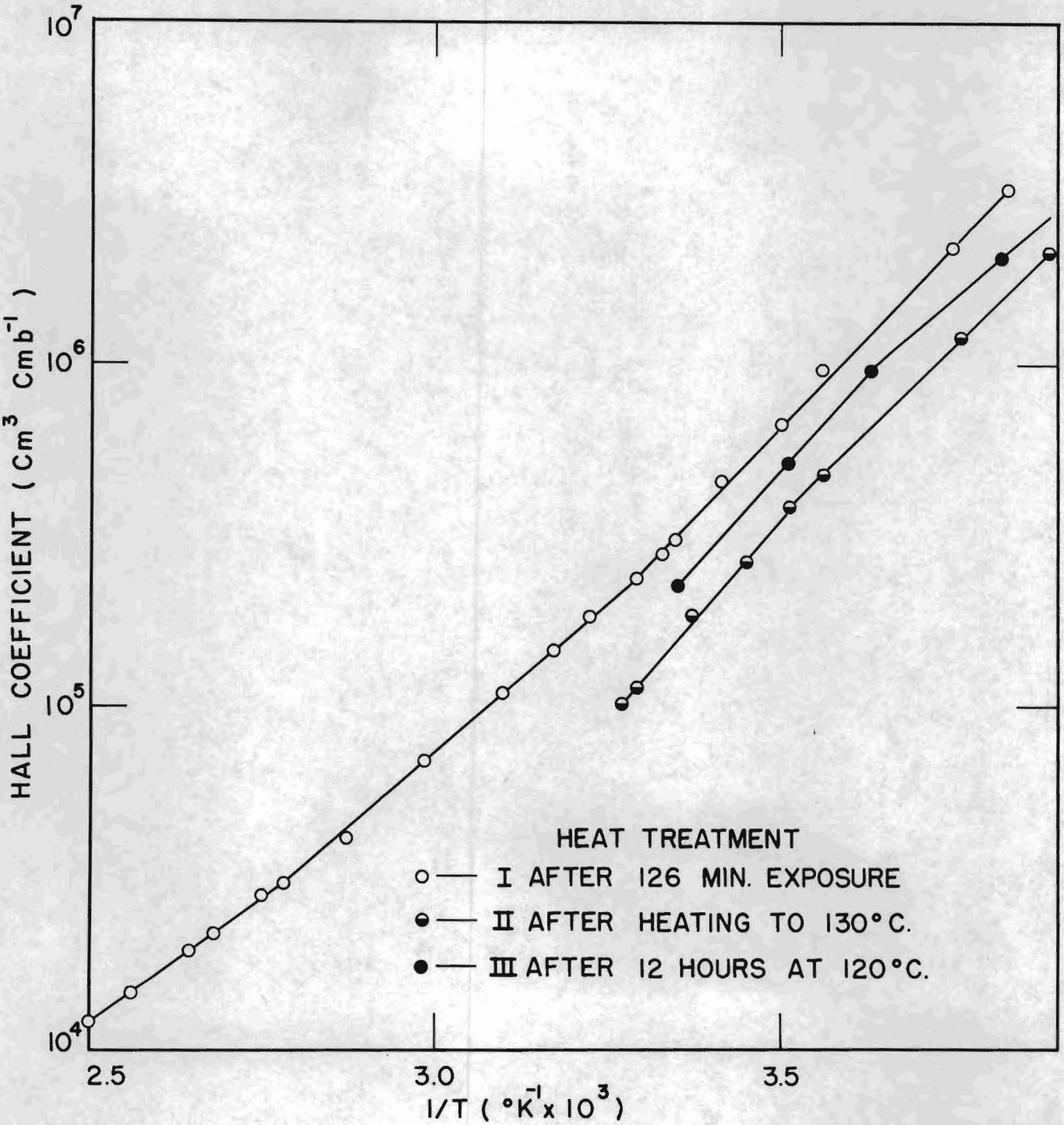

NOT CLASSIFIED

Fig. 3.5

OAK RIDGE NATIONAL LABORATORY—Physics of Solids Institute				
CUPROUS OXIDE- HALL COEFFICIENT vs RECIPROCAL TEMPERATURE OF BOMBARDED Cu_2O ANNEALED				PSI-A-111
DRAWN BY: W.E.B.	FOR: J. CRAWFORD	DATE: 5-8-51	SCALE:	DWG-11194

SILICON BOMBARDMENT EXPERIMENTS

J. W. Cleland J. H. Crawford, Jr.
K. Lark-Horovitz* J. C. Pigg

Recently it has been found desirable to obtain a quantitative correlation between the incident integrated fast-neutron flux and the magnitude of changes in electrical properties induced in silicon by fast-neutron bombardment in order to make a comparison with similar changes in germanium, for which these correlations have already been obtained. Almost no bombardment work on silicon has been carried out since the early qualitative work of Johnson and Lark-Horovitz.(5) These authors have found that the conductivity of both P- and N-type silicon decreases monotonically with bombardment over the range of exposures investigated (nvt approximately 10^{18}). The initial portion of the conductivity vs. bombardment curves for both types of material is linear, and, consequently, if the original values of the Hall coefficient and resistivity are known, the data can be analyzed to give the number of carriers removed per incident neutron in the same way in which this value was determined for germanium.(6)

Of the early samples, there was only one whose original resistivity and Hall coefficient were available. This sample, P-type silicon, was analyzed and it was found that the change in carrier concentration per incident neutron, $dn_h/d(nvt)_{fast}$, was -5.0. Recently an N-type silicon plate was exposed in the pile, and analysis gives for $dn_e/d(nvt)_{fast}$ a value of -5.1. Thus the rate of removal of carriers is the same, within experimental error, for both P- and N-type silicon. On the basis of these limited data it appears that electron and hole traps of approximately equal efficiency are introduced in equal concentrations by fast-neutron bombardment.

These results may be understood if it is assumed that vacancies act as electron traps and interstitials act as hole traps. In the case of germanium the electron traps are quite deep, lying in the forbidden energy band near the top of the filled band where they may not only trap electrons in N-type germanium but also act as acceptors in P-type germanium. The hole traps in germanium, on the other hand, are quite shallow and are, therefore, relatively

*Consultant from Purdue University.

(5) W. E. Johnson and K. Lark-Horovitz, *Neutron Irradiation of Semiconductors*, NEPA 1178-IER-23 (Oct. 20, 1949).

(6) J. H. Crawford, Jr., and K. Lark-Horovitz, "Fast Neutron Bombardment Effects in Germanium," *Phys. Rev.* 78, 815 (1950).

inefficient. Thus in germanium under ordinary experimental conditions only the effects of the electron traps are observed. Recently (see below) conclusive evidence has been found for the existence of hole traps in germanium. In contrast to the situation in germanium, bombardment-produced hole and electron traps are both quite deep in silicon, lying somewhere near the center of the forbidden energy band. In this position these traps are very inefficient as acceptors and donors but are quite efficient for trapping carriers. This difference between the relative efficiency of traps in germanium and silicon is probably due to the larger forbidden energy gap and stronger binding forces in the latter.

It is interesting to note that more traps, and therefore more atoms, are displaced per incident neutron in silicon than in germanium (~5 for silicon as compared to ~3.2 for N-type germanium). A difference in this direction is expected because of the smaller mass of the silicon atom, provided that the scattering cross-sections for fast neutrons are comparable for these two materials. It should be pointed out, however, that inelastic energy losses of knocked-on atoms, which are negligible in the case of germanium, may be appreciable in the case of silicon.

Recently a number of high-resistivity (approximately 5 ohm-cm) silicon samples, both P- and N-type, were obtained from Bell Laboratory. Consequently, more extensive silicon bombardment experiments are being planned.

EVIDENCE FOR HOLE TRAPS IN GERMANIUM RESULTING FROM FAST-NEUTRON BOMBARDMENT

J. W. Cleland J. C. Pigg
J. H. Crawford, Jr. F. W. Young, Jr.

In the preceding section the behavior of the electrical properties of silicon under fast-neutron bombardment was contrasted with that of germanium. This difference in behavior is assumed to be due to the different relative positions of the electron and hole traps in the forbidden energy band with respect to the top of the filled band. In germanium the bombardment-produced electron traps associated with lattice vacancies lie near the top of the filled band, and, in the absence of electrons in the conduction band, these may accept electrons from the filled band, thus producing holes. Hole traps

assumed to be associated with interstitial atoms, known to exist in bombarded silicon, would also be expected in bombarded germanium. In germanium, however, these hole traps are competing with acceptors (deep-lying electron traps), and, since the acceptors are more effective under normal conditions, the ability of the shallow hole traps to remove holes is overshadowed by the production of holes by the acceptors.

Lehman[7] has examined the case for germanium in which both electron traps and hole traps are introduced in equal numbers below the center of the forbidden energy band. He finds that, when only electron traps or acceptors are introduced, bombardment causes a lowering of the room temperature Fermi ζ level into the filled band of states toward some limiting value of energy. When, on the other hand, both hole and electron traps are introduced, bombardment causes a lowering of ζ for N-type and moderate-resistivity P-type material toward a limiting position approximately halfway between the positions of the two types of traps. For P-type material of low resistivity, however, ζ which initially lies below the limiting value would be expected to be raised toward this value by bombardment. Such behavior would be accompanied by a decrease in hole concentration and a corresponding decrease in conductivity.

In order to test this hypothesis a low-resistivity (0.003 ohm-cm) P-type germanium plate was bombarded in a high fast-neutron flux region of the X-10 pile in a water-cooled hole. The conductivity was recorded automatically using a Brown Electronik recorder and a constant current supply. The conductivity decreased throughout the exposure. The results are shown in Fig. 3.6, in which the conductivity is plotted against the integrated fast-neutron flux. This curve shows an initial linear decrease with later curvature, indicating an approach to saturation. Analysis of the initial linear portion of the curve gives for $dn_h/d(nvt)_{fast}$ a value of -0.48.

The efficiency of a shallow trap for removing carriers is expected to be markedly temperature-dependent, being the more efficient the lower the temperature. On the other hand the efficiency of acceptors is expected to decrease as the temperature decreases. Consequently, the effect of hole traps should be more evident at low temperatures. Three P-type germanium samples, approximately 0.1 ohm-cm, packed in dry ice were exposed in the pile, and the conductivity was followed throughout the duration of the dry ice (about 3 hr) and

(7) G. W. Lehman, "Fermi Levels in Semiconductors," *Phys. Rev.* 81, Paper T6, p. 321 (1951).

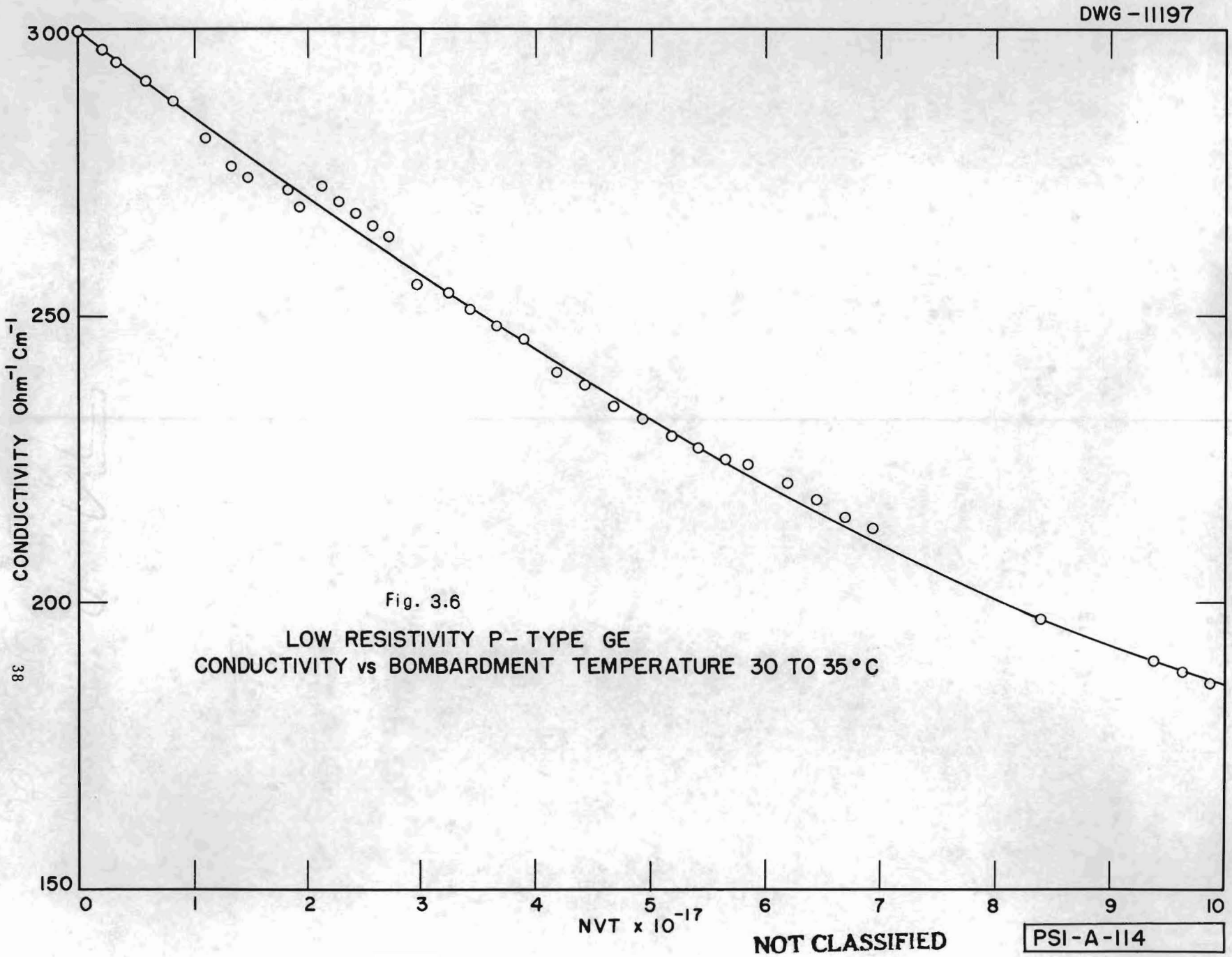

Fig. 3.6

LOW RESISTIVITY P-TYPE GE
CONDUCTIVITY vs BOMBARDMENT TEMPERATURE 30 TO 35°C

for a number of hours at pile ambient temperature (approximately 55°C). A typical conductivity vs. exposure curve is shown in Fig. 3.7. At -78°C there was a decrease in conductivity with bombardment at a rate corresponding to $dn_h/d(nvt)_{fast} = -1$. After the sample warmed to ambient temperature, the conductivity increased with bombardment. The results for the three samples are given in Table 3.2.

TABLE 3.2

Change in Conductivity of P-Type Germanium on Bombardment

SAMPLE	n_h° AT -78°C	$dn_h/d(nvt)_{fast}$ AT -78°C	$dn_h/d(nvt)_{fast}$ AT PILE AMBIENT TEMPERATURE
1	4.0×10^{16}	-0.99	0.20 (55.5°C)
2	2.7×10^{16}	-1.12	0.40 (62.0°C)
3	4.9×10^{16}	-1.03	

The above experiments demonstrate conclusively the presence of hole traps in germanium. It should be possible by studying a series of samples of increasing hole concentration at various exposure temperatures to determine the positions of hole and electron traps in the germanium band scheme. Such a study will be carried out as soon as these samples are available.

CRYOSTAT FOR PILE IRRADIATIONS

R. P. Metcalf

The future location of the cryostat in the pile was not finally decided until April 5. It will be installed in the north end of hole 52. The Engineering Department is working on those plans for the installation which could not be drawn up until this decision was made.

While the decision on the location of the cryostat was being awaited, further adjustments were made to the automatic temperature controller for the cryostat.

DWG11198

Fig. 3.7

P- TYPE GE
CONDUCTIVITY vs BOMBARDMENT
------ TEMPERATURE

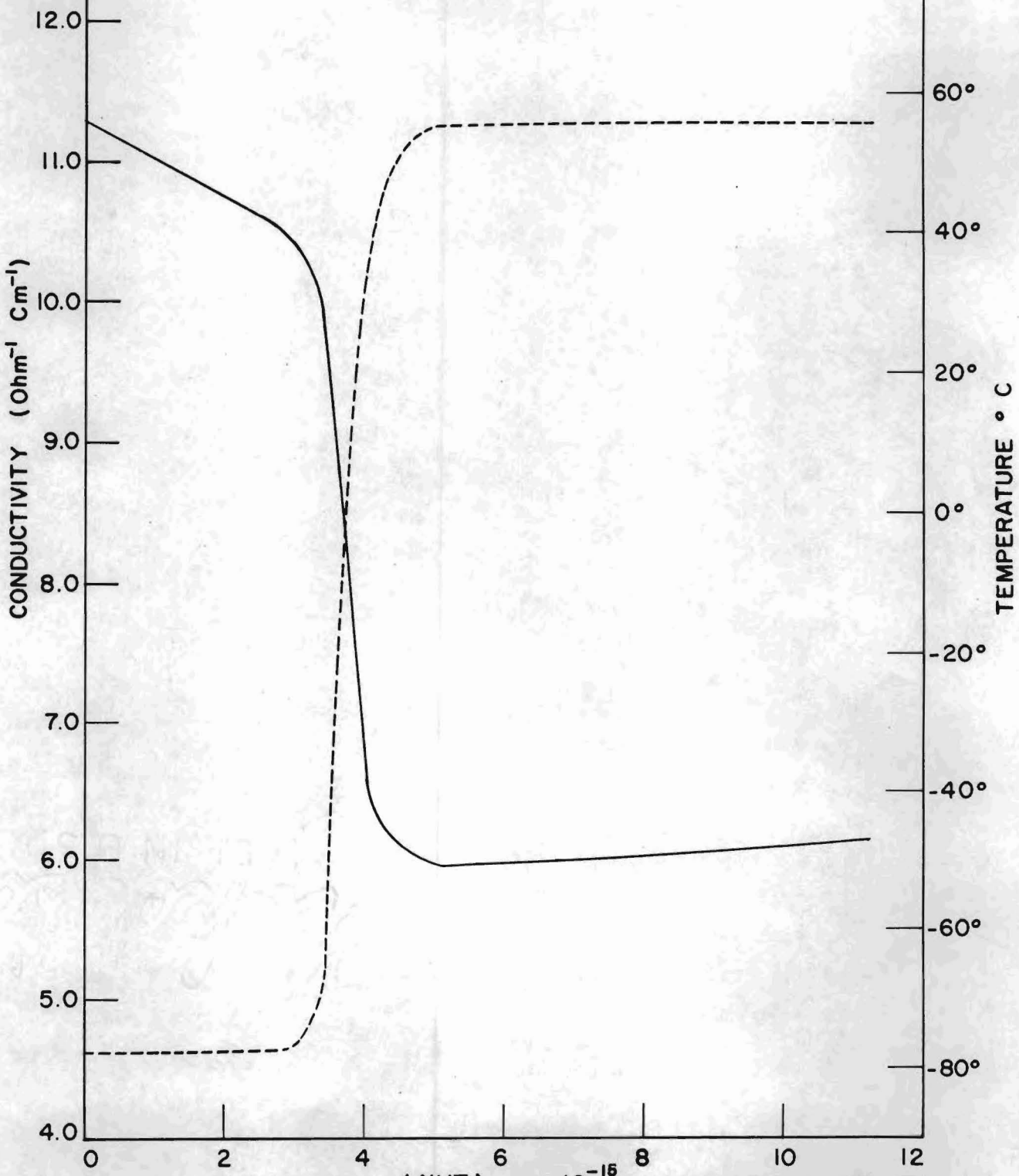

NOT CLASSIFIED

PSI-A-115

From February 8 until April 5 it appeared that the cryostat would be installed in hole 50 of the pile. In this location there would have been serious limitations on the thickness of external shielding which could be used underneath the hole. A special arrangement of shielding to meet these requirements was worked out by C. Clifford of the Shielding Section of the Physics Division. This shield and the experiments done in connection with its development are being reported by the Shielding Section in a separate report.

The floor in front of hole 52 has been removed and support beams and shielding have been added up to floor level. Material for shielding above floor level has not yet arrived.

4. RADIATION METALLURGY

INVESTIGATION OF HOMOGENEOUS DEFORMATION OF COPPER

W. E. Taylor G. T. Murray
F. M. Blacksher

The apparatus for homogeneous shearing of metal single crystals[1] is now in use. After preliminary work to refine the experimental technique, samples which have been exposed to fast-neutron flux will be deformed in order to investigate the effect of radiation on simple shearing mechanisms.

Preliminary measurements of the stress-strain curve for a pure (99.999%) copper single crystal have been made. The method of loading the specimen and controlling its deformation is shown in Fig. 4.1. The system is similar in principle to the apparatus developed by Rohm and Kochendorfer.[2] The sample was oriented so that the slip plane was perpendicular to the plane of the paper and the slip direction was in the plane of the paper. A dead-weight load was applied by means of a cable attached to the lower crystal grip through a pivoted yoke so that the shearing stress was a maximum in the selected slip system. Bending of the sample was prevented by means of tracks along which the lower crystal grip moved. Ball bearings (not shown) were mounted on the crystal grip at points of contact with the guide tracks in order to reduce errors due to friction. The measured frictional forces were small compared to the applied loads. Strain was measured by following the motion of the lower crystal grip with a transit.

The general features of the deformation were similar to those reported for aluminum by Rohm and Kochendorfer.[2] The critical shear stress (Fig. 4.2) was about 65 g/mm^2, considerably smaller than the critical shear stress of 100 g/mm^2 reported[3] for regular tension tests. In the stress-strain curve there are two distinct linear regions having a much lower slope than is shown by copper single crystals in pure tension. This stress-strain curve can only be taken as a qualitative indication of the deformation since there appeared to be some bending near the crystal grips.

(1) W. E. Taylor, G. T. Murray, and F. M. Blacksher, "Apparatus for Fundamental Investigations," *Physics of Solids Institute Quarterly Progress Report for Period Ending January 31, 1951*, ORNL-1025, p. 43 (July 17, 1951).

(2) V. F. Rohm and A. Kochendorfer, "Neue Ergebnisse über die Verfestigung bei der plastischen Verformung von Kristallen. I. Schubverformung von langen Kristalle," *Z. Metallkunde* 41, 265 (1950).

(3) C. S. Barrett, *Structure of Metals*, McGraw-Hill, New York, 1943.

NOT CLASSIFIED DWG.– 11391

Fig. 4.1
METHOD OF LOADING SINGLE CRYSTAL
FOR HOMOGENOUS SHEAR EXPERIMENT

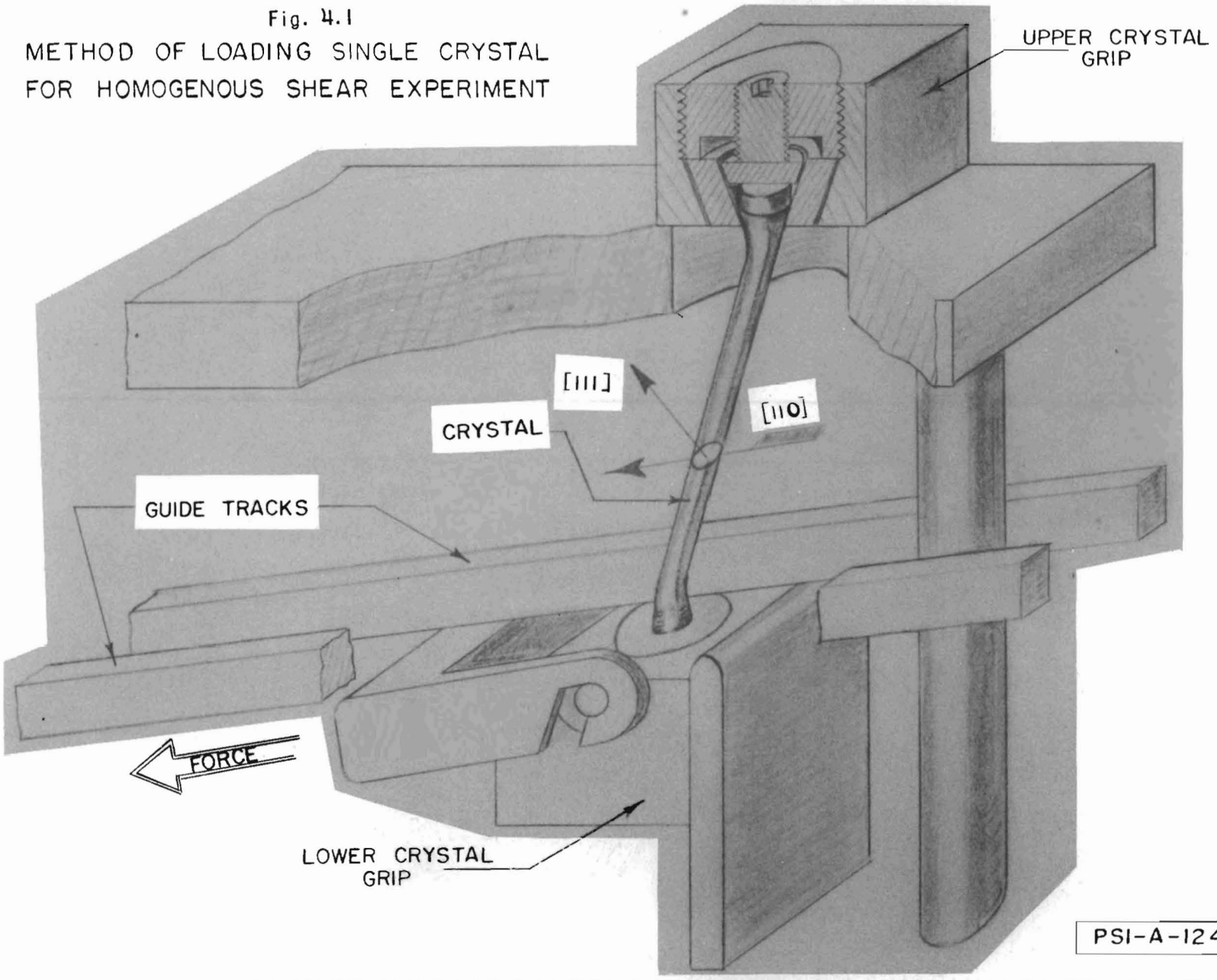

PSI-A-124

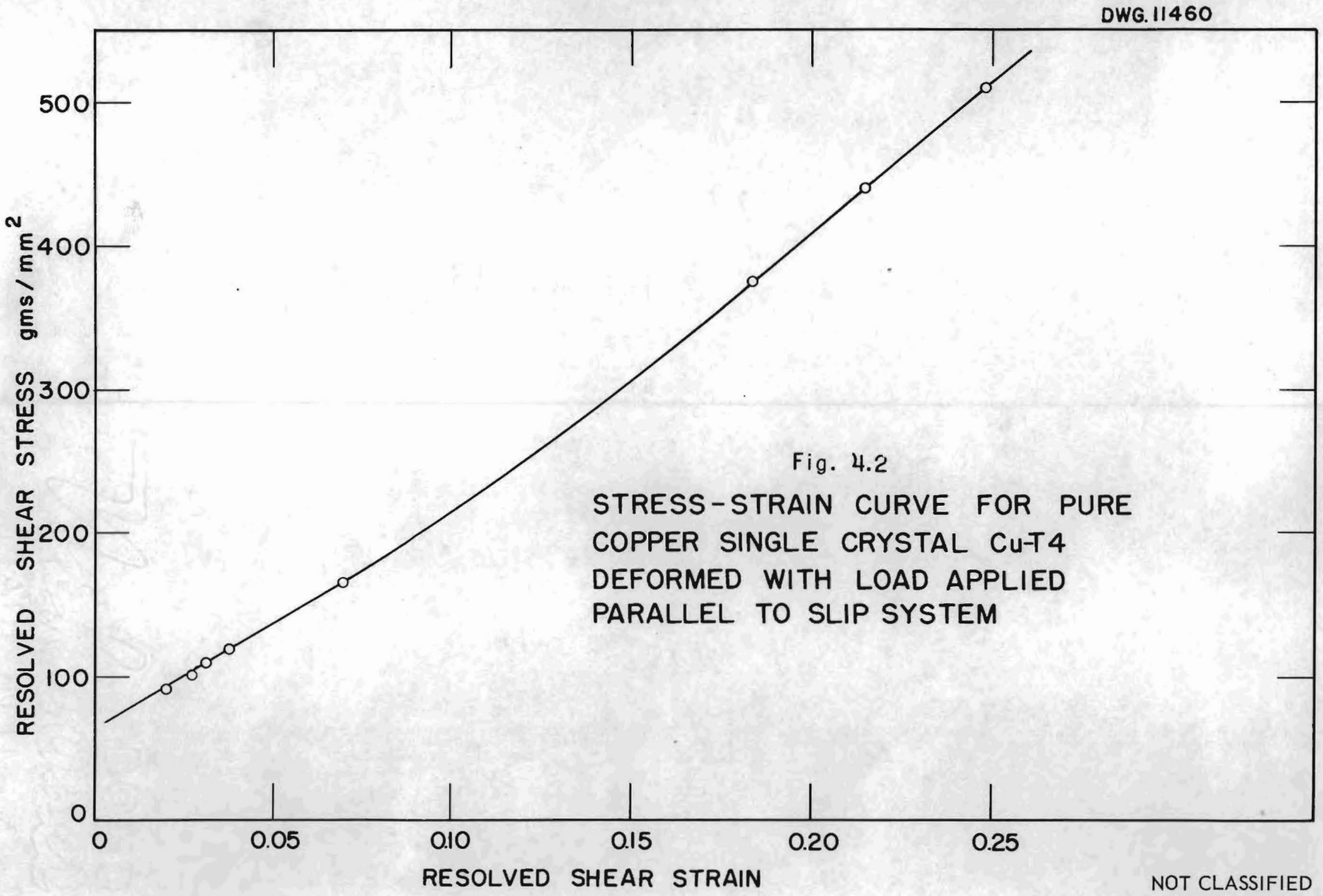

Fig. 4.2

STRESS-STRAIN CURVE FOR PURE COPPER SINGLE CRYSTAL Cu-T4 DEFORMED WITH LOAD APPLIED PARALLEL TO SLIP SYSTEM

NOT CLASSIFIED

PSI-A-120

An unsatisfactory feature of this method of loading is the existence of a shear stress parallel to the surface of the sample. At the surface of the sample this stress cannot be supported, and there must consequently be complicated deformations present in a layer near the surface. The existence of such strains was verified by X-ray techniques. Back-reflection photographs of the deformed crystal showed Laue spots which were considerably broadened and very weak. The removal of a surface layer 0.009 in. thick by electropolishing improved the appearance of the spots, and the removal of an additional 0.005 in. restored the spots to their original sharpness and relative intensities.

The results of this preliminary investigation have indicated that this method of applying the load is not entirely satisfactory. Samples are now being prepared which will be deformed by applying an axial load, with the lower (movable) crystal grip constrained to move parallel to the most favorable slip system. The use of a vertical load will eliminate the shearing stresses parallel to the surface. The bending moment will be zero at the beginning of the deformation and will gradually increase during the test, but will be much smaller than in the previous method of loading. Constraint of motion of the movable crystal grip should lead to homogeneous slip throughout most of the gage length.

ANNEALING OF RADIATION HARDENING OF COPPER AND COPPER ALLOYS

W. E. Taylor G. T. Murray
F. M. Blacksher

Isothermal annealing of radiation hardening of copper and 2 and 4 atom % alloys of zinc, gallium, germanium, and arsenic in copper has been started. The samples were exposed in the X-10 reactor to an integrated fast-neutron flux of 1.5×10^{18}. All the alloys suffered an increase of hardness of about 20 DPH numbers.[3]

One sample of each alloy was annealed in a nitrate salt bath at 300°C. Samples were quenched on removal from the bath during the early stages of annealing, which introduced some spurious effects. The annealing has not been completed for all samples, but sifficient data are available to indicate that radiation hardening anneals more readily in the alloys than in pure copper.

This effect increases as alloy content increases and also increases with increasing atomic number of the alloying element. Annealing at this temperature has not completely returned the samples to their original hardness, but to what extent this is due to quenching of the samples is uncertain. The relative ease of annealing the alloys is attributed to the effect of alloying on the self-diffusion coefficient of copper. The time required for cessation of recovery at 300°C is given in Table 4.1.

TABLE 4.1

Time Required for Cessation of Recovery of Hardness in Copper Alloys After Irradiation

ALLOY	AMOUNT OF ELEMENT ALLOYED WITH COPPER (atom %)	TIME TO CESSATION OF RECOVERY (sec)
Copper		Still recovering at 10,000 sec
Copper-zinc	2	Still recovering at 10,000 sec
Copper-zinc	4	7000
Copper-gallium	2	7000
Copper-gallium	4	2000
Copper-germanium	2	3500
Copper-germanium	4	1000
Copper-arsenic	2	100
Copper-arsenic	4	Less than 30

CREEP UNDER IRRADIATION

J. C. Wilson J. C. Zukas
W. W. Davis

Several successful in-pile cantilever creep tests have been run in the ORNL reactor using the apparatus described in ORNL-919, p. 227. Type 347 stainless steel specimens stressed to a maximum fiber stress of approximately

1700 psi at 1500°F were employed in all experiments. For a specimen with an out-of-pile creep history of about 40 hr data taken over a period of about 200 hr in the X reactor indicate that the amount of creep strain is reduced by bombardment. Creep of a virgin specimen under irradiation is characterized by an apparent dimunition of so-called "primary creep."

Figure 4.3 is the plot of the data from a test of a specimen with no previous creep history. The specimen was brought to test conditions upon insertion in the pile during a normal shutdown. A small discontinuity appearing in the curve a few hours from the origin corresponds to the time of pile start-up. This is disucssed elsewhere in this report. After some 24 hr of operation the curve becomes a straight line well within the accuracy of the strain measurements except for some slight departures occurring during short pile shutdowns when the temperature of the measuring apparatus (but not of the test specimen) departed from the control value. This in itself is rather exceptional since bench runs under similar conditions show that the creep rate is still diminishing after some 300 hr of testing. The arrow at the upper portion of the curve indicates the start-up of the pile after a 12-hr shutdown. During the shutdown the creep rate was observed to be about 3% higher than during the previous 100 hr under neutron bombardment. A few hours after the pile start-up, indicated by the arrow, the creep rate, which had started upward, leveled out at the rate for the previous 100 hr under bombardment. Thus the transient portion of the creep appears to diminish under irradiation, and, following an extended shutdown during which a slight increase in rate is observed, an upward inflection is noted followed by a resumption of the earlier rate under irradiation. Because of the difficulty of obtaining reproducible results from different specimens the constant rate established cannot be compared quantitatively with bench data.

Figure 4.4 shows the results of a test conducted on the bench for 40 hr prior to bombardment. The in-pile curve (of which only the first 40-hr portion is shown) is displaced slightly on the time axis to prevent overlapping. The starting time of the pile is indicated by the lower arrow. More correctly, the break in the curve at this point should be shown as an abrupt increase in strain rather than being smoothed. After some 12 hr of creep, 8 of them under irradiation, the creep rate is about 10% less than the

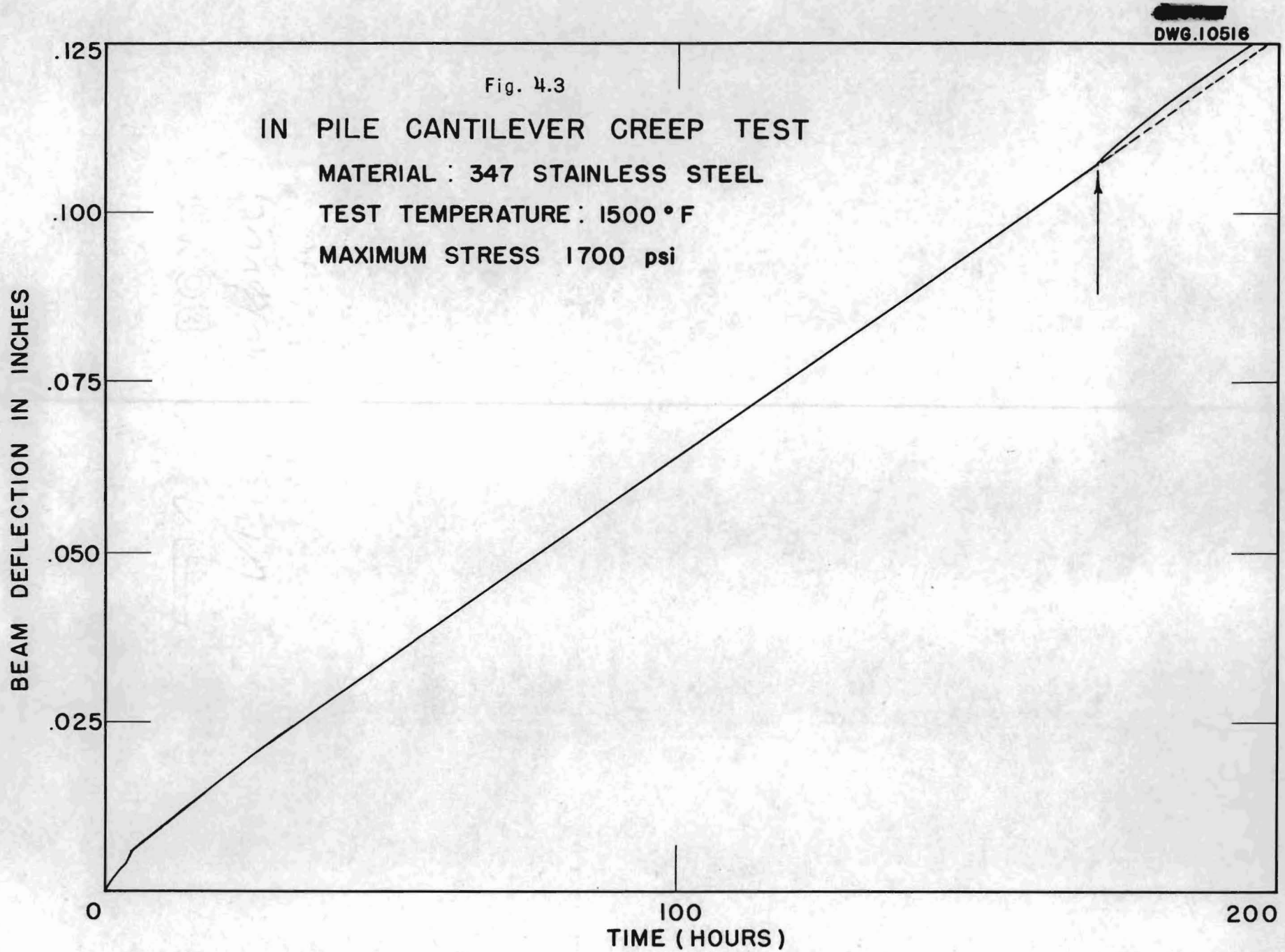
DWG.10516
Fig. 4.3
IN PILE CANTILEVER CREEP TEST
MATERIAL : 347 STAINLESS STEEL
TEST TEMPERATURE : 1500 °F
MAXIMUM STRESS 1700 psi
BEAM DEFLECTION IN INCHES
.125
.100
.075
.050
.025
0
100
200
TIME (HOURS)

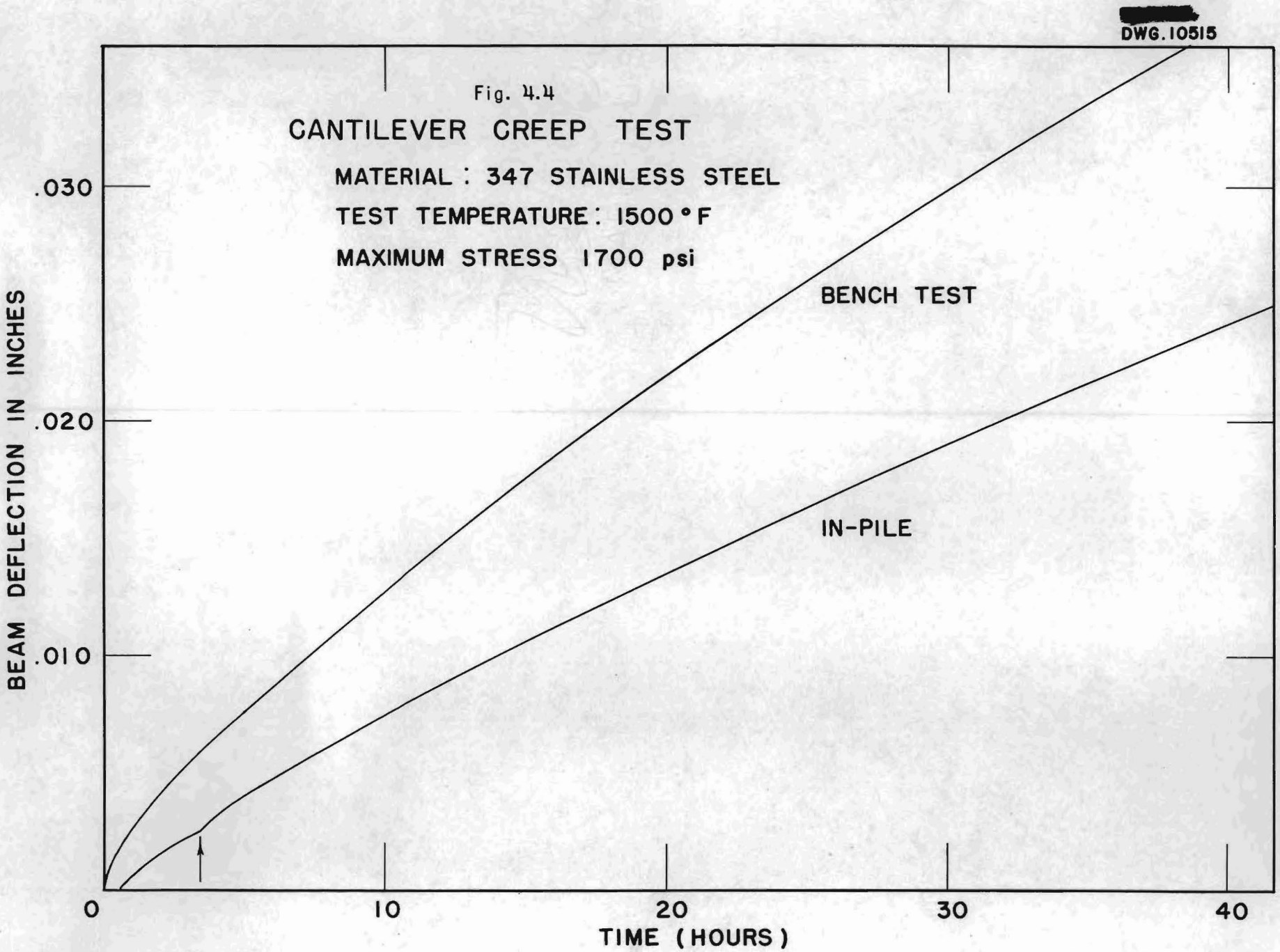
[redacted]
DWG. 10515
CANTILEVER CREEP TEST
MATERIAL : 347 STAINLESS STEEL
TEST TEMPERATURE: 1500 °F
MAXIMUM STRESS 1700 psi
BENCH TEST
IN-PILE
BEAM DEFLECTION IN INCHES
.030
.020
.010
0
10
20
30
40
TIME (HOURS)

Fig. 4.4

terminal rate in the bench test. The effect of such an interruption of the test as occurred above was studied in a similar specimen on the bench by following the same cycle of creeping, cooling, and reheating; here the creep rate 12 hr after the interruption had decreased just to the value before interruption. Qualitatively, the reduction in creep rate with respect to time appeared greater under irradiation than on the bench.

The abrupt increases in strain observed upon inception of bombardment in the accompanying plots have occurred on many occasions. Frequently a negative discontinuity has also been noted when the pile was shut down. In an effort to ascertain whether instrumental disturbances were responsible for part or all of these transients, a microformer with a locked core was placed in a temperature-controlled oven in the pile. The reactor was then operated at a series of power levels up to 3500 kw (corresponding to a fast flux of about 4×10^{10}) in 500-kw steps, between which the power was reduced to zero. The output voltage of the microformer was observed to be flux-dependent in a nonlinear manner; at somewhat less than maximum flux the voltage change appeared to reach a saturation value corresponding to that which would result from a core movement of about 0.0002 in. Although the leakage resistance of the in-pile leads is dependent on pile power and cooling air conditions, the change is not great enough to account for the phenomena observed. The possibility of intrawinding leakage is now being investigated, as are the leakage characteristics of several types of wires for in-pile service.

An experiment is being undertaken to determine if neutron bombardment affects either length or magnetic permeability sufficiently to account for the anomalous microformer noted above. Dead-weight-loaded creep tests at approximately the temperature of the LITR will also be undertaken. Type SR-4 bonded strain gages will be used for extension measurements. These appear to be fairly stable for short exposures in the ORNL reactor (see ORNL-865, p. 98).

Stress-corrosion apparatus for observing creep while the specimen is in contact with static liquid metals or salts under irradiation is being built. In view of the rather alarming effects of sodium on the creep behavior of 347 stainless steel, reported in NEPA-1720, a number of tests will be run on hollow cantilever specimens containing the corroding fluid. This will permit

metallographic comparison of the effect of the fluid on regions of different stress (both tensile and compressive) which will be present in such a specimen, and thus should lead to early establishment of a relation between stress and attack.

Metallographic examination of a specimen after 300 hr of cantilever creep on the bench at 1500°F and a maximum stress of 1600 psi revealed a small amount of an intergranular precipitate as yet unidentified. Attempts are being made to determine whether its formation is stress-dependent, and specimens are being subjected to prolonged heating to produce enough of the phase for identification.

Possible means of incorporating a creep test in the circulating-sodium loop in the LITR and the MTR are being studied. Two types of high-speed proportioning controller with rate action have been received for use in the temperature-control circuits of such an apparatus. An investigation is being made of types of strain-measuring devices whose characteristics are such as to permit their use in high gamma and neutron fluxes, where nuclear heating is of great importance. A miniature microformer weighing less than 5 g is being tested, and unbonded type wire-resistance strain gages have been ordered for trial.

RADIATION EFFECTS IN SUPERSATURATED SOLID SOLUTIONS

W. E. Taylor G. T. Murray
F. M. Blacksher

X-Ray Investigations. Previous investigations[4,5] of the effect of radiation on supersaturated solid solutions suggest two explanations, (1) localized distortion due to atom displacements and (2) pre-precipitation due to thermal spikes. Data are presented in this report to support the pre-precipitation hypothesis. The work has been concerned primarily with the copper-beryllium system. In an effort to check the hypothesis that radiation induces a nucleated condition in a solution-annealed alloy, X-ray line-broadening measurements have been made employing the Geiger counter spectrometer method of recording the diffracted beam. It was found that the line broadened

(4) D. S. Billington and S. Siegel, *Effect of Nuclear Reactor Radiation on Metals*, AECD-2810 (decl. Mar. 22, 1950).

(5) W. E. Taylor, G. T. Murray, and F. M. Blacksher, "Effect of Radiation on Pure Metals and Simple Solid-Solution Alloys," ORNL-1025, *op. cit.*, p. 41.

considerably with a shift of the peak toward larger values of Bragg angle, θ. This indicates a contraction of the lattice, i.e., a smaller a_0, which would occur if the amount of beryllium in solution were increased. The shape of the (331) line before and after an exposure of 6.31×10^{18} nvt is shown in Fig. 4.5. In Fig. 4.6 the change in the diffraction angle is plotted as a function of the integrated flux. Since these specimens contained beryllium in excess of that for complete solid solution, a small amount of beta phase was detected in the solution-annealed alloys. These experiments are being repeated using complete solid-solution specimens in order to exclude the excess beryllium as a variable.

Gunier-Preston zones due to thermal aging have been identified in copper-beryllium alloys.[6] Single crystal specimens of 0.005 in. thickness were irradiated to determine whether these zones were induced by irradiation. There was no evidence of streaks on the Laue photographs of such specimens after an exposure of 2.44×10^{18} nvt. This is being repeated using longer neutron exposure times.

Metallographic Investigation. Single-crystal specimens are being aged after irradiation to determine the effect of radiation on the subsequent rate of precipitation. Comparison of metallographic samples with resistance changes indicated that the rate is affected only in the submicroscopic stage of the subsequent aging process.

Comparison of Thermal Aging with "Irradiation Aging." Previously reported data[7] on the change of resistance during irradiation indicates the possibility of a low-temperature aging effect. This experiment has been repeated, giving attention to the early stages of the process as shown in Fig. 4.7. The comparison of the change in resistance during irradiation with that of thermal aging is shown in Fig. 4.8. The variation of the thermal aging curves with temperature suggests the possibility that the effect is similar to thermal aging at approximately 75°C. This could be considered as an increase of precipitation rate due to irradiation, since the temperature during irradiation is approximately 25°C. Apparatus is now being bench-tested which will permit measurements to be made of the precipitation rate at higher temperatures during irradiation. In addition, a nonirradiated specimen is being aged at 75°C.

(6) A. G. Guy, C. S. Barret, and R. F. Mehl, "Mechanism of Precipitation in Alloys of Beryllium in Copper," *Am. Inst. Mining. Met. Engrs.*, 175, 216 (1948).

(7) "Effect of Neutron Irradiation on Copper Alloys," *Metallurgy Division Quarterly Progress Report for Period Ending July 31, 1950*, ORNL-827, p. 72 (Dec. 4, 1950).

UNCLASSIFIED
DWG. 10498

Fig. 4.5

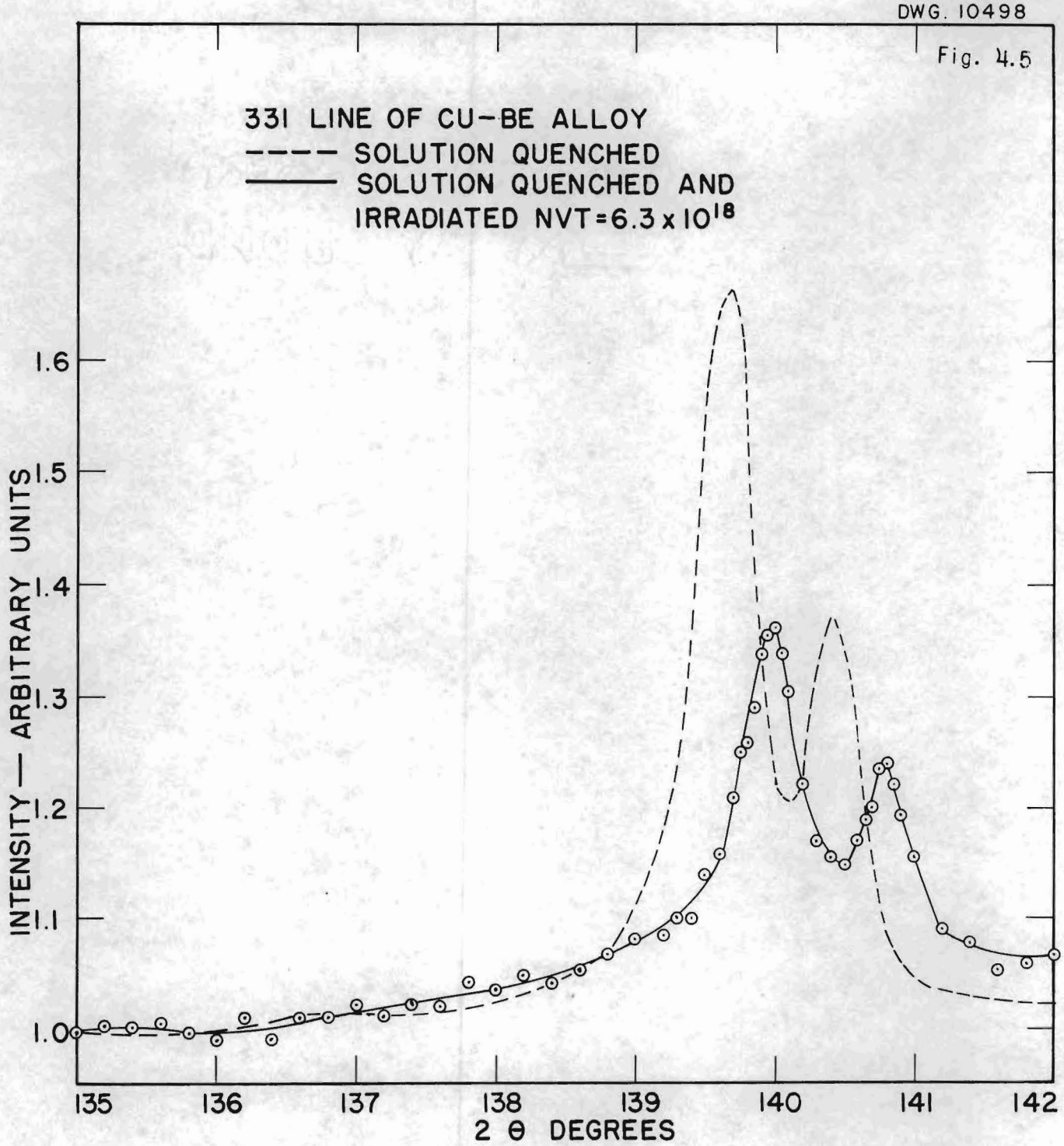

PSI-A-156

UNCLASSIFIED
DWG. 10500

Fig. 4.6

SHIFT OF 331 LINE OF CU-BE
DUE TO IRRADIATION.

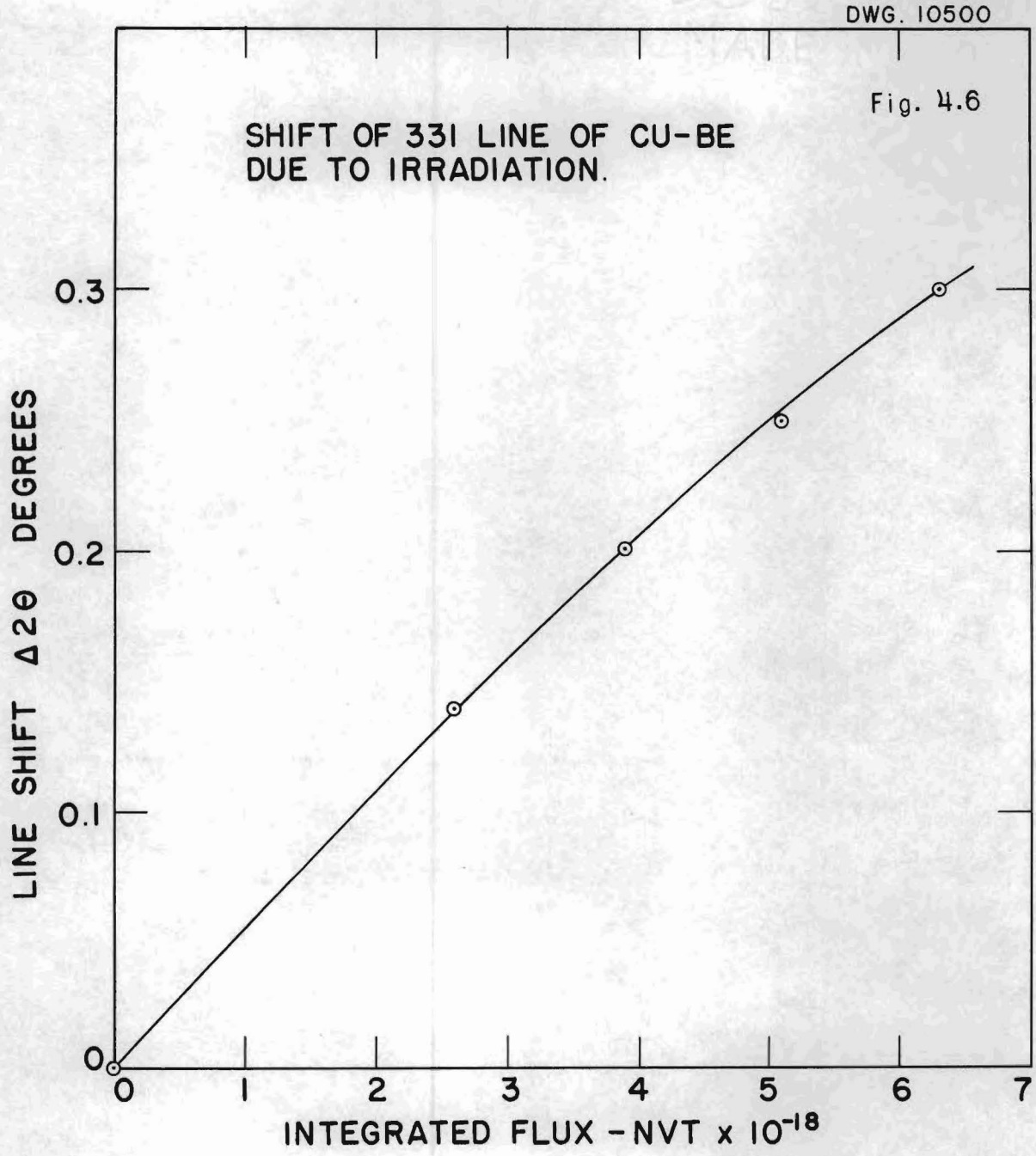

PSI-A-157

UNCLASSIFIED
DWG. 10839

Fig. 4.7

EARLY STAGES OF RESISTANCE CHANGE OF SOLUTION QUENCHED CU-BE DURING EXPOSURE TO REACTOR RADIATIONS

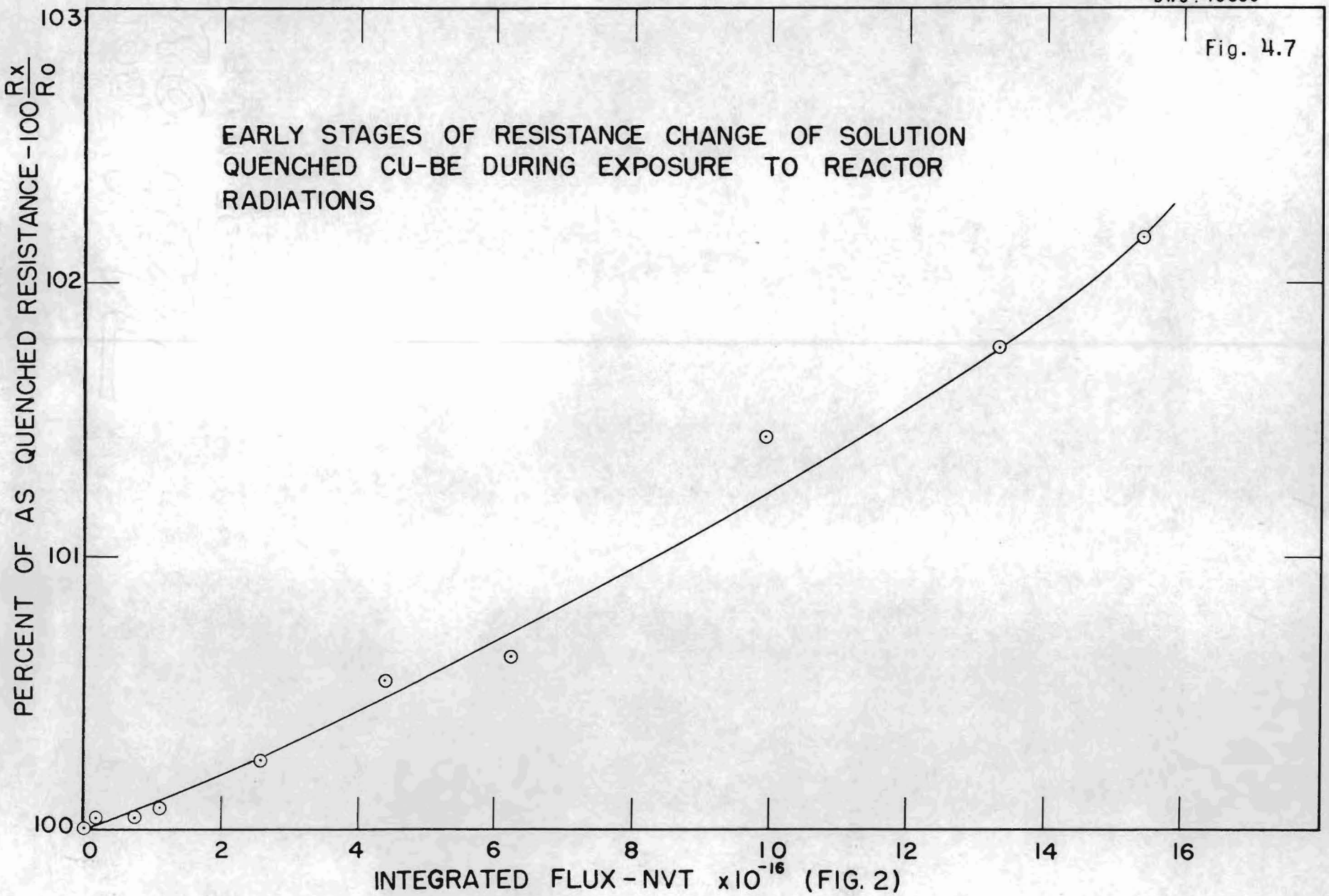

DWG.-10499

Fig. 4.8

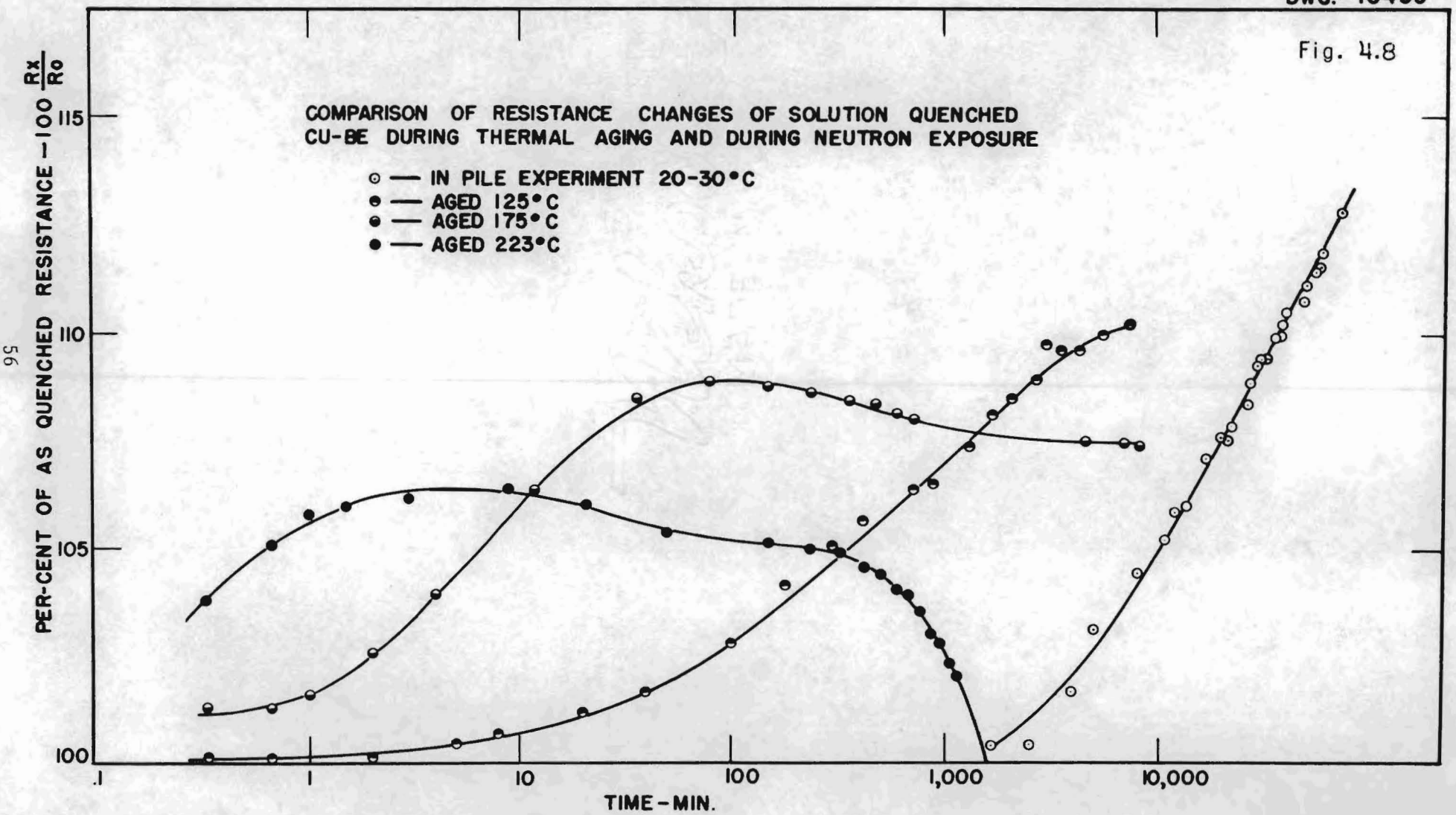

NOT CLASSIFIED

PSI-A-125

Billington and Siegel report[4] that essentially all the changes in resistance and hardness induced by irradiation in copper-beryllium alloys are removed after 30 sec in a 660°F (349°C) salt bath. This supported the hypothesis of localized distortion rather than a precipitation induced by neutron bombardment. However, aging of a solution-annealed resistance specimen for 122 hr in a 125°C bath produced a resistance increase of 10.2%. This is the same order of magnitude as that produced during exposures of 2×10^{18} nvt. A 20-sec immersion at 325°C of the 125°C thermally aged specimen and the irradiation-aged specimen changed the resistance of both to within 1% of their solution-annealed value. On further aging at 325°C the irradiated specimen appeared to age at a more rapid rate than the one pre-aged at 125°C. This will be checked using single-crystal specimens since the grain boundary effect hampers comparison of thermal- and irradiation-aging phenomena. The possibility of redissolving of nuclei also must be considered here.

Billington and Siegel reported[4] that irradiation of copper-beryllium specimens which were cold-worked from the solution-annealed state led to a smaller increase in resistance than in specimens that were only solution-annealed. It has been generally accepted that cold-working accelerates the subsequent aging process. The use of resistance measurements as a measure of aging may lead to confusion. It was found that on aging at low temperatures the resistance of the solution-annealed specimen increased considerably faster than the cold-worked solution-annealed specimen, as shown in Fig. 4.9. This can be explained on the basis that recovery of the work hardening acts in opposition to the resistance increase due to aging to give a net effect much smaller than if no work hardening were introduced. It is supposed that similar behavior would be found if hardness were used as a measure of the aging process, although this has not been verified.

The results of these experiments support the hypothesis that the effect of radiation on copper-beryllium is similar to that of low-temperature thermal aging. The increase in hardness of pure copper under irradiation indicates that other mechanisms will be present, but will not be detected in resistance measurements. When thermally aged samples are compared with irradiation-aged samples the grain boundary effect must be considered. During thermal aging the effect of the precipitation at the grain boundary is predominant in the early stages whereas the irradiation effects are concerned with the interior

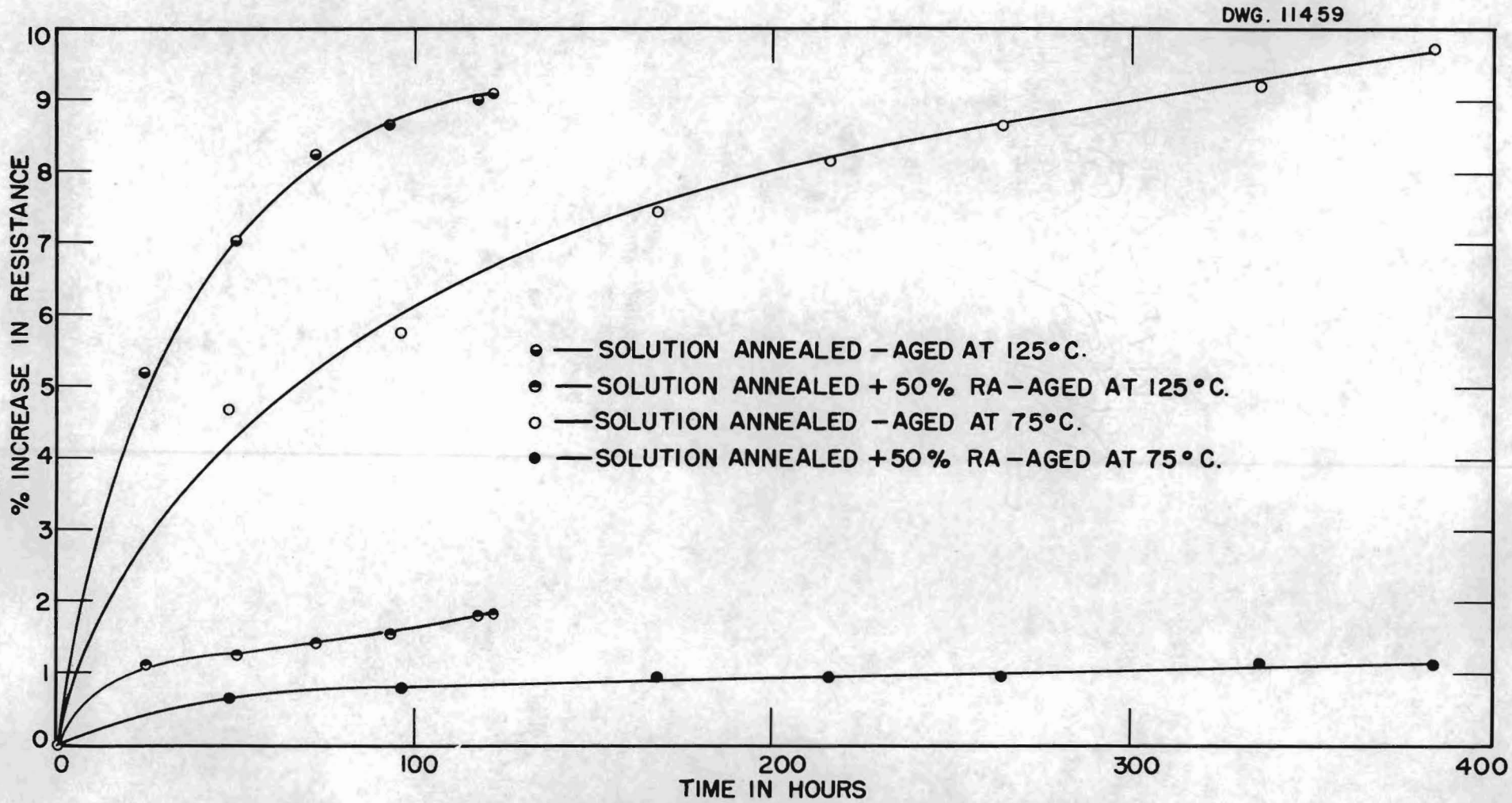

EFFECT OF PRIOR COLD WORK ON THE CHANGE OF RESISTANCE DURING AGING

Fig. 4.9

NOT CLASSIFIED

PSI-A-119

of the grains in addition to the grain-boundary effect. Single-crystal resistance specimens will be grown to exclude the effect of the grain-boundary precipitate on subsequent aging and irradiation aging.

Effects of Dissolved Beryllium. Billington and Siegel concluded[4] that the more beryllium there is in solution, the greater will be the effect of irradiation. This was verified by holding specimens at various temperatures until they reached equilibrium, as indicated by resistance measurements. Specimens quenched from higher temperatures contained more beryllium in solid solution than those quenched from lower temperatures. The specimens were then exposed to an integrated flux of 2.29×10^{18} nvt in the ORNL reactor. The results are summarized in Table 4.2.

TABLE 4.2

Effect of Overaging at Various Temperatures on Radiation-Induced Resistance Changes in Copper-Beryllium

TEMPERATURE OF SOLUTION-ANNEAL (°C)	INCREASE IN RESISTANCE DUE TO EXPOSURE OF 2.29×10^{18} nvt (%)
300	1.5
400	1.3
550	9.8
650	12.2
800	11.0

Although the higher increase for the 300°C anneal over the 400°C anneal was reproducible, it is difficult to explain. The greater increase of the 650°C specimen over the 800°C also was reproducible and may be due to the presence of the beta phase. Quenching from above the beta-alpha transformation temperature (600°C) results in all the beryllium being in a metastable phase. The effect of irradiation on the metastable beta phase may be greater than that on the metastable alpha phase since the 650°C quenched specimen contained approximately 20% beta whereas the 800°C quenched specimen contained less than 5% beta.

Investigations of Other Age-Hardenable Alloys. These investigations have been extended to other age-hardenable alloys. No significant changes in hardness or resistance of aluminum-silicon alloy specimens containing approximately 2% silicon were noted after exposures of 2.47×10^{18} and 4.84×10^{18} nvt. These alloys were irradiated in the solution-quenched condition. A possible explanation of these results can be based on the fact that the energy of a knocked-on atom in aluminum is dissipated primarily by the process of ionization rather than by interaction with the lattice ions.

A copper-titanium alloy containing 2.50 wt % titanium has been exposed in the solution-quenched condition to an integrated flux of 2.28×10^{18} nvt. The resistance increased 0.55%, which is comparable to that of simple solid-solution alloys of copper which have been irradiated. The hardness increase of 17.7 DPH is also of the same order of magnitude as that experienced in pure copper and simple solid-solution copper alloys. This has raised the possibility that the irradiation effect may be characteristic of the solute element, i.e., beryllium. However, we have been unable to obtain a low-temperature aging effect thermally in copper-titanium similar to that in copper-beryllium. A silver-copper age-hardening alloy has been fabricated, and a nickel-beryllium alloy will be made to investigate both of these possibilities.

Samples of microscope-slide glass were irradiated to an integrated flux of 1×10^{19} nvt in order to determine whether the unstable amorphous structure would crystallize. No evidence of crystallization was found using the Philips recording X-ray spectrometer.

5. ENGINEERING PROPERTIES

LITHIUM-IRON CYCLOTRON BOMBARDMENT

North American Aviation, Inc., W. W. Parkinson

In connection with the design of compact mobile nuclear reactors, information is needed about the behavior of structural materials in contact with the liquid-metal coolants which might be used. Owing to its low density and its favorable thermal properties, lithium is interesting as a possible coolant, and the resistance of iron to attack by lithium and its ease of fabrication make iron important as a structural material. To study the iron-lithium system under conditions similar to those prevailing in a reactor, an experiment is being conducted in which iron in contact with molten lithium is irradiated in the direct alpha beam of the Berkeley 60-in. cyclotron.

Capsules shown in Fig. 5.1 and 5.2 were machined out of iron stock, Globe iron, supplied by the Globe Steel Tubes Co. The circular faces of the capsules were used as the iron specimens and were made to a thickness equal to or just smaller than the range of the alpha particles from the cyclotron. These disks were annealed, polished, and given a "nital" etch. Hardness measurements were made with a Tukon machine and Knoop indenter over a pattern covering both the area to be irradiated and an unirradiated area, and photomicrographs were made of both these areas. The capsules were assembled by heliarc-welding the disks to the flange at the end of the capsule, with the polished and tested surface of the disks inward, so that the disk would be in contact with the lithium charge. The capsules were filled in an argon-atmosphere glove box with slugs bored from lumps of lithium of the low-sodium grade supplied by the Metalloy Corp.

Continued difficulties were encountered in the development of a heater durable enough to heat the capsule above 900°C and withstand the force of interaction with the cyclotron magnetic field. To reduce the probability of heater failure a bombardment was carried out at a temperature of 625°C at the irradiated zone. The capsule was mounted on the cyclotron as shown in Fig. 5.3 in the target box described in the previous quarterly report (ORNL-1025, p. 21) to provide temperature control and inert atmosphere. A thermocouple of 0.005-in. Chromel-Alumel was spot-welded on the face of the capsule in the

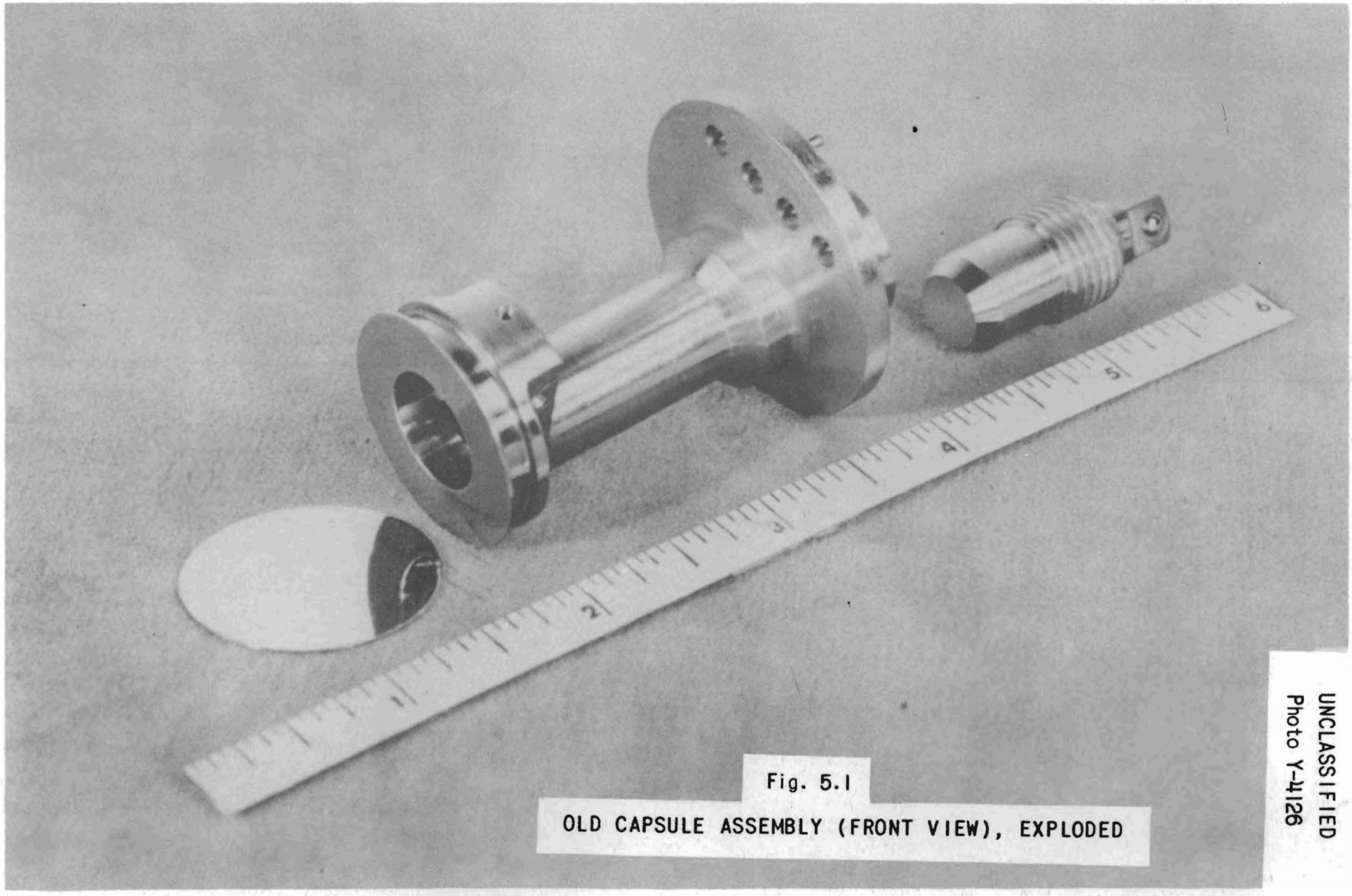

Fig. 5.1

OLD CAPSULE ASSEMBLY (FRONT VIEW), EXPLODED

UNCLASSIFIED
Photo Y-4126

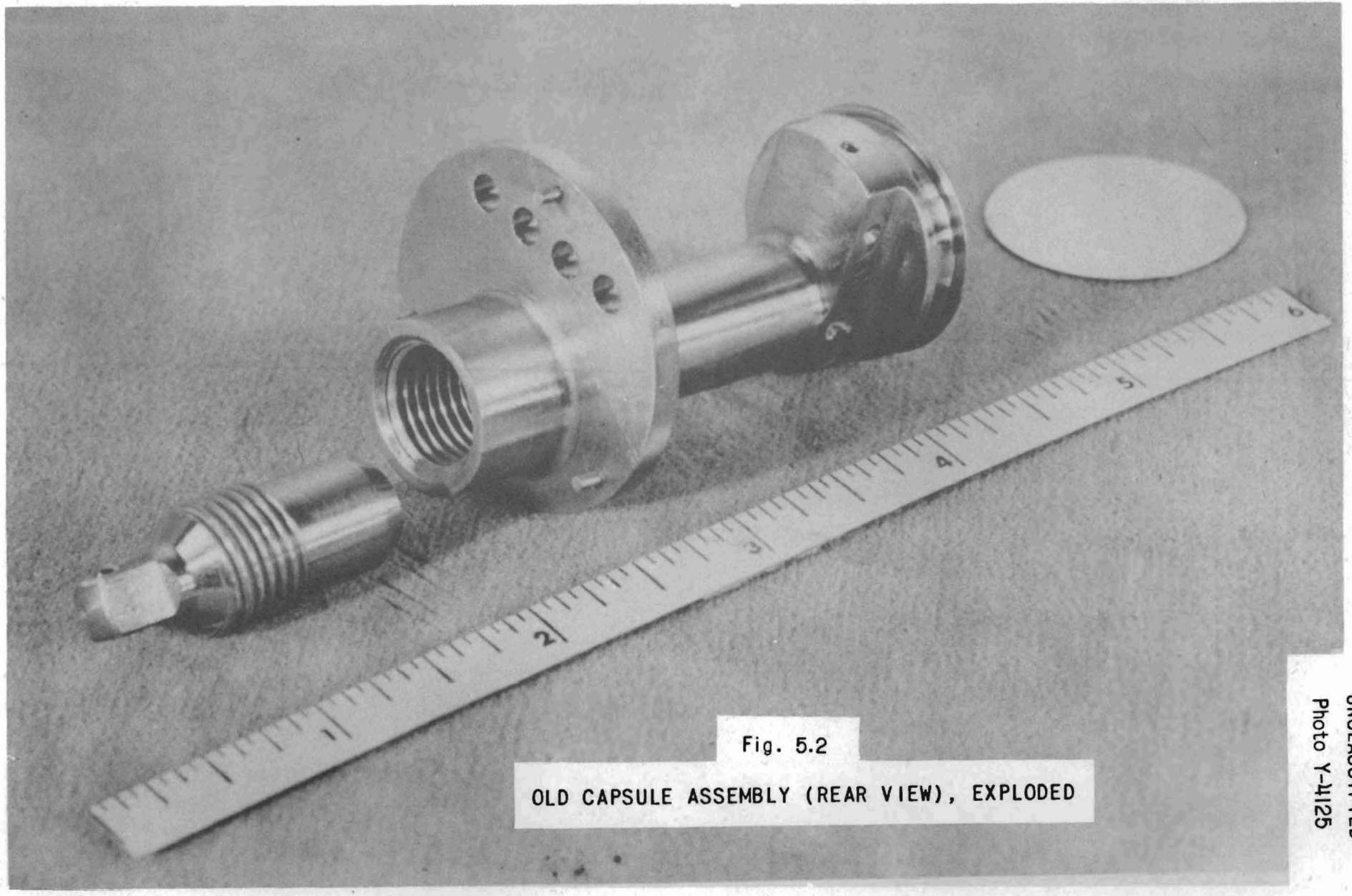

Fig. 5.2

OLD CAPSULE ASSEMBLY (REAR VIEW), EXPLODED

UNCLASSIFIED
Photo Y-4125

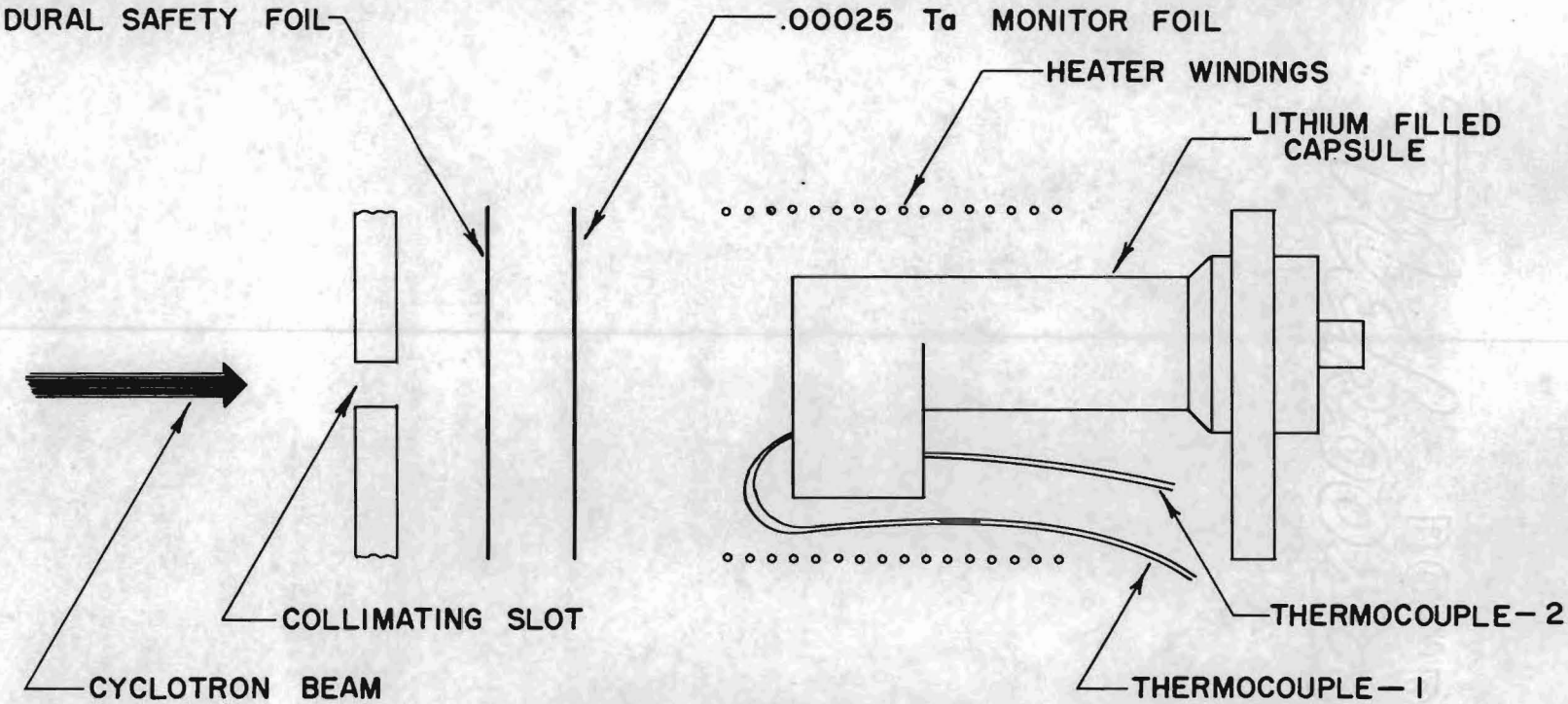

Fig. 5.3

NOT CLASSIFIED

OAK RIDGE NATIONAL LABORATORY — Physics of Solids Institute				
ARRANGEMENT OF CAPSULE AND ASSOCIATED EQUIPMENT				PSI-A-116
DRAWN BY: W.E.B.	FOR: W.W. PARKINSON	DATE: 5-10-51	SCALE:	DWG. 11218

irradiated area to record temperature during irradiation and to control the power to the target-box heater in conjunction with an electronic power regulator. A second thermocouple was clamped in a well at the rear of the bombarded chamber on the end of the capsule. This thermocouple recorded the temperature of this massive chamber.

The capsule was bombarded with 36.6 ± 0.6 Mev alphas for 9 hr for a total exposure of 25.5 μa-hr over an area 0.608 by 0.250 in. or 0.98 sq cm. During the irradiation the temperature at the irradiated zone was 625°C, dropping occasionally for short periods (up to 3 min) to 25°C below this and rising 10°C above this for shorter periods. At the rear of the chamber the temperature was 650°C, varying ±25°C for short periods. At the cool end of the stem of the capsule which was partially filled with lithium the temperature was 400 to 430°C, as shown by a previous trial heating. The activity of the face of the capsule 1½ hr after completion of irradiation was 0.6 r/hr as shown by a survey type instrument. A comparison of the exposure to irradiation with neutrons may be made by the estimate[1] that 1 μa-hr of 33-Mev alpha particles $\equiv 6 \times 10^{18}$ neutrons $\equiv$ 160 hr in the Hanford reactor. The data from the experiment in which the capsule was irradiated at 625°C are given in the following outline.

1. *Analysis of iron before irradiation.* All the elements were determined spectrographically except carbon, manganese, sulfur, and phosphorus, which were determined chemically. The following amounts were found:

Cu	Low	Cr	Trace	C	0.03%
Co	0	Ni	Trace	Mn	0.23%
Nb	0	Mo	Trace	S	0.02%
Ti	0	V	0	P	0.01%
Be	0				

2. *Chemical analysis of lithium.* The charge was dissolved in absolute ethyl alcohol, and the Li_2O was filtered off; Li_3N was determined by Kjeldahl analysis, and iron and manganese were determined colorimetrically. Analysis of a slug, cut in the glove box to simulate conditions of filling a capsule, gave the following values:

Li_3N	0.3%	Li_2O	<0.1%

(1) A. B. Martin, M. Tarpinian, and R. R. Eggleston, *The Effect of Cyclotron Irradiation on the Physical Properties of Metals*, North American Aviation report NAA-SR-75 (Jan. 8, 1951).

Analysis of the lithium from a capsule irradiated at 625°C gave the following values:

Li_3N	5.3%	Fe	0.008%
Li_2O	3.2%	Mn	None

It should be noted that solution of the lithium charge in the capsule was carried out by immersing the entire capsule in hot alcohol and required a period of three days. Although this treatment was carried out in an argon-filled glove box, the atmosphere was not completely inert, and the nitrogen and oxygen might have been introduced during this process rather than before or during irradiation. The significance of the iron found is also uncertain since it represents only 0.0001 g in the lithium charge and might have flaked off the outside of the capsule during immersion in the alcohol, or this much iron may have been present in the lithium charge before it was inserted in the capsule. This possibility will be investigated by analysis of the batch of lithium from which the charge came.

3. *Radioactivity of capsule face and of alcohol-insoluble residue from lithium charge.* A Tracerlab model SU-1A instrument was used to determine the radioactivity of the capsule face, and 90 mr/hr of β-γ activity was found 29 days after irradiation; the activity of the alcohol-insoluble residue was not appreciably more than background after the same period.

4. *X-ray-diffraction measurements.* The following values of the lattice parameter were found:

Before irradiation	2.8605 K-X units
After irradiation	2.8605 K-X units

Line width of the (211) line with Cr $K\alpha_1$ radiation:

Before irradiation, half-width	0.3°
After irradiation, irradiated zone	0.5°
After irradiation, unirradiated zone	1°

The specimen disk was seen to be bent slightly when it was removed from the capsule. The curvature required to broaden the half-width of the line from 0.3 to 0.5° was calculated to be 0.0016 in. in 1 in. It was felt that the specimen was deformed to this extent and that this was responsible for the line broadening. The even greater broadening in the unirradiated zone where deformation was more severe supports this conclusion.

5. *Photomicrographs of the inner surface of the specimen disk.* The following illustrations show the results of the irradiation: Fig. 5.4, unirradiated zone, before irradiation, after being annealed and nital-etched for 2 sec; Fig. 5.5, zone to be irradiated, before irradiation, after being annealed and nital-etched for 2 sec; Fig. 5.6, unirradiated zone, after irradiation, no additional etching or hardness denting done after bombardment; Fig. 5.7, irradiated zone after irradiation, no additional etching or harness denting done after bombardment.

The only result of the bombardment of iron and lithium at 625°C observed so far is an increase in grain size of the iron in the irradiated area. There cannot have been much iron dissolved by the lithium, as indicated by chemical analysis, by the lack of radioactivity in the residue after solution of the lithium, and by the sharpness of the original hardness dents in the post-irradiation photomicrographs.

An attempt was made to irradiate a capsule at 910°C after the substitution in the heater of a winding of tantalum wire of larger diameter and closer spacing to improve the performance of the heaters. For the first 2 hr of this irradiation the temperature at the irradiated zone of the face was 906°C, varying +6 and -36°C momentarily but dropping to about 840°C when the beam was off for an extended period. The rear of the bombarded chamber ran at 950°C varying +6 and -40°C during this time. At the end of 2 hr the thermocouple on the face of the capsule pulled loose, and the power to the heater was controlled by the temperature at the rear of the chamber. The controller was adjusted to make this temperature 910°C to prevent melting of the thin capsule face in the event of a sudden large increase in cyclotron beam. Under these conditions the temperature of the irradiated zone was 850 to 900°C. At the end of 7 hr of bombardment, when the capsule had received 13.6 μa-hr of alpha particles, the heater failed, rupturing the safety window in the front plate of the target box to stop the run. When the target box was disassembled the face of the capsule was found to have a small leak, probably where the thermocouple was spot-welded, and it is uncertain whether this capsule can provide useful data.

A third irradiation was carried out at 700°C, but the beam intensity of the cyclotron was abnormally low. After 20 hr of bombardment the specimen had received only 3.8 μa-hr, too small an exposure to compare with a reasonable period in a reactor.

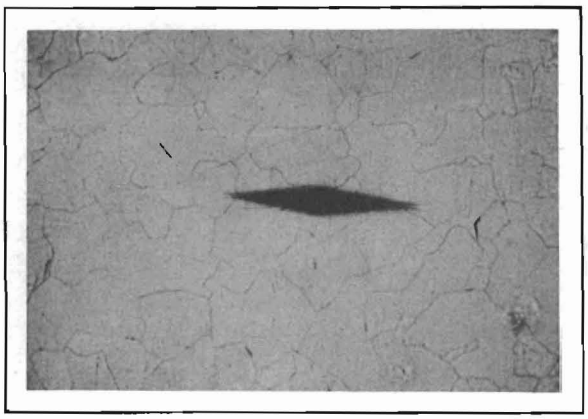

GLOBEIRON MAG. 250 X

UNIRRADIATED ZONE: BEFORE IRRADIATION, ANNEALED 20 MINUTES AT 870°C NITAL ETCH BEFORE DENTING FOR HARDNESS

Fig. 5.4

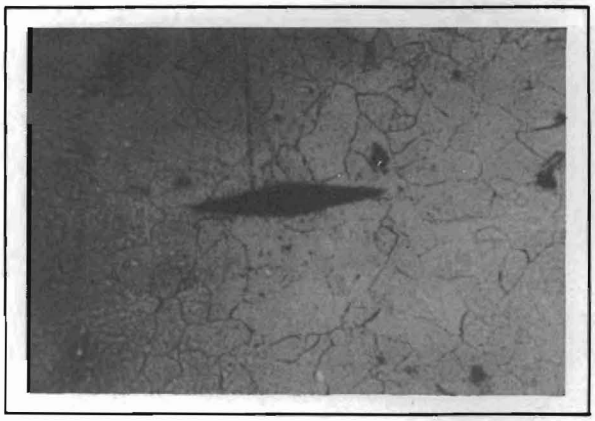

GLOBEIRON MAG. 250 X

ZONE TO BE IRRADIATED:
BEFORE IRRADIATION, IDENTICAL TREATMENT AS UNIRRADIATED ZONE AT LEFT.

Fig. 5.5

NOTE: MAGNIFICATIONS GIVEN ARE THOSE AT WHICH PHOTOGRAPHS WERE TAKEN. REDUCED APPROXIMATELY ONE-HALF IN REPRODUCTION.

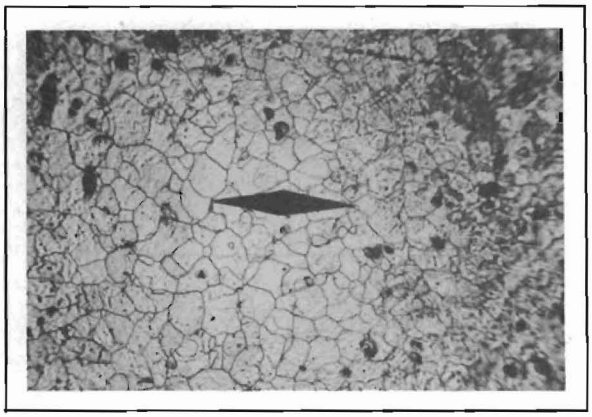

GLOBEIRON MAG. 150 X

UNIRRADIATED ZONE: AFTER IRRADIATION, ORIGINAL HARDNESS DENT, NO ETCH.

Fig. 5.6

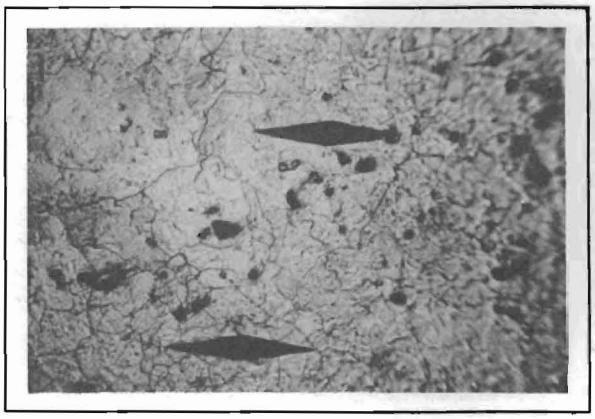

GLOBEIRON MAG. 150 X

IRRADIATED ZONE: AFTER IRRADIATION, ORIGINAL DENTS, NO ETCH.

Fig. 5.7

In order to conduct a bombardment at the conditions of interest for reactor design, both the heater and capsule are being redesigned to permit operation in a target box developed by the North American Aviation group at Berkeley. This box has given satisfactory operation with both metal and graphite samples at temperatures above 900°C. Figures 5.8 and 5.9 show these new capsules, exploded and assembled.

LIQUID-METAL LOOPS

C. D. Baumann R. M. Carroll
O. Sisman

Liquid metals are being considered as coolant and heat-transfer media for power reactors. Because little is known concerning the behavior of liquid metals at high temperatures under radiation, several problems of practical interest arise. Among these are the activity of the liquid-metal stream when outside the reactor, the radiation and corrosion damage to the container wall material, and the radiation effects on the liquid metal itself. In order to find answers to some of these problems, a loop for circulating liquid metals at elevated temperatures through the X-10 pile has been designed, built, and bench-tested and is currently being made ready for installation in the pile early in July.

The first loop will be run with lithium at 1000°F. It was designed primarily for the study of Bremsstrahlung activity and activity introduced into the liquid metal by corrosion and recoil atoms from the container tube. The loop was designed so that it could be used as the basis for development of other high-temperature liquid-metal in-pile experiments, such as creep and stress-corrosion studies.

In the development of the loop it was decided to use electromagnetic pumps and flowmeters since, having no moving parts, they eliminate packing, seal, and bearing problems. However, it was questionable whether an electromagnetic pump would pump liquid lithium (the first coolant to be tested) at high temperatures. The output of an electromagnetic pump depends upon the resistivity of the fluid being pumped. The meager data available on the resistivity of lithium at high temperatures indicate that the resistivity increases markedly with temperature and, in fact, could be so high that the pump would be inoperative or would lack the desired capacity.

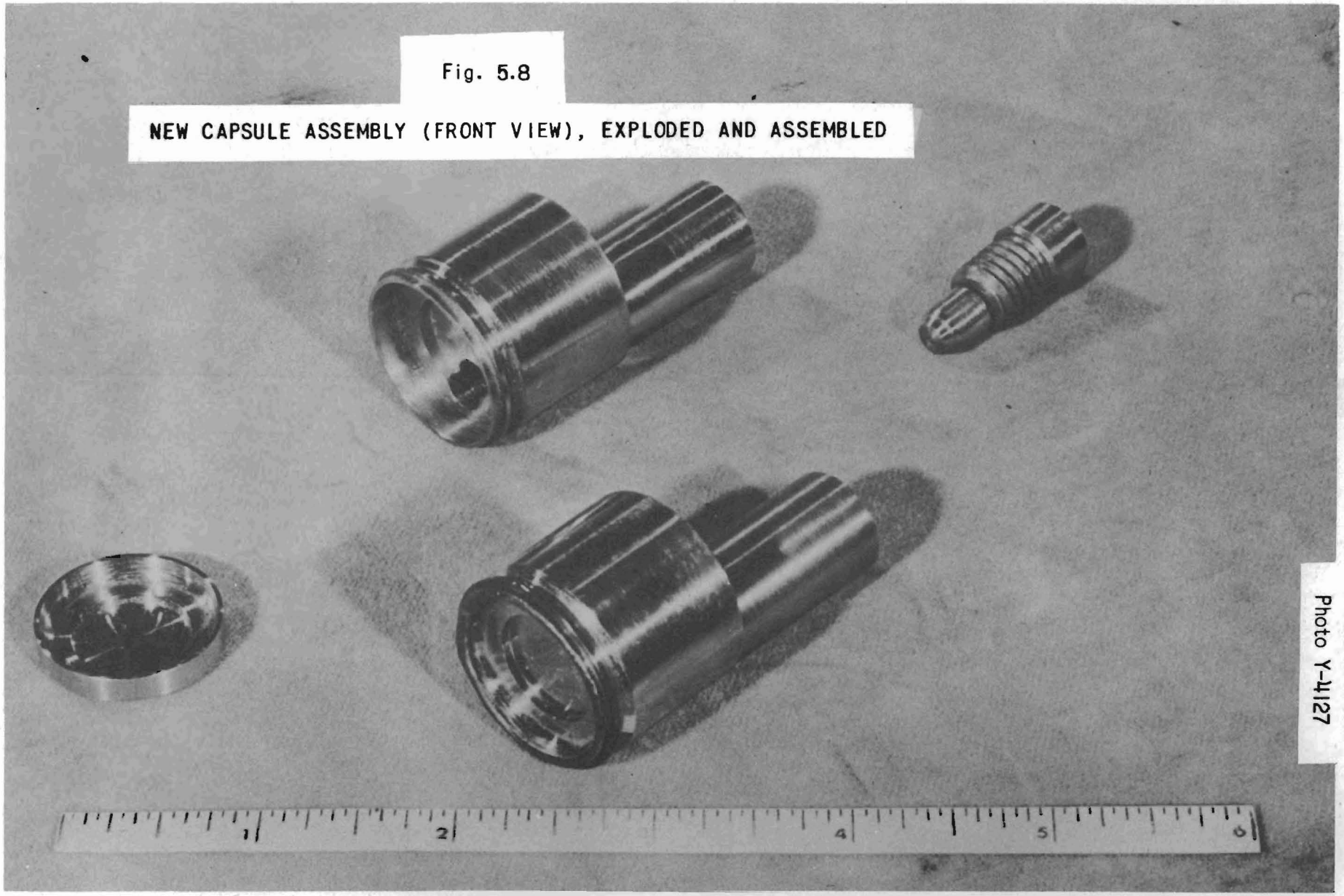

Fig. 5.8

NEW CAPSULE ASSEMBLY (FRONT VIEW), EXPLODED AND ASSEMBLED

UNCLASSIFIED
Photo Y-4127

Fig. 5.9

NEW CAPSULE ASSEMBLY (REAR VIEW), EXPLODED AND ASSEMBLED

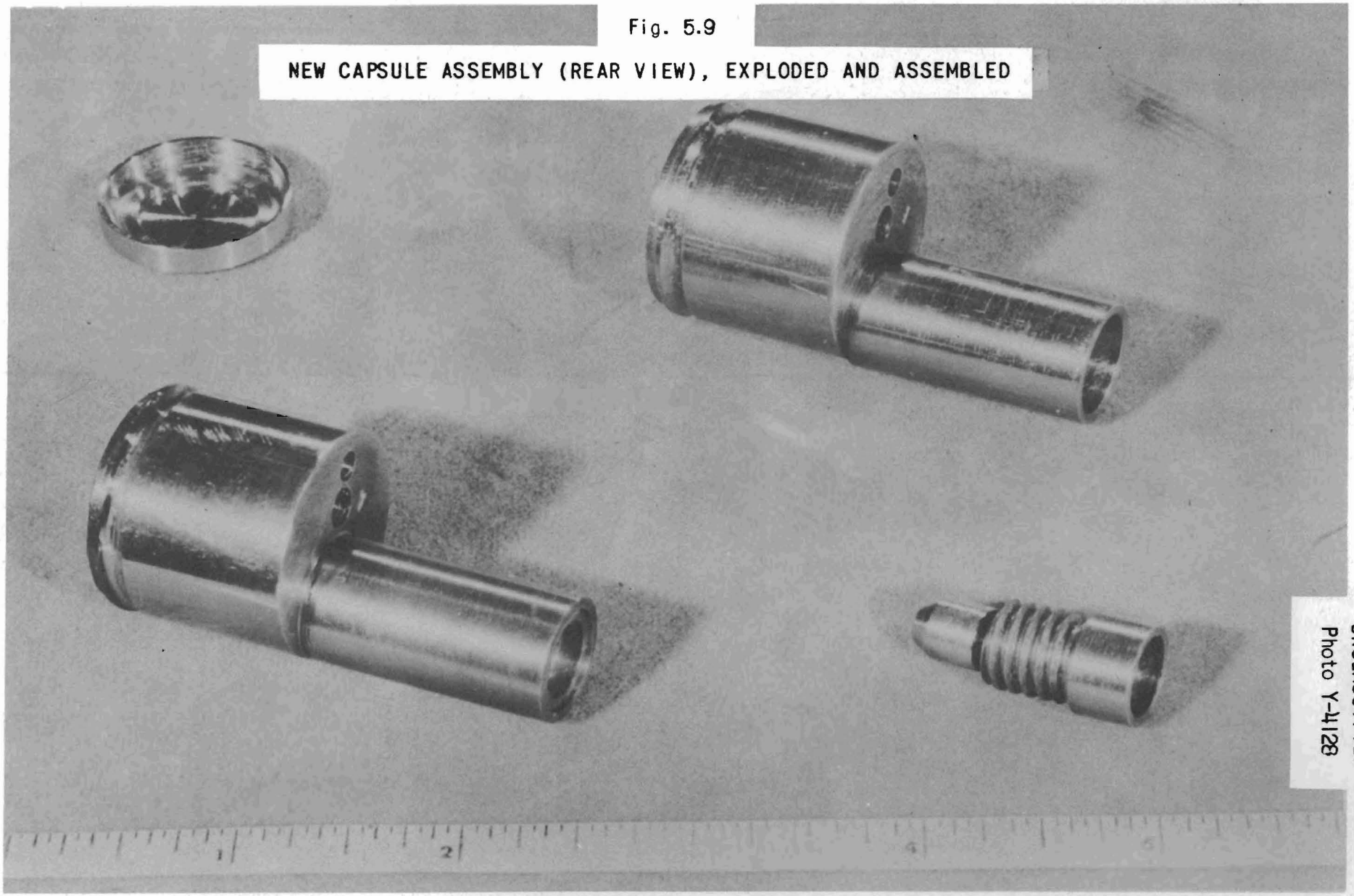

UNCLASSIFIED
Photo Y-4128

A prototype test loop (Fig. 5.10) for the calibration of an electromagnetic flowmeter and evaluation of electromagnetic pump performance with lithium at 1000°F was built. It consisted of a metal load tank in which degreased lithium was melted and filtered before being introduced to the system, a catch tank, a combination surge and measuring tank, several flowmetering stations of different sizes and configurations, the pump cell, a drop tank, and associated tubing, all made of 316 stainless steel. The system was operated for varying periods of time at elevated temperatures and for one continuous period of 170 hr at 1000°F. Both pump and flowmeter were found very satisfactory for the desired application. The velocity varied approximately linearly with the applied pump voltage. The emf generated by the flowmeter varied directly as the velocity, was relatively independent of temperature, was greater for small tubes than for larger tubes at constant mass flow, and was very sensitive to variations in flow. After the loop was dismantled, there were no visible signs of corrosion. A similar system was built for testing with sodium.

Using the results of the test loop, the design of the in-pile loop was completed and the loop was constructed, loaded, and tested with lithium at 1000°F. The apparatus (Fig. 5.11) consists of an external loop approximately 5 ft long, an internal loop approximately 18½ ft long, and a jacket assembly approximately 20 ft long. The external loop consists of a melt or load tank (removed from the system after loading was accomplished), a surge tank, a drop tank for collecting the liquid metal at the end of the run, an electromagnetic flowmeter, an electromagnetic pump, and associated tubing (5/16 in. o.d. and 3/16 in. i.d., 316 stainless steel). All parts are heated with calrod tubular heaters and insulated with 2 in. of magnesia.

The internal loop (3/8 in. o.d. and 1/4 in. i.d., 316 stainless steel tubing, 18½ ft long) is heated with calrod tubular heaters and surrounded by stainless steel radiation shields and mica insulation. The internal loop is positioned inside a 2-in. pipe mounted in the jacket assembly. The jacket assembly is a water-cooled 3¾-in.-square aluminum box enclosing the 2-in. pipe which contains the inner loop. Diatomaceous earth is packed in the space between the pipe and the jacket wall as a heat insulator.

During test operation of the loop it was found that the heat capacity of the system is such that once the system was up to temperature (i.e., 1000°F) the heat input to the external loop could be discontinued and the temperature

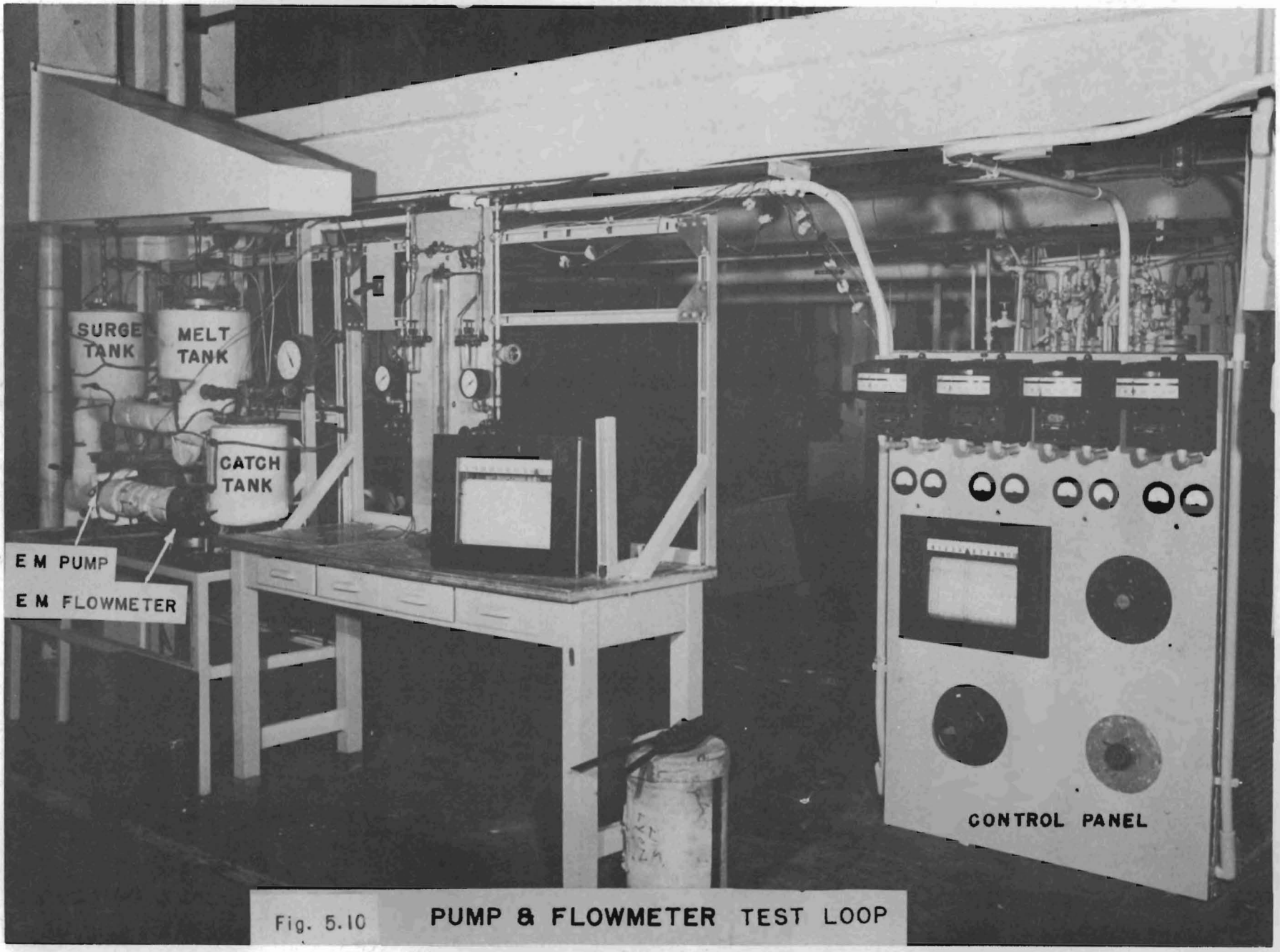

Fig. 5.10 PUMP & FLOWMETER TEST LOOP

PHOTO Y-62274

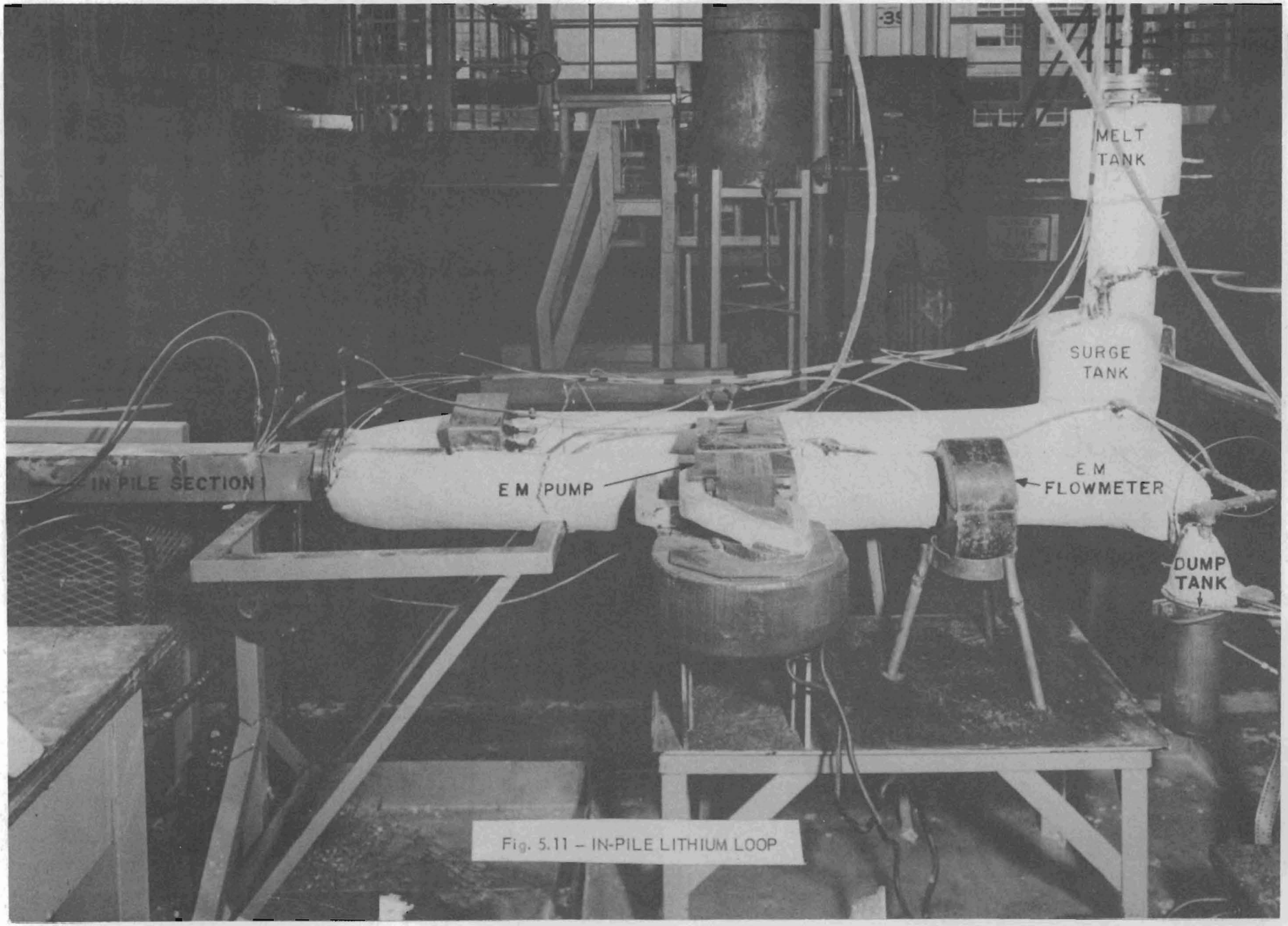

Fig. 5.11 – IN-PILE LITHIUM LOOP

PHOTO Y-10714

of the internal loop still maintained at 1000°F with very little additional heat input. The reverse situation also exists, i.e., the internal loop remains at approximately 750°F with no heat input while the external loop is maintained at 1000°F. Although the conditions of the test were not the same as will be met in the pile, results indicate that it should be possible to continue operations in the pile in the event of failure of either the external or the internal loop heaters. In fact, ambient conditions with the pile are more favorable than the test conditions because the graphite temperature is higher than normal air temperatures.

The desired liquid-lithium velocity of 3 ft/sec through the external loop was obtained at approximately one-sixteenth maximum pump power.

PHYSICAL PROPERTIES OF PLASTICS

O. Sisman C. D. Bopp
R. L. Towns W. K. Kirkland

Plastics. The physical properties of pile-irradiated plastics are described in ORNL-928.[2] Equipment is being built for similar studies with light particles (beta and gamma). Studies are being initiated to determine the effect of the presence of oxygen on the radiation damage to plastics and to determine the effect of aging subsequent to irradiation. It is planned also to irradiate some materials in cadmium-shielded containers to determine the damage contributed by thermal neutrons and to determine the effect of irradiation rate by subjecting some materials to a higher flux (LITR, or Hanford or Chalk River reactors).

Elastomers. Work on radiation damage to elastomers has just been begun. Very preliminary results are given in Tables 5.2 to 5.11. The data presented are for pile-irradiated elastomers of the compositions shown in Table 5.1. Measurements of the physical properties were made by standard ASTM methods.

A modification of the ASTM tensile test D 412 49 T[3] was employed. The tensile strength is the breaking load divided by the original cross-sectional area. The percent set at break is the percentage increase in the distance between gage marks measured by piecing together the halves of the broken specimen. The percent elongation is the percentage increase in the distance between gage marks that occurs before the specimen breaks.

(2) O. Sisman and C. D. Bopp, *Physical Properties of Irradiated Plastics*, ORNL-928 (June 29, 1951).

(3) 1949 Book of A.S.T.M. Standards, Part 6, *Electrical Insulation, Plastics, Rubber*, p. 881, American Society for Testing Materials, Philadelphia, 1950.

TABLE 5.1

Composition of Elastomers

MATERIAL	COMPOSITION (parts by weight)							
	NATURAL RUBBER	HYCAR OR-15	GR-150	THIOKOL ST	SILASTIC 7/170*	GR-S50	NEOPRENE W	HYCAR PA-21
Base rubber	100.0	100.0	100.0	100.0	x	100.0	100.0	100.0
Zinc oxide	5.0	5.0	5.0	0.5	x	5.0	5.0	
SRF black	70.0	55.0	75.0	60.0	x	70.0	45.0	
Stearic acid	1.0		2.0	3.0	x		0.5	1.0
Sulfur	3.0	1.5	1.5			1.75		0.5
Captax	0.6		0.5					
Altax		1.0						
Tetramethyl thiuram disulfide			1.0					
Phenyl-β-napthylamine	1.0						2.0	
p-Quinone dioxime				1.5	x			
Ca-10				2.0	x			
Magnesium oxide							2.0	
HMF (Philblack O)								40.0
Trimene base								3.0
Permalux							0.5	
Santocure						1.5		

*Exact composition not yet known.

TABLE 5.2

Tensile Strength of Elastomers After Radiation Exposure

MATERIAL	NO EXPOSURE	TENSILE STRENGTH (psi)		
		0.24×10^{18} nvt EXPOSURE	0.59×10^{18} nvt EXPOSURE	1.05×10^{18} nvt EXPOSURE
Natural rubber	2700	2000	1300	700
Hycar OR-15	2000	2200	2700	1300
GR-S50	1200	Became gummy		
GR-S50	1700	1700	800	900
Neoprene W	2800	1100	1400	1200
Hycar PA-21	1800	1200	700	600
Thiokol ST	800	600	300	400
Silastic 7-170	400	300	200	200

TABLE 5.3

Set at Break of Elastomers After Radiation Exposure

MATERIAL	NO EXPOSURE	SET AT BREAK (%)		
		0.24×10^{18} nvt EXPOSURE	0.59×10^{18} nvt EXPOSURE	1.05×10^{18} nvt EXPOSURE
Natural rubber	31	12	3	0
Hycar OR-15	4	2	0	0
GR-S50	35	Became gummy		
GR-S50	5	1.5	0	0
Neoprene W	6	0	2	0
Hycar PA-21	10	0	0	0
Thiokol ST	2	1.5	0	0
Silastic 7-170	0	0	0	0

TABLE 5.4

Elongation of Elastomers After Radiation Exposure

MATERIAL	ELONGATION (%)			
	NO EXPOSURE	0.24×10^{18} nvt EXPOSURE	0.59×10^{18} nvt EXPOSURE	1.05×10^{18} nvt EXPOSURE
Natural rubber	450	240	120	30
Hycar OR-15	250	100	40	3
GR-S50	530	Became gummy		
GR-S50	270	90	30	20
Neoprene W	450	55	20	3
Hycar PA-21	315	100	40	30
Thiokol ST	160	115	70	65
Silastic 7-170	100	12	9	7

TABLE 5.5

Compression Set of Elastomers After Radiation Exposure

MATERIAL	COMPRESSION SET (%)			
	NO EXPOSURE	0.24×10^{18} nvt EXPOSURE	0.59×10^{18} nvt EXPOSURE	1.05×10^{18} nvt EXPOSURE
Natural rubber	11.6	7.5	5.0	2.1
Hycar OR-15	9.1	1.6	1.0	2.5
GR-S50	6.5	Became gummy		
GR-S50	5.0	1.6	1.2	0.8
Neoprene W	8.9	2.4	2.4	1.7
Hycar PA-21	4.9	2.9	2.0	1.1
Thiokol ST	9.0	50.0	68.0	76.0
Silastic 7-170	1.4	0.02	0.2	1.2

TABLE 5.6

Specific Gravity of Elastomers After Radiation Exposure

MATERIAL	SPECIFIC GRAVITY, 25°/4°C			
	NO EXPOSURE	0.24×10^{18} nvt EXPOSURE	0.59×10^{18} nvt EXPOSURE	1.05×10^{18} nvt EXPOSURE
Natural rubber	1.186	1.187	1.192	1.194
Hycar OR-15	1.229	1.239	1.258	1.278
GR-S50	1.195	Became gummy		
GR-S50	1.210	1.215	1.221	1.230
Neoprene W	1.418	1.424	1.444	1.456
Hycar PA-21	1.268	1.270	1.271	1.274
Thiokol ST	1.451	1.451	1.446	1.340
Silastic 7-170	1.431	1.387	1.399	1.422

TABLE 5.7

Change in Weight of Elastomers After Radiation Exposure

MATERIAL	CHANGE IN WEIGHT (%)			
	NO EXPOSURE	0.24×10^{18} nvt EXPOSURE	0.59×10^{18} nvt EXPOSURE	1.05×10^{18} nvt EXPOSURE
Natural rubber		-0.03	-0.05	
Hycar OR-15		-0.01	+0.05	
GR-S50		Became gummy		
GR-S50		+0.01	+0.01	
Neoprene W		+0.23	+0.16	
Hycar PA-21		-0.17	-0.40	
Thiokol ST		-0.08	-0.14	
Silastic 7-170		-0.06	-0.19	

TABLE 5.8

Shore Durometer Hardness of Elastomers After Radiation Exposure

MATERIAL	SHORE DUROMETER HARDNESS			
	NO EXPOSURE	0.24×10^{18} nvt EXPOSURE	0.59×10^{18} nvt EXPOSURE	1.05×10^{18} nvt EXPOSURE
Natural rubber	61	72	79	86
Hycar OR-15	74	88	100	100
GR-S50	67	Became gummy		
GR-S50	69	86	91	95
Neoprene W	79	89	99	100
Hycar PA-21	62	72	81	85
Thiokol ST	74	76	70	70
Silastic 7-170	59	91	95	99

TABLE 5.9

Shore Elasticity of Elastomers After Radiation Exposure

MATERIAL	SHORE ELASTICITY			
	NO EXPOSURE	0.24×10^{18} nvt EXPOSURE	0.59×10^{18} nvt EXPOSURE	1.05×10^{18} nvt EXPOSURE
Natural rubber	100	100	50	25
Hycar OR-15	75	70	Too hard for test	
GR-S50	85	Became gummy		
GR-S50	100	65	37	25
Neoprene W	82	45	Too hard for test	
Hycar PA-21	70	70	35	25
Thiokol ST	30	30	30	30
Silastic 7-170	20	10	10	10

TABLE 5.10

Volume Resistivity of Elastomers After Radiation Exposure

MATERIAL	VOLUME RESISTIVITY (ohm-cm)			
	NO EXPOSURE	0.24×10^{18} nvt EXPOSURE	0.59×10^{18} nvt EXPOSURE	1.05×10^{18} nvt EXPOSURE
Natural rubber	2×10^{10}	2×10^{10}	3×10^{11}	3×10^{11}
Hycar OR-15	2×10^{9}	1×10^{10}	1×10^{11}	6×10^{9}
GR-S50	3×10^{3}	Became gummy		
GR-S50	6×10^{13}	6×10^{13}	2×10^{13}	1×10^{9}
Neoprene W	1×10^{11}	3×10^{8}		2×10^{8}
Hycar PA-21	6×10^{10}	6×10^{10}		3×10^{9}
Thiokol ST	10^{5}	10^{7}		10^{6}
Silastic 7-170	$>10^{14}$	$>10^{14}$	$>10^{14}$	$>10^{14}$

TABLE 5.11

Dielectric Strength of Elastomers After Radiation Exposure

MATERIAL	DIELECTRIC STRENGTH (volts/mil)			
	NO EXPOSURE	0.24×10^{18} nvt EXPOSURE	0.59×10^{18} nvt EXPOSURE	1.05×10^{18} nvt EXPOSURE
Natural rubber	170	190	110	120
Hycar OR-15	190	200	240	300
GR-S50	80	Became gummy		
GR-S50	160	300	330	320
Neoprene W	290	320	210	160
Hycar PA-21	90	90	90	90
Thiokol ST	105	105	105	105
Silastic 7-170	>380	>380	>380	>380

The compression set test used is described in reference 3. It was designed to measure the ability of rubber compounds to retain elastic properties during prolonged action of compressive stress. The percent compression set is the percentage decrease in thickness of a test specimen measured after removal from a loading device in which the specimen has been subjected for 22 hr to compressive deformation under 400 psi at 70°C.

The elastomers tested are compounded for gasketing material rather than for electrical insulation. The dielectric strength (ASTM D 149-44[4]) and volume resistivity (ASTM D 257-49 T[5]) were measured, however, since materials compounded for electrical insulation will probably change under irradiation in the same way as gasketing materials.

Durometer hardness (ASTM D 676-49 T[6]) was determined with a Shore durometer. A spring in the durometer forces a pressure foot to indent the rubber, and the amount of indentation is indicated by a pointer. The Shore elasticity is obtained with another instrument which pushes a needle into the rubber. The needle is released and the amount it is forced back by the spring of the rubber is indicated on the scale of the instrument.

PILE-INDUCED RADIATION

C. D. Bopp W. K. Kirkland
O. Sisman R. L. Towns

The decay of several concretes and of several steels and other metals after six months of irradiation in the ORNL reactor has been recorded for 180 to 360 hr. These materials are part of a list of materials of construction on which induced activity is being determined so that the radiation intensity to be encountered when equipment is removed from the pile for repairs or for other reasons may be predicted more accurately. The data have not yet been analyzed, but the gamma decay curves are presented in Figs. 5.12 to 5.19. These curves were taken on very thin specimens with an ionization chamber which was calibrated with Co^{60} standards (1.2-Mev gamma rays).

Absorption curves are being determined for the same materials, but the data are not complete and are not presented at this time.

Long-time decay data will be presented as soon as they are accumulated.

(4) *Ibid.*, p. 411.

(5) *Ibid.*, p. 390.

(6) *Ibid.*, p. 1039.

	MATERIAL	IRRADIATION TIME	AV. FLUX - N/(CM^2)(SEC.)
X	309	4536 HRS.	.52 X 10^{12}
O	302	4700 "	.48 "
●	303	4536 "	.52 "
∇	304	4283 "	.59 "

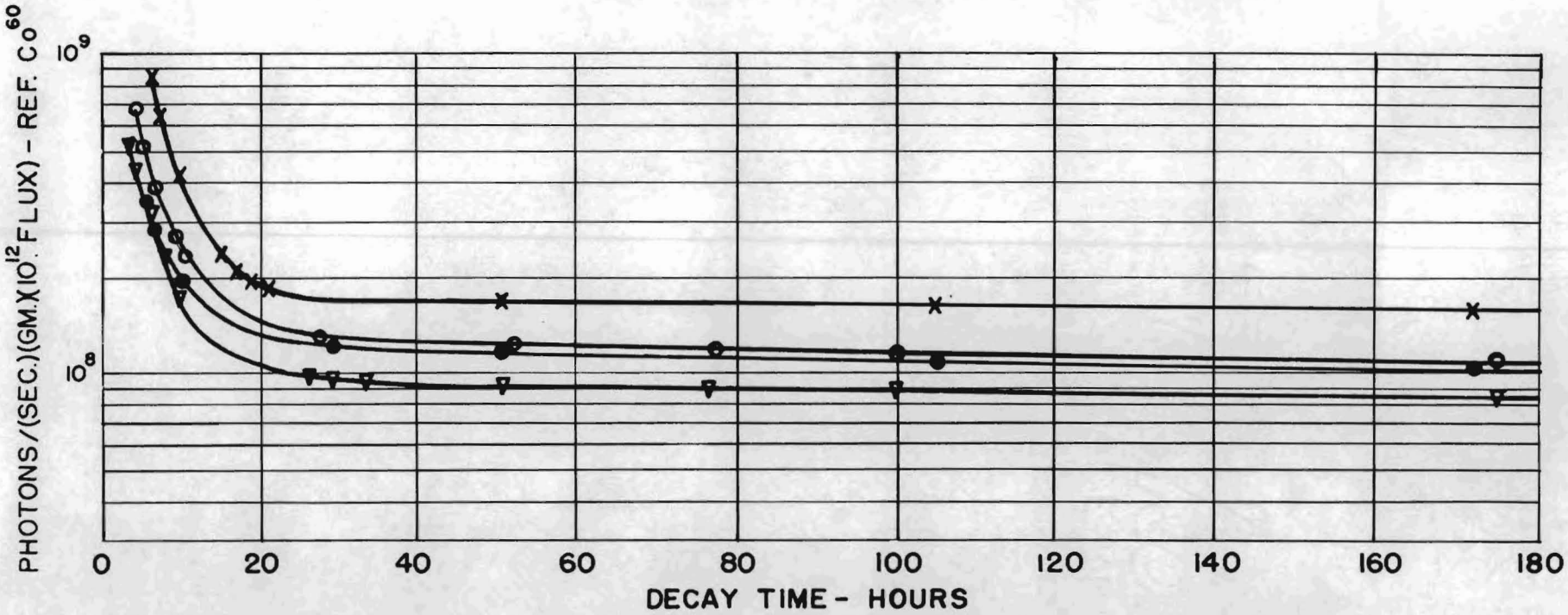

NOT CLASSIFIED

Fig. 5.12 GAMMA DECAY OF STAINLESS STEELS

PSI-A-138
DWG-11627

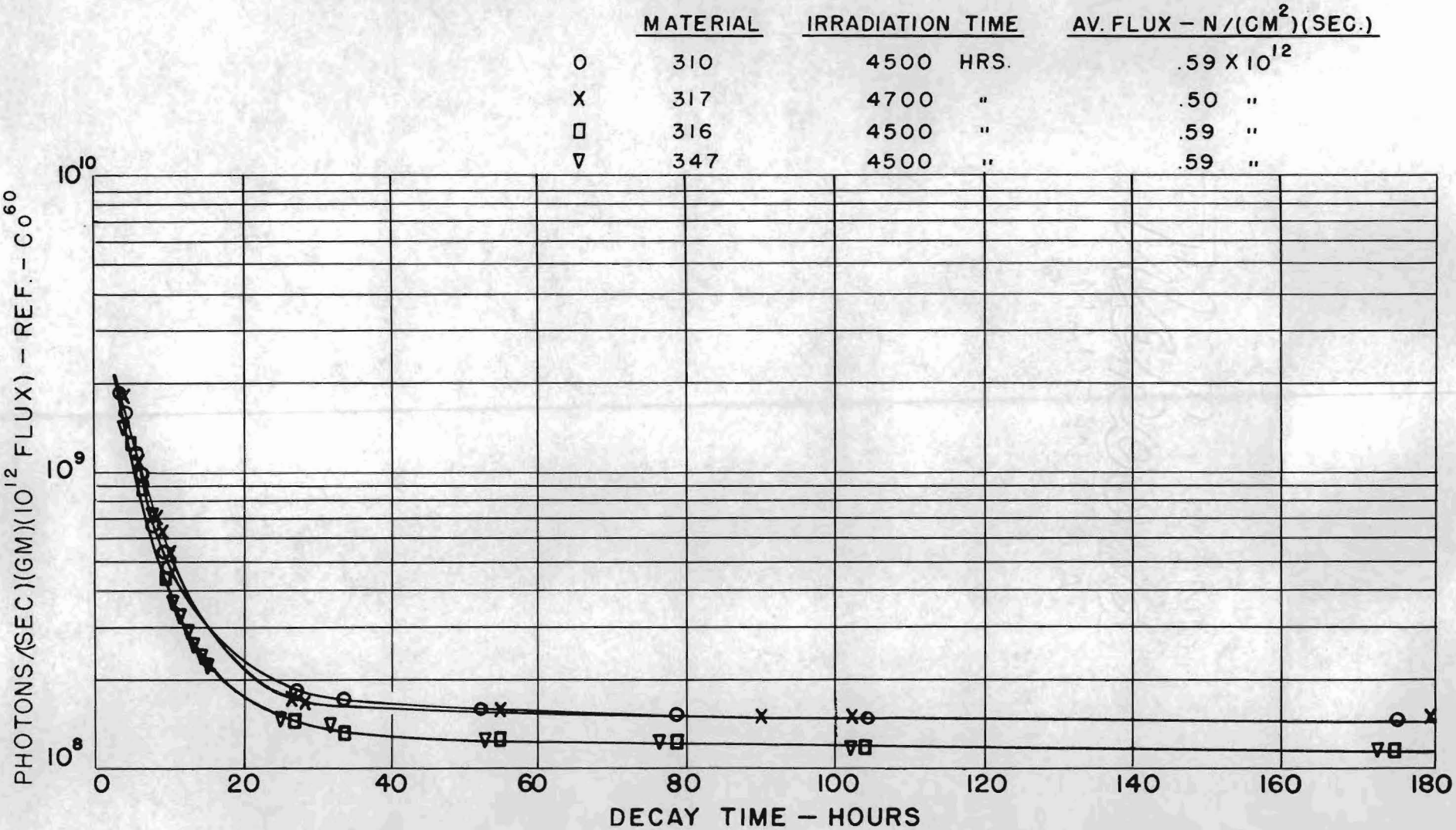

NOT CLASSIFIED

Fig. 5.13 GAMMA DECAY OF STAINLESS STEELS

PSI-A-139
DWG.-11628

	MATERIAL	IRRADIATION TIME	AV. FLUX - N/(CM^2)(SEC.)
○	405	4502 HRS.	.59 X 10^{12}
○	446	4283 "	.59 "
□	430	4283 "	.59 "
▽	502	4512 "	.51 "

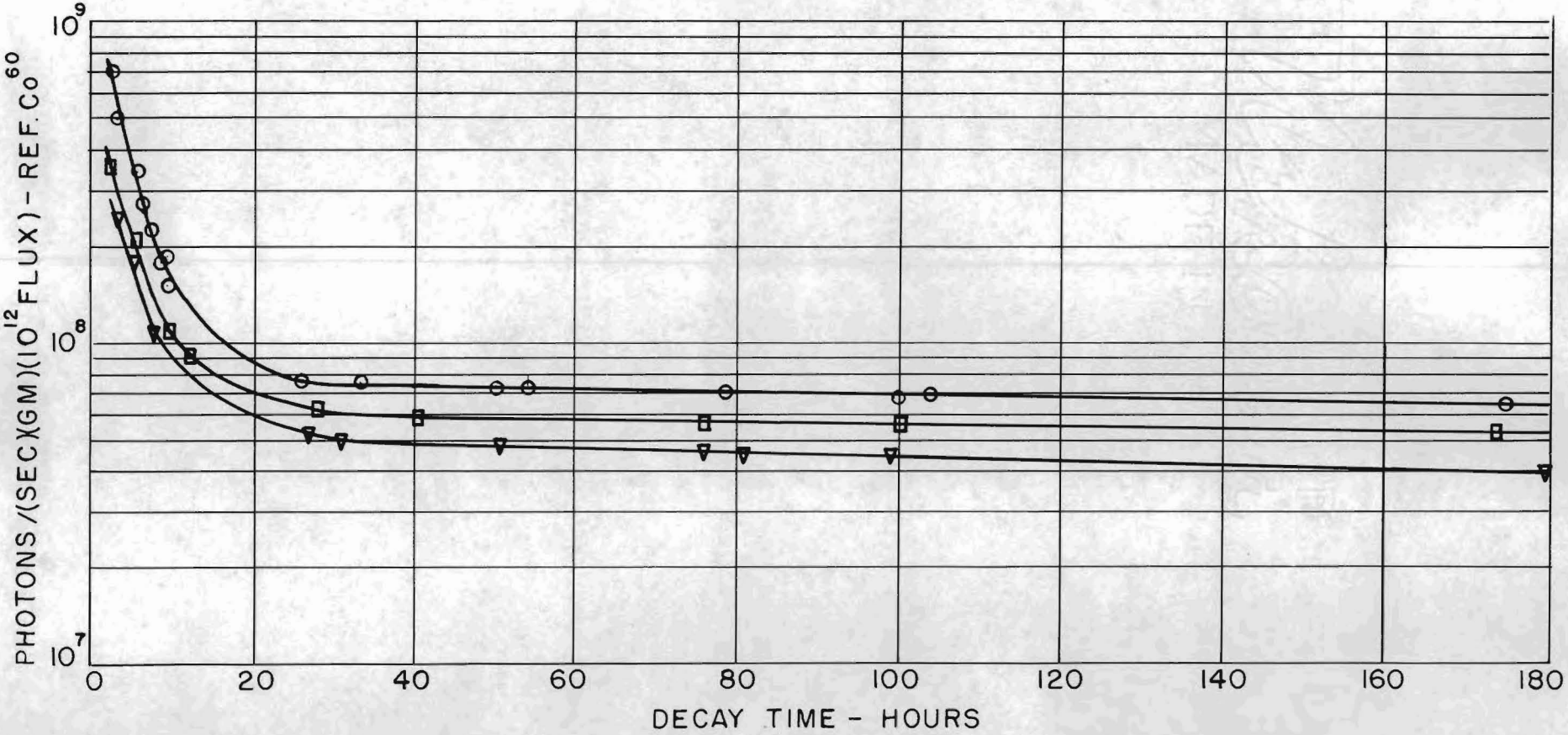

Fig. 5.14 GAMMA DECAY OF STAINLESS STEELS

NOT CLASSIFIED

PSI—A—140
DWG.—11629

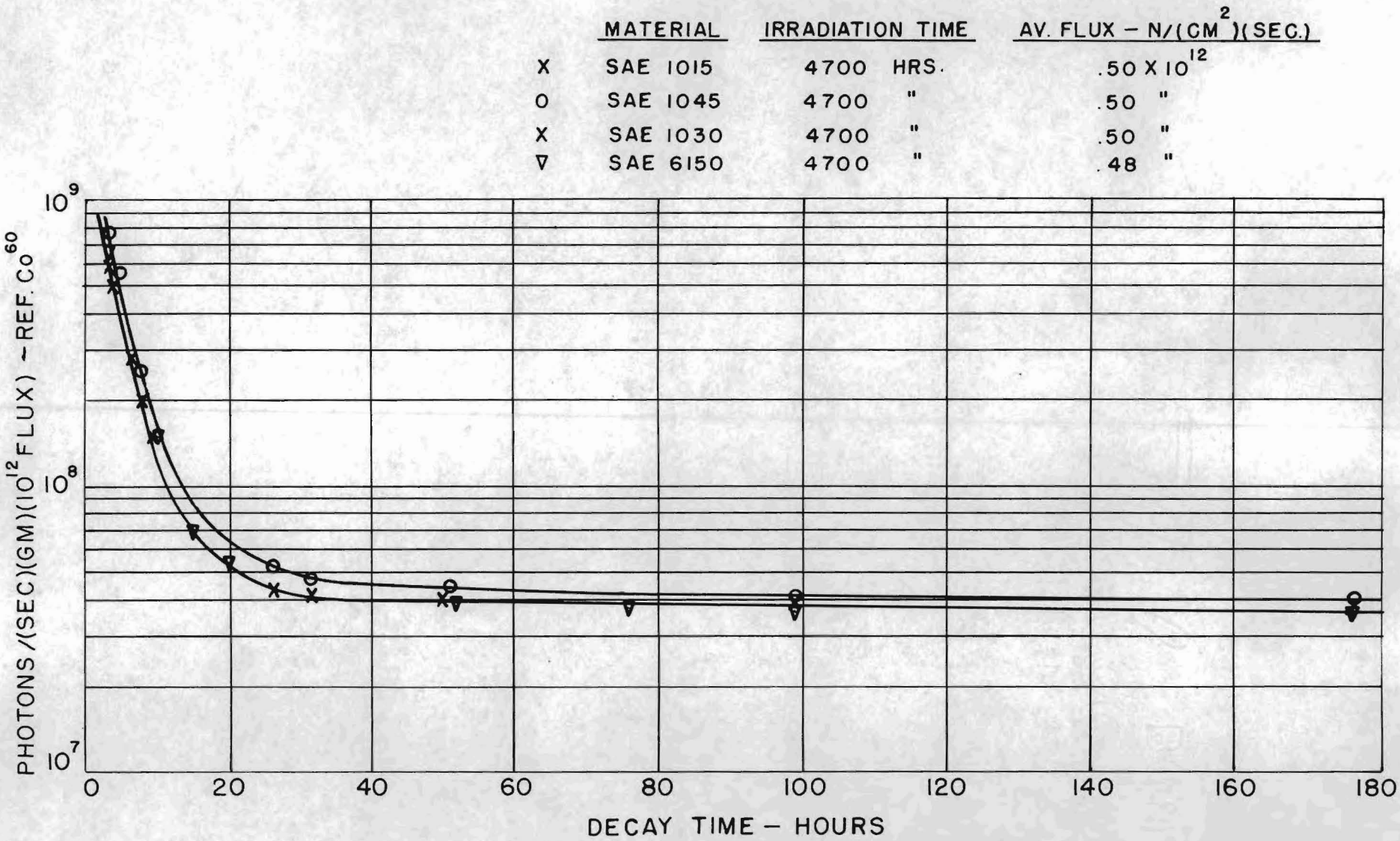

Fig. 5.15 GAMMA DECAY OF STEELS

NOT CLASSIFIED

PSI–A–141
DWG.-11630

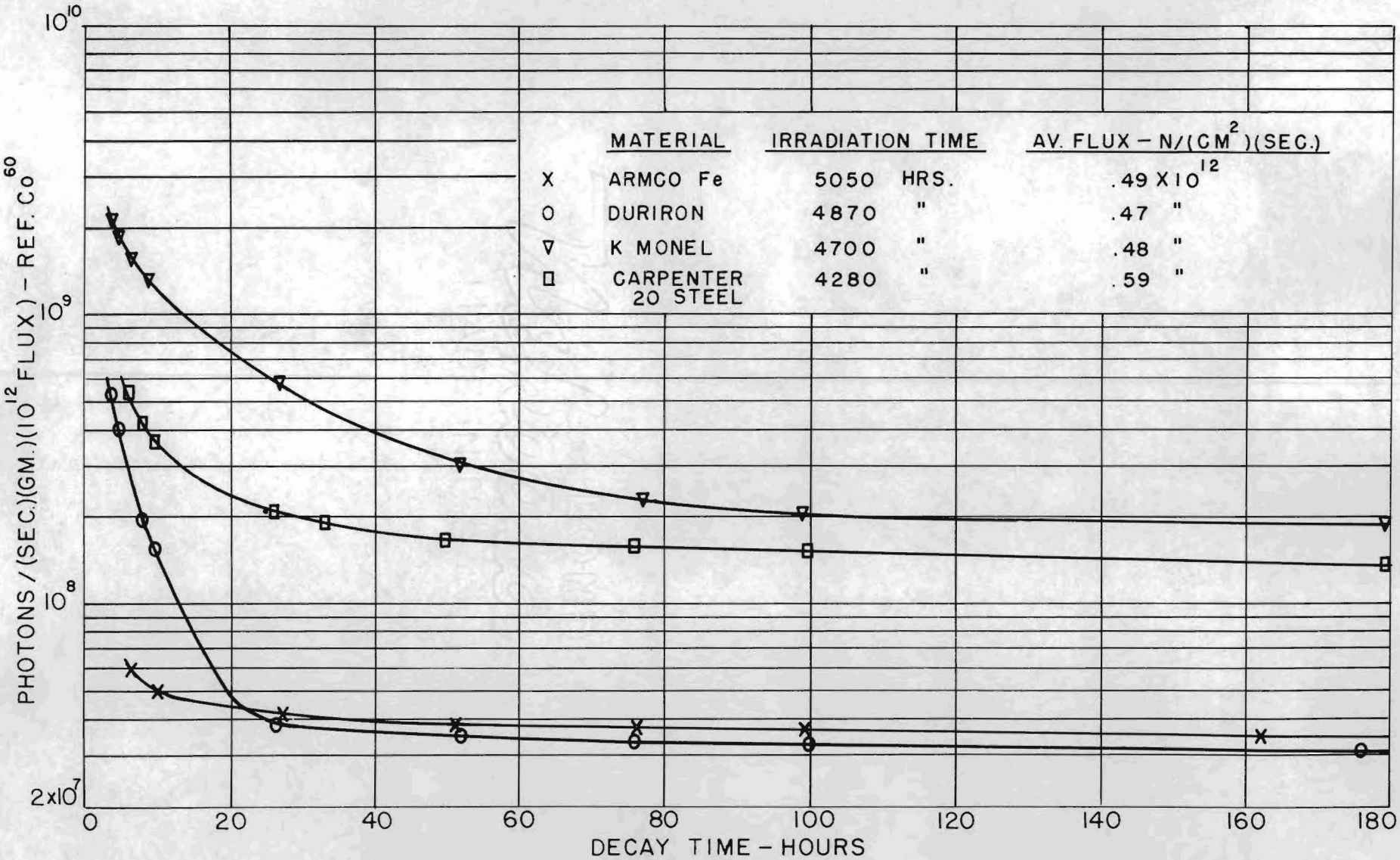

Fig. 5.16 GAMMA DECAY OF METALS

NOT CLASSIFIED
PSI-A-142
DWG.-11631

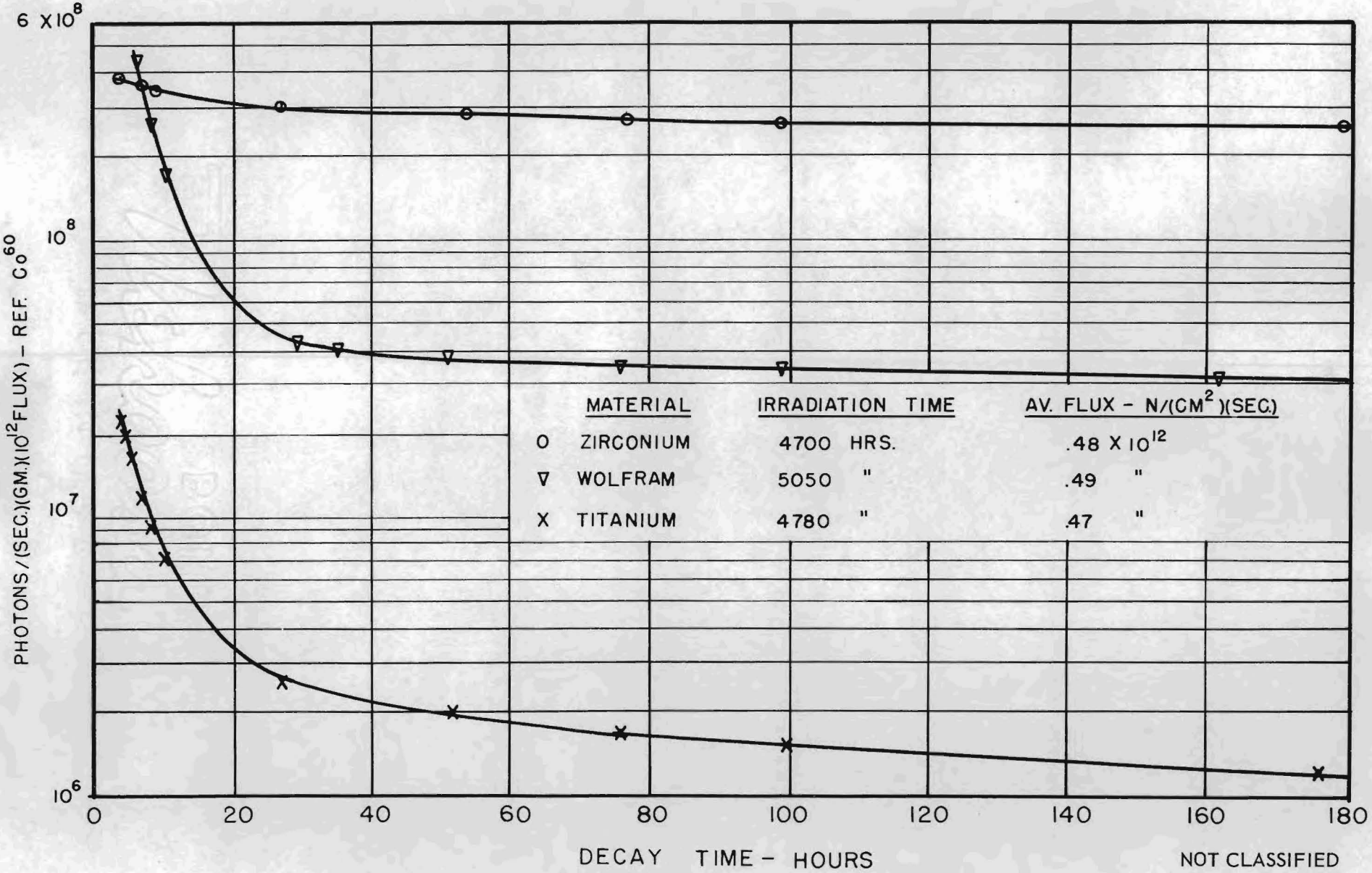

NOT CLASSIFIED

Fig. 5.17 GAMMA DECAY OF METALS

PSI-A-143
DWG.-11632

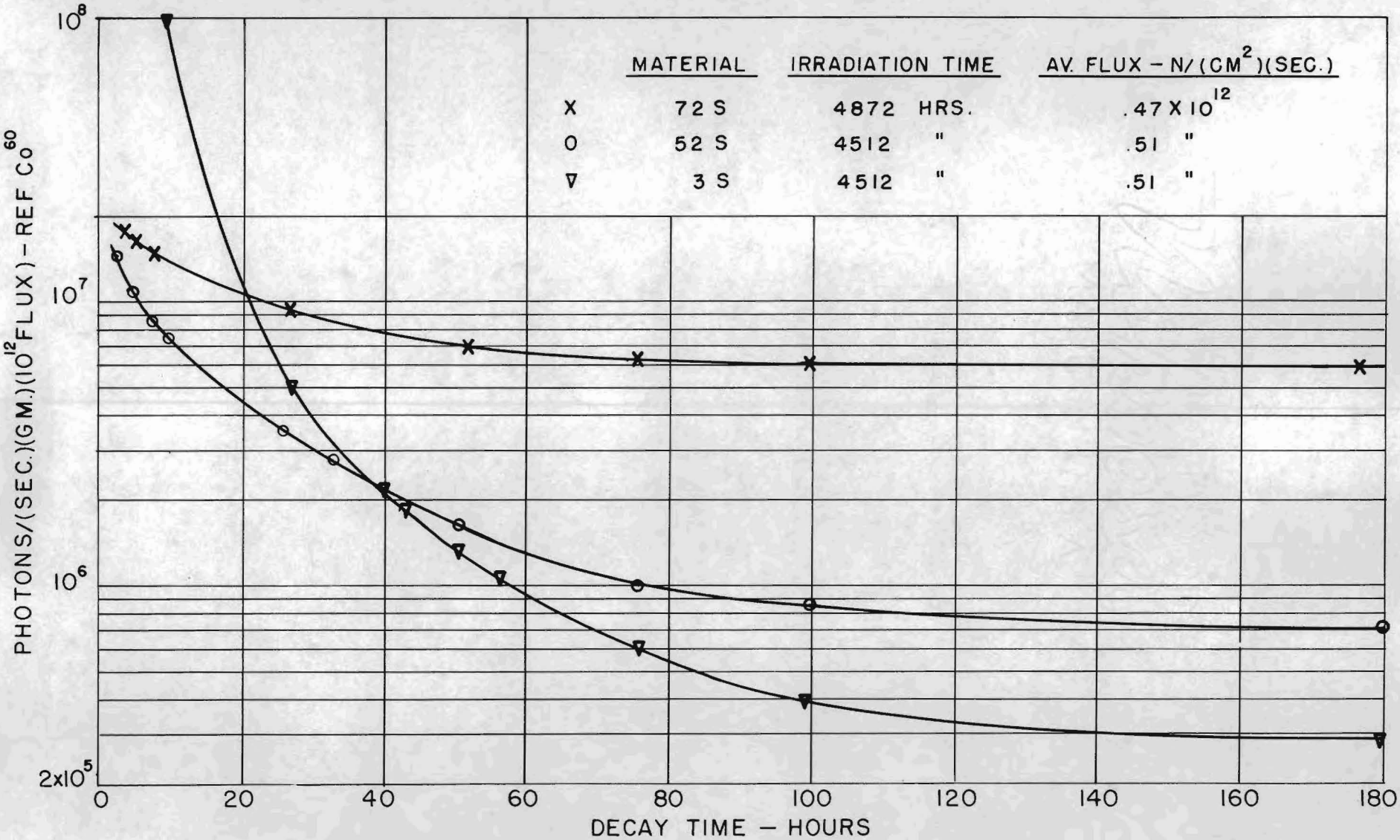

Fig. 5.18 GAMMA DECAY OF ALUMINUM

NOT CLASSIFIED

PSI-A-144
DWG.-11633

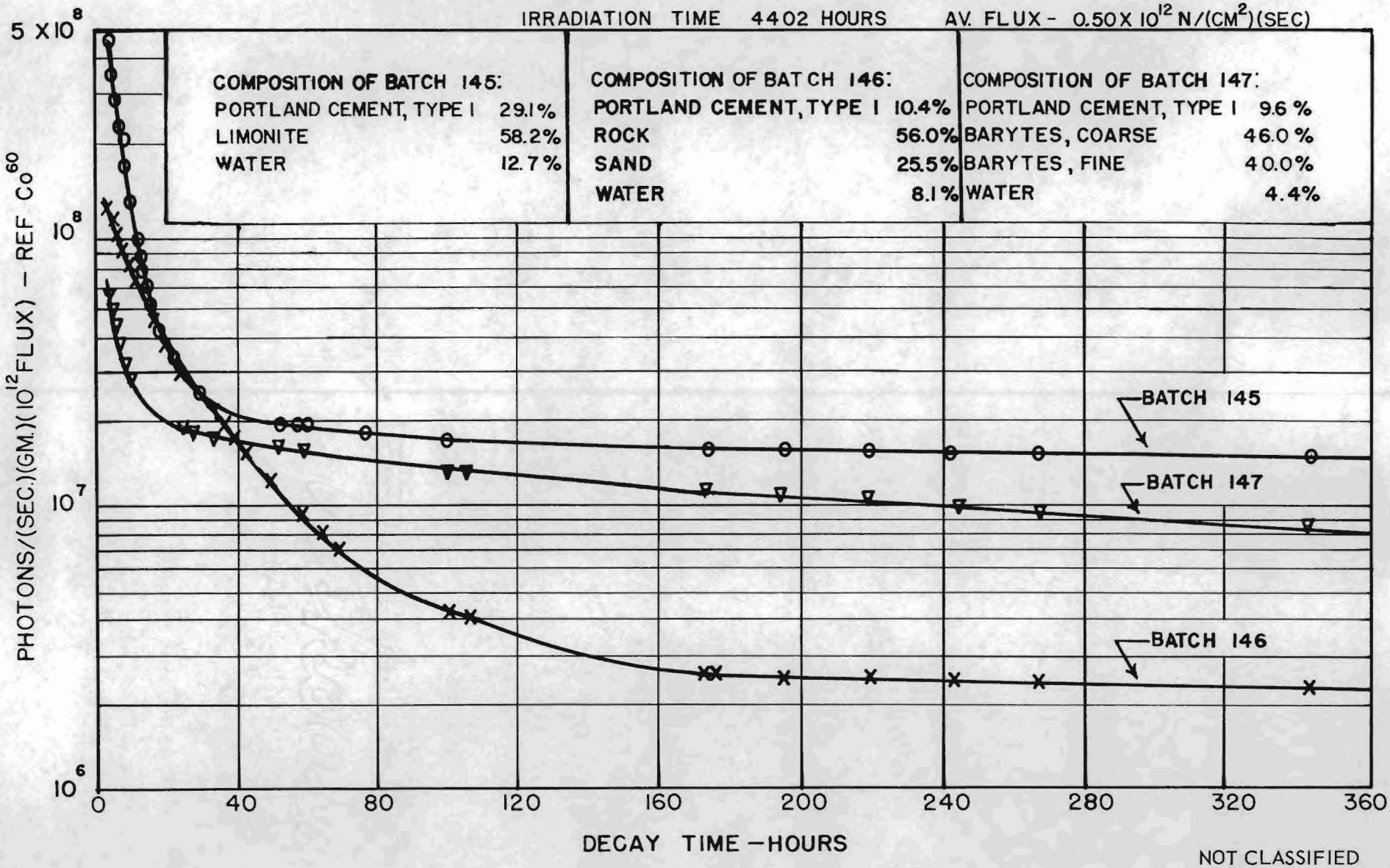

NOT CLASSIFIED

Fig. 5.19 **GAMMA DECAY OF CONCRETES**

PSI-A-145
DWG.-11634

RADIATION EFFECTS ON KOVAR

L. C. Templeton

Six specimens, 0.15 by 0.15 by 3 in., were cut from each of two pieces of Kovar stock, Nos. 6166 and 6167. An analysis of the stock is found in Table 5.10. The 12 specimens were annealed in vacuum for 1 hr at 800°C and furnace-cooled. Three specimens from each stock were then quenched from room temperature for 10 min in liquid nitrogen.

Examination by X-ray diffraction showed that the crystal structure of the annealed-only specimens was largely face-centered-cubic, and that the structure of the quenched specimens was chiefly body-centered-cubic. The quenched specimens from stock 6167 contained more of the body-centered-cubic phase than the quenched specimens from stock 6166. The annealed-only specimens were annealed in vacuum for 1 hr at a higher temperature (900°C) and furnace-cooled. It was then found that the structure of the annealed-only specimens was completely face-centered-cubic. The quenched specimens received no further heat treatment.

Length, specific volume, hardness, and electrical conductivity were measured before the second anneal and after irradiation. The average reproducibility (average range of repeated measurements) of the measurements was as follows: length, 0.02%; specific volume, 0.05%; hardness, 1 Rockwell B number; electrical conductivity, 0.2%.

The postirradiation measurements for both exposure groups were made at about the same time. Conductivity of three of the four control specimens had increased appreciably since the original measurements were made, and hardness had increased a small amount. Hardness and conductivity data were corrected to eliminate the effect of similar changes in the irradiated specimens. The curves were plotted from corrected data. Points were connected with straight lines because there were not enough to establish a smooth curve.

Length was measured with an apparatus equipped with a dial gage marked with 0.0001-in. graduations. The increase in length, if any, was of the order of magnitude of the accuracy of measurement, ~0.3 mil or better. The data are given in Table 5.12.

The changes in density reported in ORNL-1025, p. 50, were based on measurements made before the specimens were etched to remove corrosion products. After a 2-min etching with a solution of 5 g of ferric chloride, 50 ml

TABLE 5.12

Analysis of Kovar Stock*

STOCK NO.	AMOUNT OF ELEMENT PRESENT (%)					
	Fe	Ni	Co	Mn	Si	C
6166	53.60	26.70	19.06	0.36	0.10	0.02
6167	54.37	26.21	18.80	0.32	0.06	0.03

*Kovar stock and analysis supplied by Westinghouse Co.

TABLE 5.13

Classification of Kovar Specimens

SPECIMEN NO.	STOCK NO.	CONTROL SPECIMEN	HEAT TREATMENT
6-2, 6-3	6166	6-1	Annealed only
6-5, 6-6	6166	6-4	Annealed, quenched
7-2, 7-3	6167	7-1	Annealed only
7-5, 7-6	6167	7-4	Annealed, quenched

of concentrated hydrochloric acid, and 100 ml of distilled water, density was again measured. The densities, converted to specific volume, are given in Table 5.13 and Fig. 5.20. Specimens which had the longer exposure seemed to have corroded more.

Specific volume was calculated from specimen weights in air and in carbon tetrachloride. An analytical balance which had been adapted for remote operation was used for weighing. The change given for specimen 7-2 is particularly inconsistent with values obtained for other specimens. However, both the initial and final (after irradiation) measurements were verified. The values of percent change in specific volume are of doubtful significance for the following reasons: (1) length measurements, which were more accurate, showed that there were no significant changes in that direction, (2) scatter in the data was large compared to the magnitude of the changes, and (3) an increase of 1°C in the temperature of the carbon tetrachloride, caused by heat produced by the radioactivity of the specimen while immersed, would cause an apparent increase of approximately 0.1% in the specific volume of the specimen.

Hardness was measured on a Rockwell tester. The B scale, 1/16-in. ball and 100-kg load, was used. Tests were made at three points along the length of the specimens. Annealed-only specimens slowly increased in hardness approximately 5 numbers during an integrated flux of 3.04×10^{20} nvt. The quenched specimens initially increased in hardness much faster, 8 numbers during an integrated flux of 7.65×10^{19} nvt, than the annealed-only specimens. However, the quenched specimens reached a maximum hardness, after which continued irradiation resulted in a decrease. Since there were only two irradiation periods, it is not possible to determine the integrated flux at which maximum hardness occurred. The data are presented in Table 5.14 and in Figs. 5.21 and 5.22.

Electrical conductivity was calculated from potential measurements made across the specimens and across a 0.1-ohm standard resistor, through which 2 amp of current was passed. A potentiometer and galvanometer were used for measuring potential by the null-current method. During the shorter irradiation period the conductivity of the quenched specimens increased approximately 11%, more than twice as much as that of the annealed-only specimens. In the quenched specimens conductivity also reached a maximum, followed by a decrease.

DWG - 11374
NOT CLASSIFIED

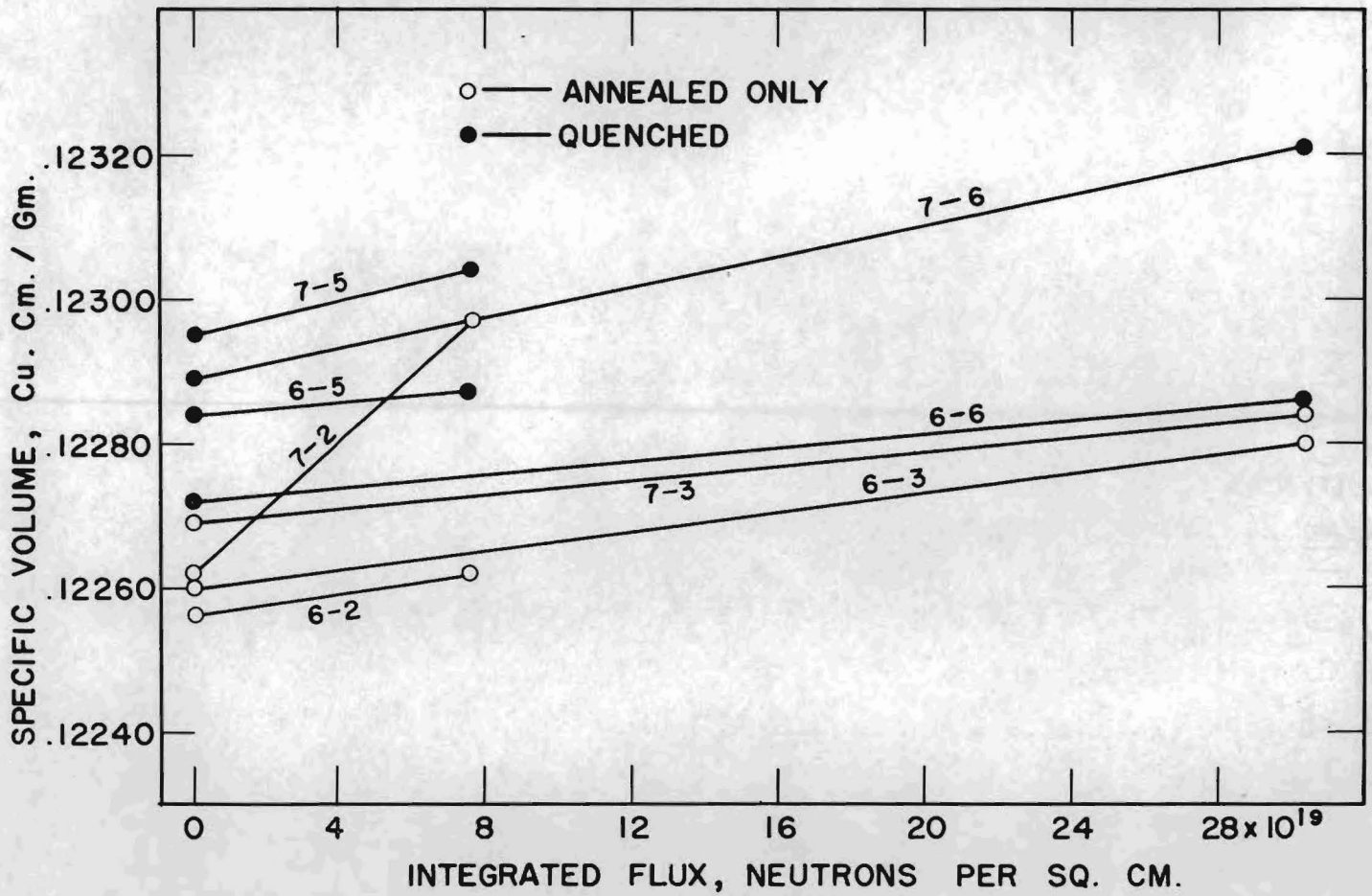

Fig. 5.20

SPECIFIC VOLUME OF KOVAR

VS

NEUTRON IRRADIATION

PSI-A-117

TABLE 5.14

Length of Kovar Specimens

SPECIMEN	HEAT TREATMENT	RADIATION DOSAGE (nvt)	LENGTH BEFORE IRRADIATION (in.)	LENGTH AFTER IRRADIATION (in.)	INCREASE (%)
6-1	Annealed only	Control	3.0005	3.0008	0.01
6-2	Annealed only	7.65×10^{19}	2.9981	2.9988	0.02
6-3	Annealed only	3.04×10^{20}	2.9955	2.9953	-0.01
6-4	Annealed and quenched	Control	2.9985	2.9987	0.01
6-5	Annealed and quenched	7.65×10^{19}	2.9985	3.0004	0.06
6-6	Annealed and quenched	3.04×10^{20}	2.9974	2.9984	0.03
7-1	Annealed only	Control	3.0139	3.0142	0.01
7-2	Annealed only	7.65×10^{19}	3.0133	3.0180	0.16
				3.0136*	0.01
7-3	Annealed only	3.04×10^{20}	3.0101	3.0114	0.04
7-4	Annealed and quenched	Control	3.0117	3.0119	0.01
7-5	Annealed and quenched	7.65×10^{19}	3.0120	3.0127	0.02
7-6	Annealed and quenched	3.04×10^{20}	3.0115	3.0118	0.01

*After removing foreign matter from end of specimen

DWG -11376
NOT CLASSIFIED

Fig. 5.21

HARDNESS OF KOVAR
VERSUS
NEUTRON IRRADIATION

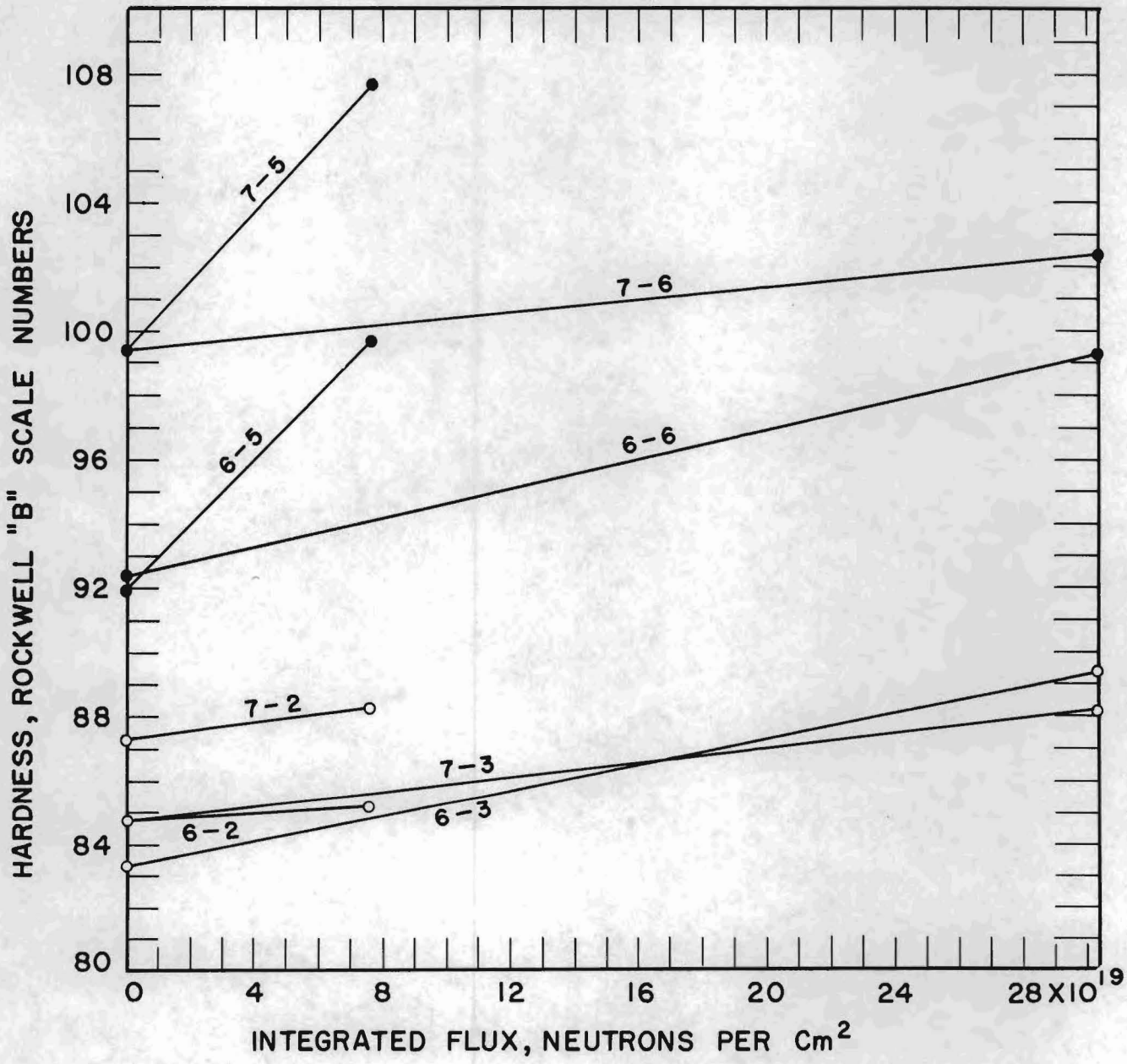

○—— ANNEALED AT 900° C FOR ONE HOUR.
●—— ANNEALED AT 800° C FOR ONE HOUR QUENCHED IN LIQUID NITROGEN.

PSI—A-122

NOT CLASSIFIED
DWG — 11377

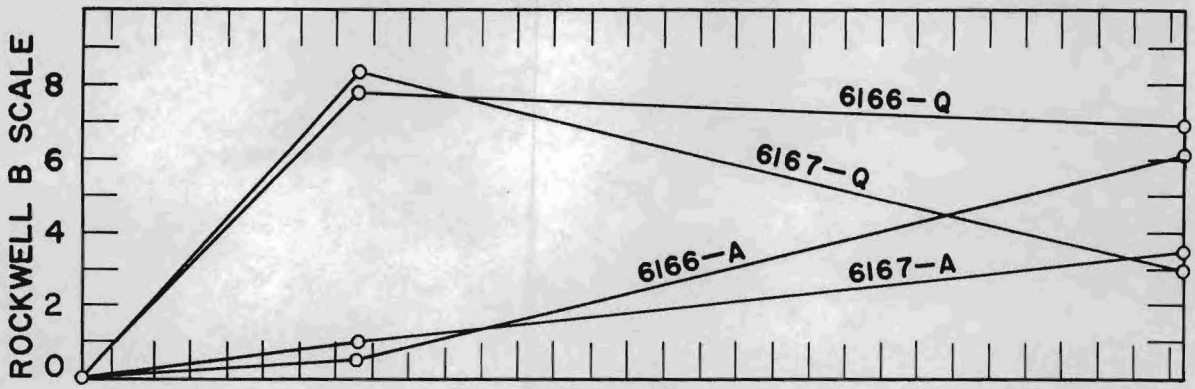

Fig. 5.22a CHANGE IN HARDNESS OF KOVAR VERSUS NEUTRON IRRADIATION

A-ANNEALED ONLY
Q-QUENCHED

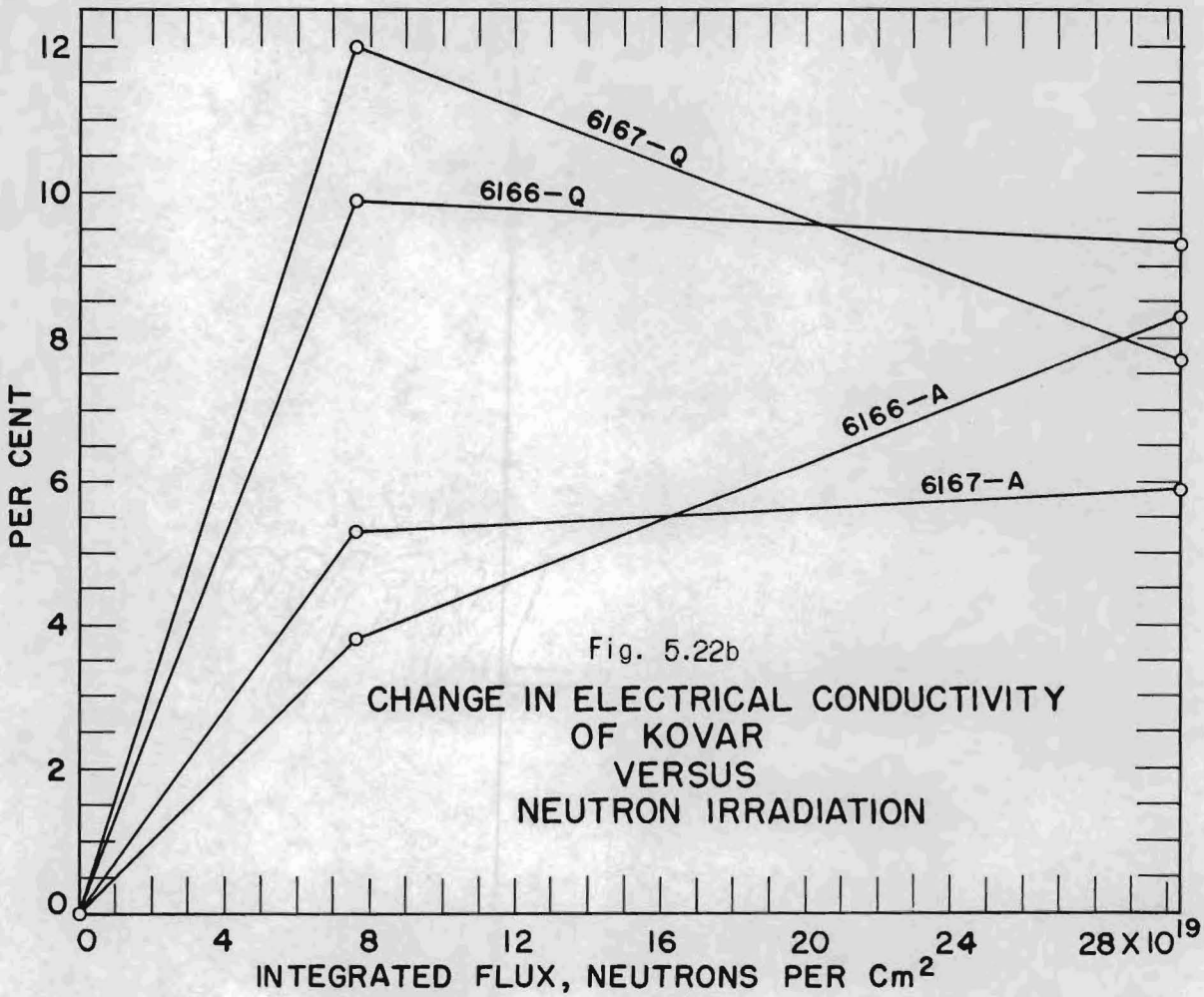

Fig. 5.22b
CHANGE IN ELECTRICAL CONDUCTIVITY OF KOVAR VERSUS NEUTRON IRRADIATION

PSI-A-123

The symmetry between the curves for hardness and conductivity suggests the possibility of a relation between the mechanisms which caused the observed changes. The data are given in Tables 5.15, 5.16, 5.17 and Figs. 5.22 and 5.23.

TABLE 5.15

Specific Volume of Kovar

SPECIMEN	HEAT TREATMENT	RADIATION DOSAGE (nvt)	SPECIFIC VOLUME BEFORE IRRADIATION (cc/g)	SPECIFIC VOLUME AFTER IRRADIATION (cc/g)	INCREASE (%)
6-1	Annealed only	Control	122.77×10^{-3}		
6-2	Annealed only	7.65×10^{19}	122.56	122.62×10^{-3}	0.05
6-3	Annealed only	3.04×10^{20}	122.60	122.80	0.16
6-4	Annealed and quenched	Control	122.69	122.72	0.03
6-5	Annealed and quenched	7.65×10^{19}	122.84	122.87	0.02
6-6	Annealed and quenched	3.04×10^{20}	122.72	122.81	0.07
7-1	Annealed only	Control	122.65	122.70	0.04
7-2	Annealed only	7.65×10^{19}	122.62	122.97	0.28
7-3	Annealed only	3.04×10^{20}	122.69	122.84	0.12
7-4	Annealed and quenched	Control	122.94	122.95	0.00
7-5	Annealed and quenched	7.65×10^{19}	122.95	123.04	0.07
7-6	Annealed and quenched	3.04×10^{20}	122.89	123.21	0.26

NOT CLASSIFIED
DWG-11375

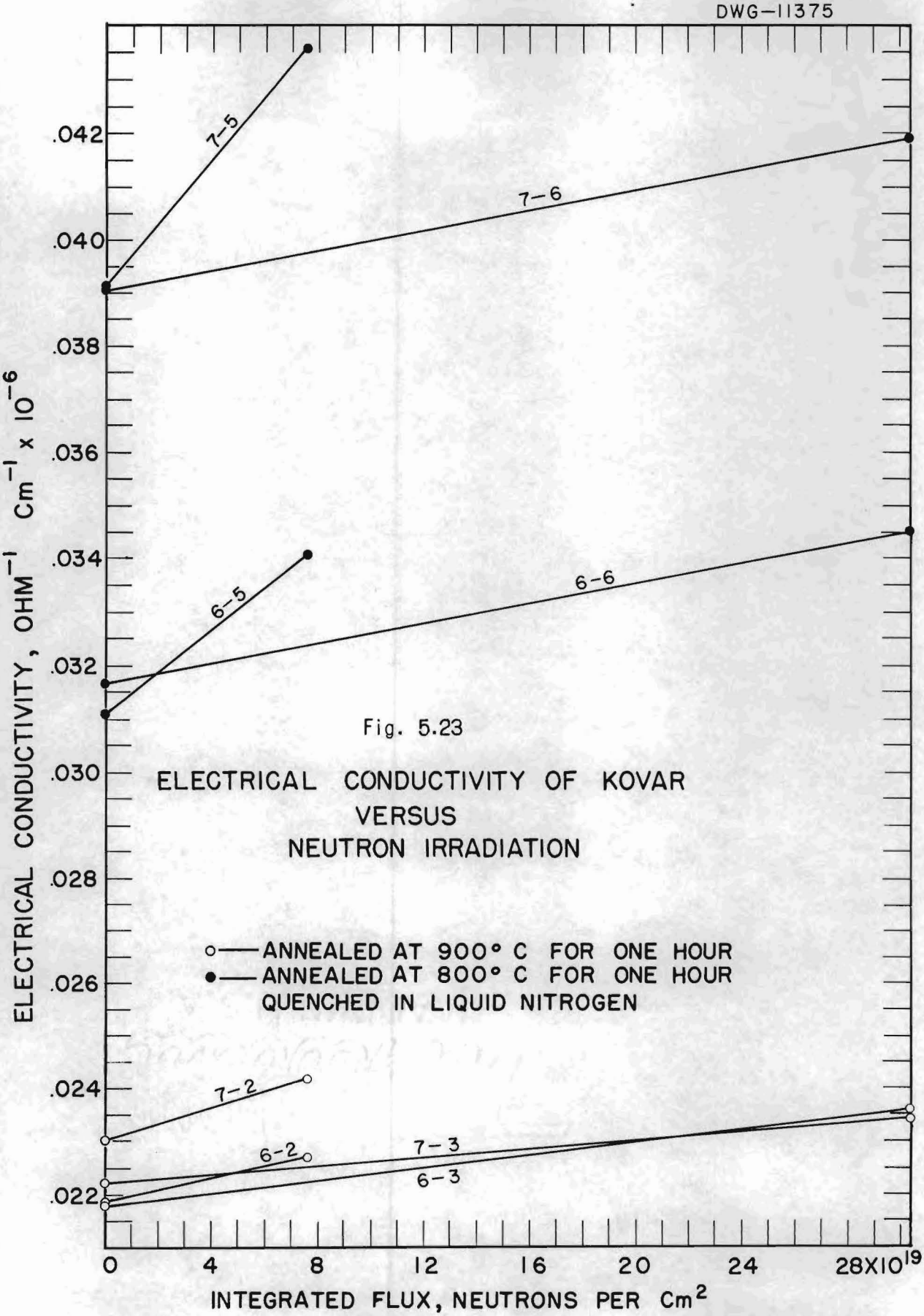

Fig. 5.23

ELECTRICAL CONDUCTIVITY OF KOVAR
VERSUS
NEUTRON IRRADIATION

PSI-A-121

TABLE 5.16

Hardness of Kovar

SPECIMEN	HEAT TREATMENT	RADIATION DOSAGE (nvt)	HARDNESS (Rockwell B)				
			BEFORE IRRADIATION	AFTER IRRADIATION		INCREASE	
				MEASURED	CORRECTED*	MEASURED	CORRECTED
6-1	Annealed only	Control	84.2	84.9	84.2	0.7	0.0
6-2	Annealed only	7.65×10^{19}	84.7	85.9	85.2	1.2	0.5
6-3	Annealed only	3.04×10^{20}	83.3	90.1	89.4	6.8	6.1
6-4	Annealed and quenched	Control	92.8	93.9	92.8	1.1	0.0
6-5	Annealed and quenched	7.65×10^{19}	91.9	100.8	99.7	8.9	7.8
6-6	Annealed and quenched	3.04×10^{20}	92.4	100.4	99.3	8.0	6.9
7-1	Annealed only	Control	87.0	87.9	87.0	0.9	0.0
7-2	Annealed only	7.65×10^{19}	87.3	89.2	88.3	1.9	1.0
7-3	Annealed only	3.04×10^{20}	84.7	89.1	88.2	4.4	3.5
7-4	Annealed and quenched	Control	99.0	100.7	99.0	1.7	0.0
7-5	Annealed and quenched	7.65×10^{19}	99.4	109.4	107.7	10.0	8.3
7-6	Annealed and quenched	3.04×10^{20}	99.4	104.1	102.4	4.7	3.0

*Measured hardness minus the change in hardness of the control specimen.

TABLE 5.17

Electrical Conductivity of Kovar at 20°C

SPECIMEN	HEAT TREATMENT	RADIATION DOSAGE (nvt)	CONDUCTIVITY (ohm^{-1} cm^{-1}) BEFORE IRRADIATION, (σ_B)	AFTER IRRADIATION MEASURED, (σ_A)	AFTER IRRADIATION CORRECTED,* (σ_C)	CONDUCTIVITY INCREASE (%) MEASURED	CONDUCTIVITY INCREASE (%) CORRECTED
6-1	Annealed only	Control	21.71×10^3	21.71×10^3	21.71×10^3	0.0	0.0
6-2	Annealed only	7.65×10^{19}	21.86	22.70	22.70	3.8	3.8
6-3	Annealed only	3.04×10^{20}	21.79	23.60	23.60	8.3	8.3
6-4	Annealed and quenched	Control	31.46	31.88	31.46	1.3	0.0
6-5	Annealed and quenched	7.65×10^{19}	31.09	34.58	34.08	11.2	9.9
6-6	Annealed and quenched	3.04×10^{20}	31.65	35.03	34.52	10.7	9.3
7-1	Annealed only	Control	23.46	24.37	23.46	3.9	0.0
7-2	Annealed only	7.65×10^{19}	23.03	25.14	24.17	9.2	5.3
7-3	Annealed only	3.04×10^{20}	22.21	24.39	23.44	9.8	5.9
7-4	Annealed and quenched	Control	39.29	40.13	39.29	2.1	0.0
7-5	Annealed and quenched	7.65×10^{19}	39.11	44.62	43.59	14.1	12.0
7-6	Annealed and quenched	3.04×10^{20}	39.05	42.88	41.93	9.8	7.7

*$\sigma_C = \sigma_A - \frac{\sigma_B \times P}{100}$, where P is the percent change of the control specimen.

THERMAL CONDUCTIVITY OF URANIUM-BEARING MATERIALS*

R. G. Berggren R. M. Carroll
W. Primak, Consultant, Argonne National Laboratory

Irradiations of BeU and ZrU alloys reported previously[7] have been continued through the present quarter. No significant changes in thermal conductivity were observed. A Zr—6 wt % U alloy sample of the dimensions shown in Fig. 5.24 has been received and is being mounted in the longitudinal thermal-conductivity apparatus previously illustrated[8] for irradiation in an X reactor fuel channel.

The second device suggested previously[9] for determining the rate of fission heating in the X reactor was developed and inserted into the reactor. The difference in temperature between a fission heater suspended in air and the walls of the chamber is measured. An electrical heater incorporated with the fission heater permits calibration. The device is found to be very stable. It responds fairly rapidly, having a relaxation time of 2 to 3 min, which is a sufficiently rapid response for detection of slight movements in the control rods. The general features of construction are shown in Fig. 5.25. The device has shown that the fission heating is not proportional to the pile power as recorded by the pile operator. It now seems that this is fundamental, since the pile operator measures a somewhat different quantity, makes the measurement in a different part of the reactor, and then controls this quantity by altering the flux pattern as well as the flux. Hence any data depending on fission heating when reduced to standard pile power are irregular. These devices for measuring the fission heating rate have been inserted with a number of thermal conductivity samples. Even when the thermal conductivity data are reduced to the readings of the device there still remain irregularities in the data which may be due in part to the flux pattern shifting across the space separating the device and the thermal conductivity torpedo, the limits of precision of the instruments, and spurious emf's. It is believed, however, that long-term data given in terms of the calibrated fission-heating rate meter are much more reliable than the data reported heretofore.

(7) *Physics of Solids Institute Quarterly Progress Report for Period Ending January 31, 1951*, p. 49, ORNL-1025 (July 17, 1951); *Physics Division Quarterly Progress Report for Period Ending September 20, 1950*, ORNL-864, pp. 11 and 14 (Jan. 8, 1951).

(8) ORNL-864, *op. cit.*, p. 11.

(9) *Ibid*, p. 14.

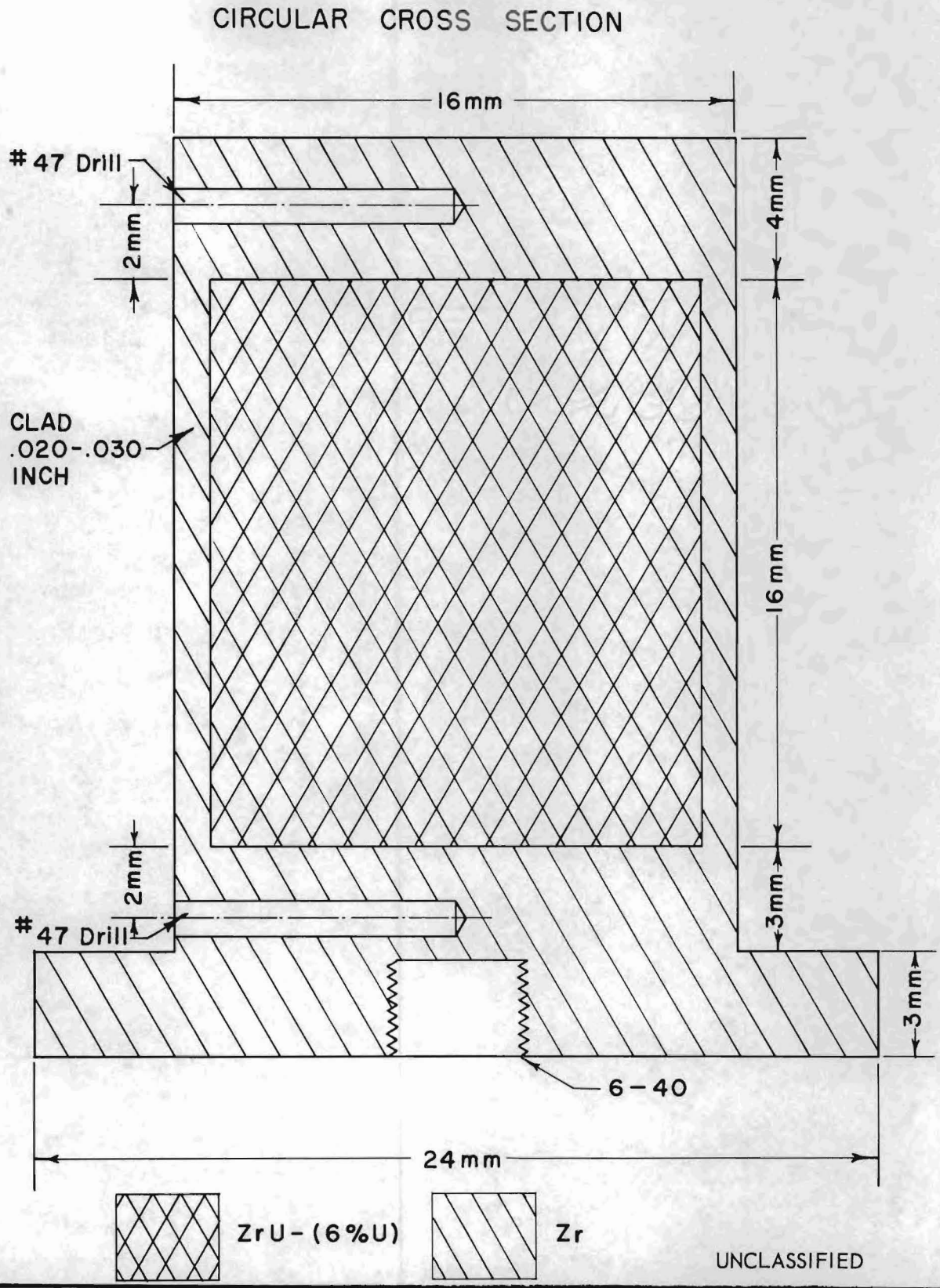

UNCLASSIFIED

OAK RIDGE NATIONAL LABORATORY - Physics of Solids Institute

Fig. 5.24 THERMAL CONDUCTIVITY SAMPLE

PSI-A-147

DRAWN BY: W.E.B. | FOR: R.G.BERGGREN | DATE: 6/20/51 | SCALE:

DWG.-11663

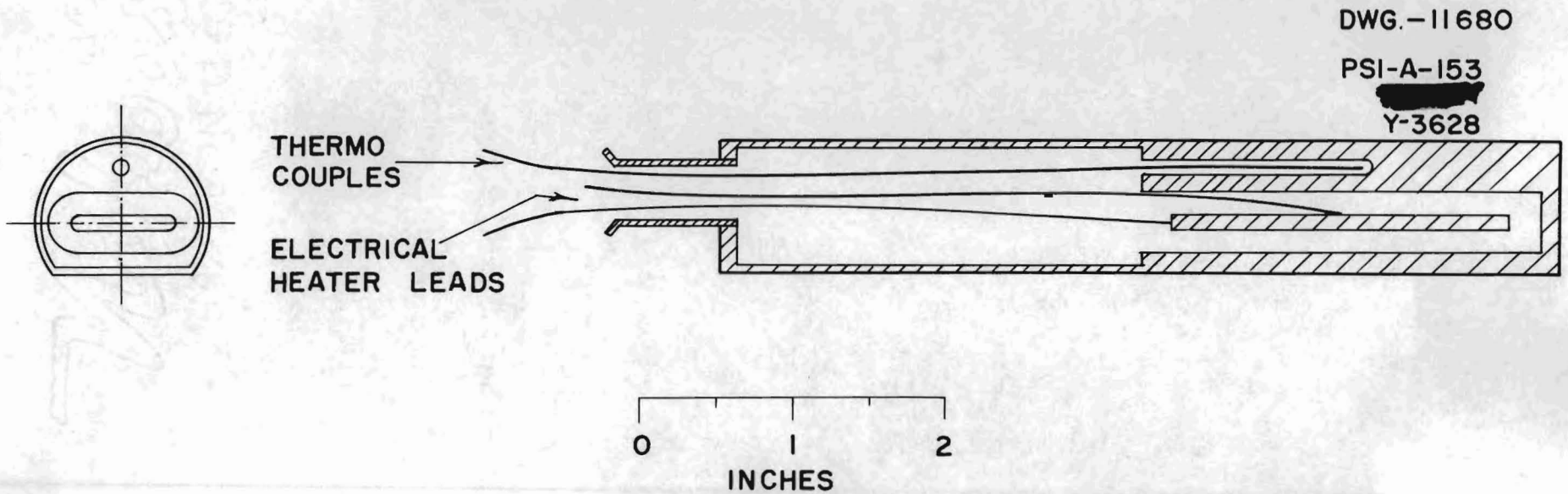

FLUXMETER

Fig. 5.25a

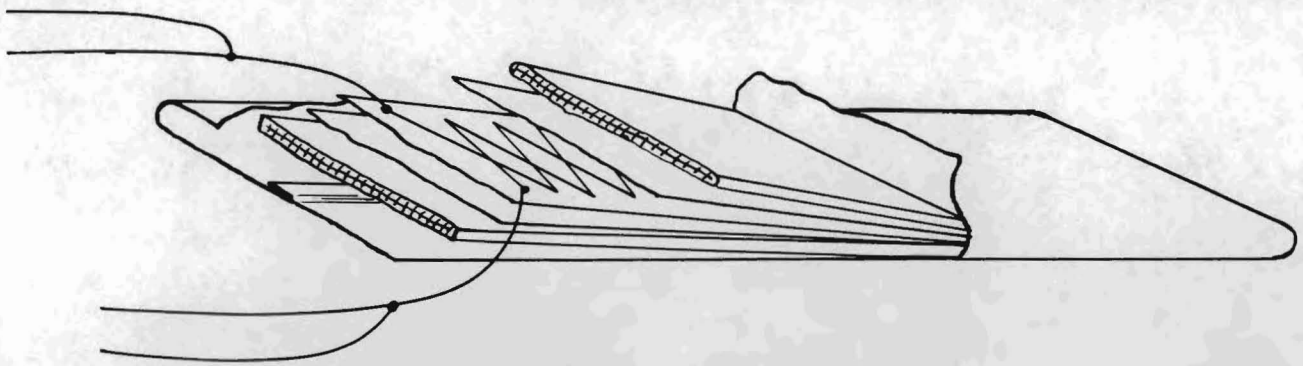

HEATER CONSTRUCTION
(NOT TO SCALE)

Fig. 5.25b

A uranyl nitrate hexahydrate—impregnated carbon[10] sample and a similarly impregnated graphite sample have been irradiated during this quarter. The carbon sample showed, as expected, a lower rate of change of thermal conductivity than the graphite previously irradiated. The results are shown in Fig. 5.26. The impregnated graphite sample was irradiated in the low-temperature radial-conductivity apparatus. It did not reproduce the results reported for a previous sample.[11] In two and a half months the conductivity has decreased by a factor of only 3-1/3, and the center temperature, originally 215°C, reached 315°C. The reason for this marked difference in behavior is unexplained.

Two Zr—3 wt % U alloy samples have been mounted in a slug for insertion into a fuel channel and an HEW reactor.

DEAD WEIGHT CREEP*

W. E. Brundage A. S. Olson
W. Primak, Consultant, Argonne National Laboratory

Following news of excessive heating in a NEPA creep apparatus inserted in the HEW reactor, calculations were made of gamma heating to be expected in the apparatus developed here[12] for measuring creep of zirconium using a dead weight load. It became clear that the gamma heating would not upset temperature control in the torpedo shown in Fig. 5.27, but it would seriously affect the temperature distribution, making the temperature different in the operating and shutdown reactor and thus invalidating the experiment. For the HEW experiment it would be necessary to redesign the torpedo, placing the LVDT and the yoke outside the furnace holding the specimen. However, since several torpedoes were available, it was decided to use them for bench tests.

The LVDT instrumentation previously developed[13] was found to be inadequate and was rebuilt.**

During this period five bench tests were set up using components described previously. The performance of the various components was as follows:

(10) An extensive progress report covering the past two and one-half years of work will be issued shortly.

(11) This work was previously reported in Progress Reports of the ORNL Physics Division.

(12) Argonne National Laboratory report ANL-4613.

*Sponsored by Argonne National Laboratory.

(13) ORNL-864, p. 16.

**We are indebted to W. E. Johnson (WAPD) and J. C. Wilson (ORNL) for several suggestions which were incorporated in the instrumentation.

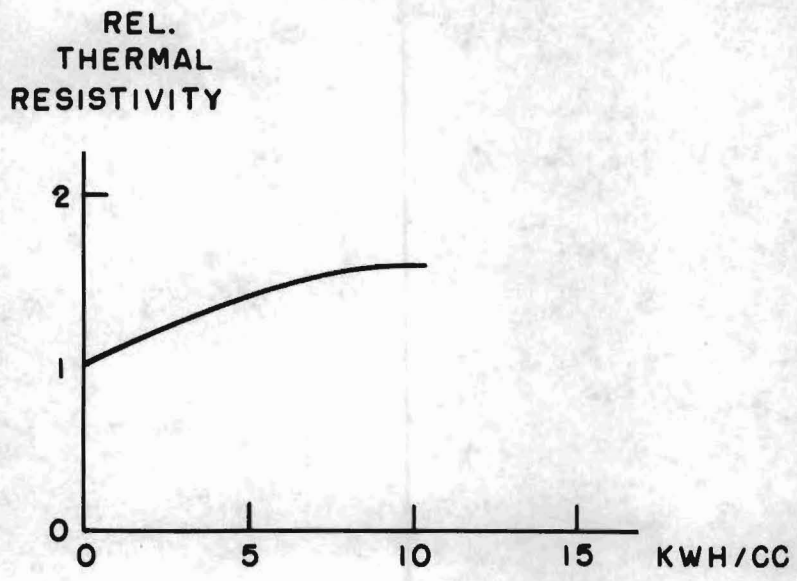

Fig. 5.26

THE RELATIVE THERMAL RESISTIVITY OF A UNH IMPREGNATED CARBON SAMPLE IRRADIATED IN X-10.

DWG.-11666
PSI-A-150

NOT CLASSIFIED

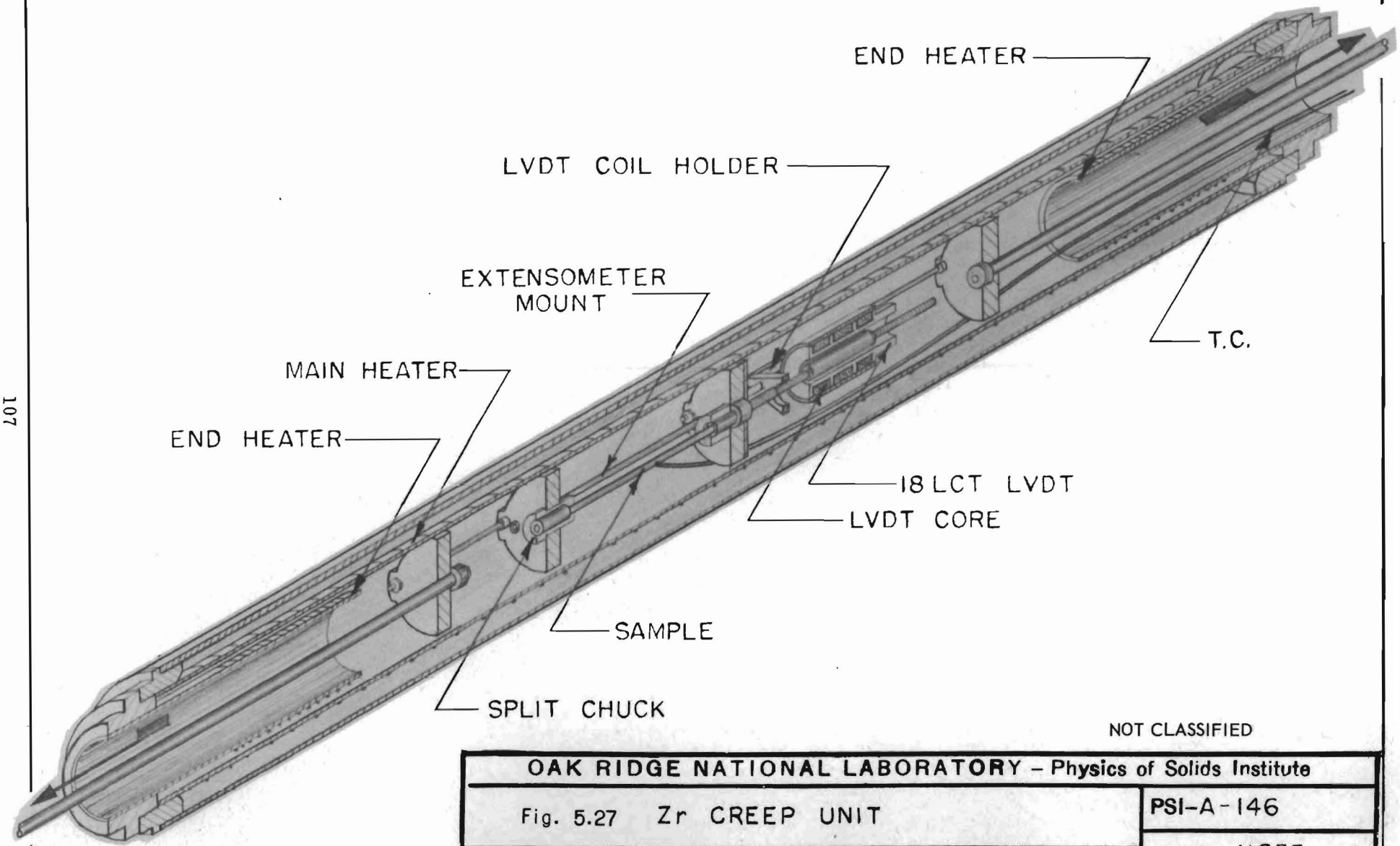

NOT CLASSIFIED

OAK RIDGE NATIONAL LABORATORY – Physics of Solids Institute				
Fig. 5.27 Zr CREEP UNIT				PSI-A-146
DRAWN BY: W.E.B	FOR: W.L. PRIMAK	DATE: 5/28/51	SCALE:	DWG.-11635

1. *Temperature control.* Although much better results had been achieved during short runs, it was not found possible to control the temperature at the surface of the specimen in the creep torpedo to better than ½°C over long periods of time. This is no better than could presumably be done with commercial control instruments. Occasional failures from various causes indicated the desirability of comparing the performance of a commercial controller on the torpedo.

2. *Samples.* One sample slipped in the steel chucks.[12] Since this was the only one that did, it is assumed that the sample was defective in some way and that the method used for preparing the ends of the specimen is in general satisfactory.

3. *Extensometer.* None of the LVDT units placed in the torpedoes read properly. Some difficulty was experienced at first with mounting them, and, after this was corrected, a number of electrical problems were also encountered. None of the LVDT units indicated the same motion in the torpedoes as they did outside. It is concluded that it is essential to calibrate an LVDT in place. It was originally hoped to read these instruments to 0.02 to 0.05 mil, but it now seems that 0.05 to 0.1 mil would be a fortunate achievement.

The circuit used for the extensometer is shown in Fig. 5.28. An electrical equivalent (neglecting some of the capacity) for one of the LVDT's is given in Fig. 5.29, and an approximate vector diagram is shown in Fig. 5.30. Placing the extensometer in a metal jacket (i.e., furnace) increases i_e, hence i_η, and therefore decreases i' and alters its phase. This decreases the sensitivity by decreasing E_1 and E_2 and also shifts the phase of E_1 and E_2. Thus, in general, the output $\mathcal{E}$ of two LVDT's not in the same environment will differ in phase by a value θ. When the core is moved, x_1 and x_2 are altered, causing the phase of $\mathcal{E}_1$ and $\mathcal{E}_2$ to alter. Since the extensometer and reference LVDT do not in general have the same sensitivity, θ will vary with core position. Varying the potentiometer contact will alter the phase, as can be seen from Fig. 5.30, but will in general also alter the amplitude.

If the potentiometer is not adjusted, the condition for a null, ϵ_0, is obtained by moving the reference core, changing $\mathcal{E}_r$ until the vacuum-tube

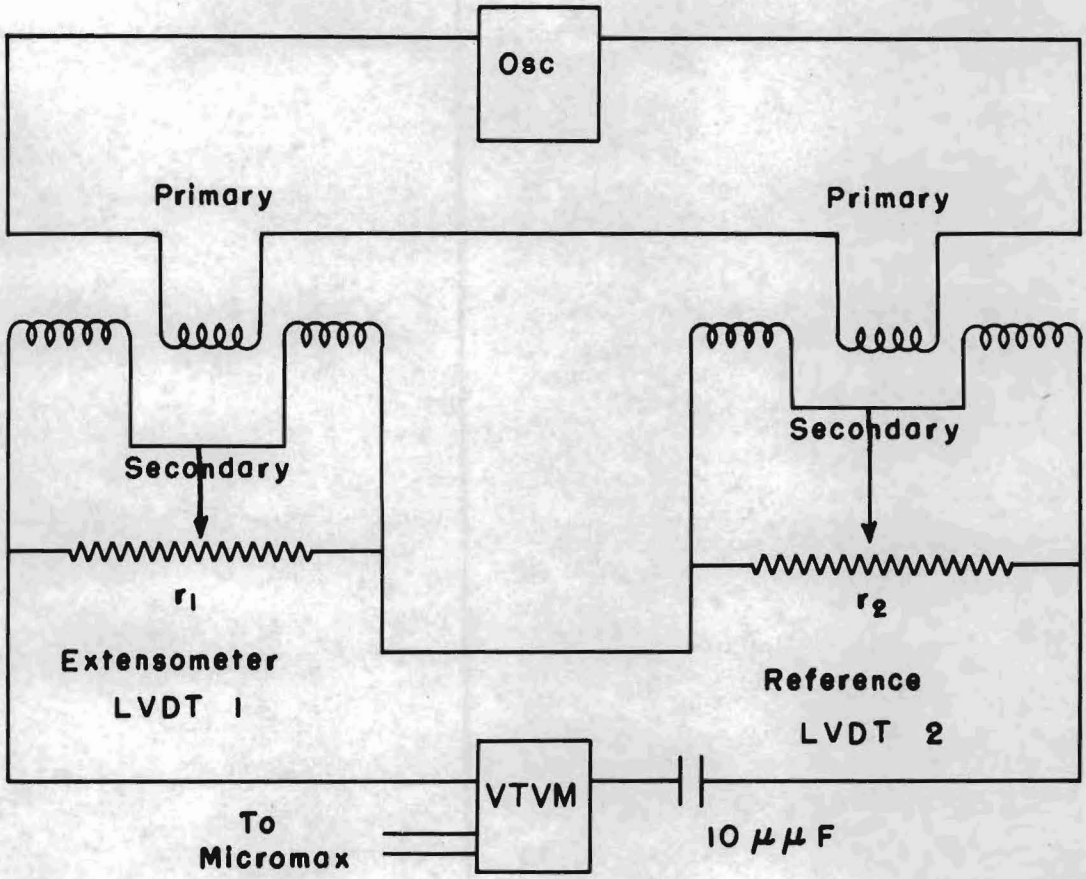

Fig. 5.28

CIRCUIT FOR LVDT.

Osc Hewlett-Packard Oscillator 100 A set at 3000 CPS.
VTVM Hewlett-Packard Vacuum tube voltmeter 400 C.
LVDT—1 Mounted in torpedo.
LVDT—2 Mounted on micrometer.
r_1, r_2 Phasing resistors.

DWG.-11668
PSI-A-152

NOT CLASSIFIED

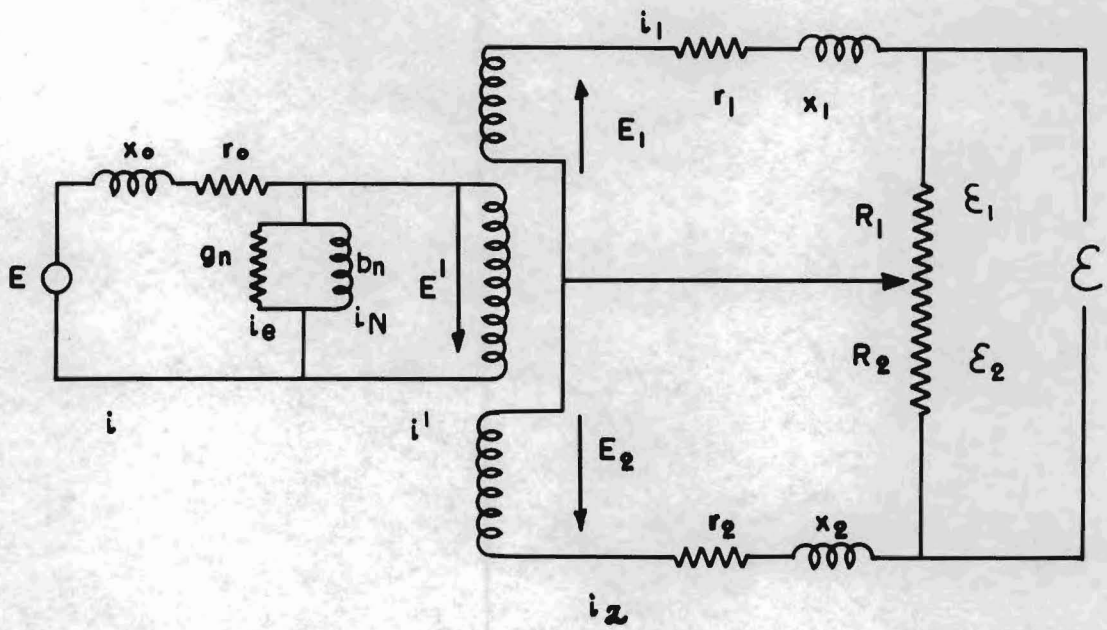

Fig. 5.29

ELECTRICAL EQUIVALENT OF AN LVDT.

$x_o\ r_o$, $x_1\ r_1$, $x_2\ r_2$	Leakage resistances & reactances.
g_n	Core losses
b_n	Susceptance
i_N	Magnetizing current
$i_\eta = i_e + i_N$	
E', i'	Voltage and current in equivalent ideal transformer primary.
i	Total current in primary.
$E, E_1, E_2, \mathcal{E}_1, \mathcal{E}_2, \mathcal{E}$	Voltages

DWG.-11667
PSI-A-151

NOT CLASSIFIED

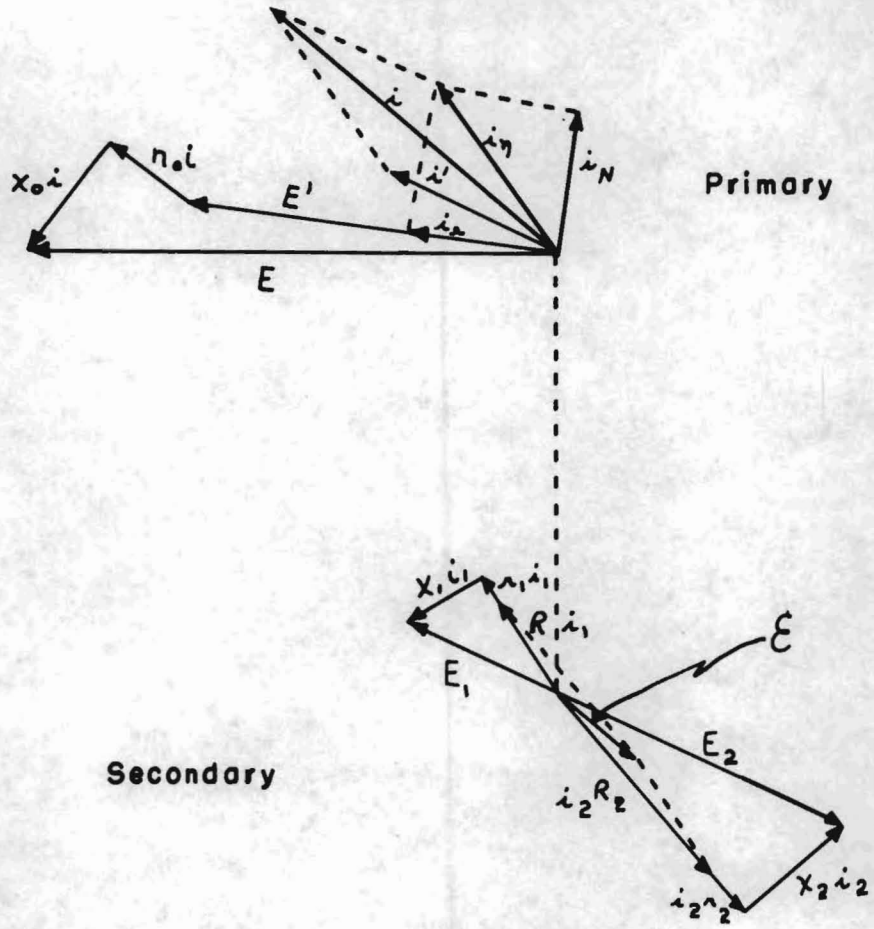

Fig. 5.30

VECTOR DIAGRAM OF TRANSFORMER
SHOWN IN Fig. 5.29

DWG.-11665
PSI-A-149
NOT CLASSIFIED

voltmeter reads a minimum. The extensometer output is $\mathcal{E}_e$ and the resultant $\mathcal{E}_r + \mathcal{E}_e = \epsilon$. Then obviously,

$$\epsilon = \sqrt{\mathcal{E}_e^2 - 2\mathcal{E}_r\mathcal{E}_e \cos\theta + \mathcal{E}_r^2}$$

which is a minimum at

$$\mathcal{E}_r = \mathcal{E}_e \cos\theta$$

as shown in Fig. 5.31. The reference core then moves by the fraction $\cos\theta$ of the relative sensitivities. ϵ_0 is obviously a minimum, i.e., equal to zero, when $\theta = 0$. The more complicated behavior obtained when the potentiometer is varied to make $\theta = 0$ has not yet been analyzed because the necessary electrical constants have not yet all been determined.

The record on the micromax is more complex. Here $\mathcal{E}_e$ is kept constant and $\mathcal{E}_r$ varies as the core of the extensometer moves. Since the range of the micromax is small, it can be assumed that θ has changed only by a small amount. Then the micromax record $\epsilon + \delta\epsilon$ is

$$\epsilon + \delta\epsilon = \sqrt{\mathcal{E}_r - 2\mathcal{E}_r\mathcal{E}_e \cos\theta - 2\mathcal{E}_r\,\delta\mathcal{E}_e + \mathcal{E}_e^2 + 2\mathcal{E}_e\,\delta\mathcal{E}_e + \delta\mathcal{E}_e^2}$$

which can be recognized as

$$\epsilon + \delta\epsilon = \sqrt{\epsilon^2 + (\delta\mathcal{E}_r)^2}$$

Here ϵ is ϵ_0 and $\mathcal{E}_r$ and $\mathcal{E}_e$ are the respective voltages at this point as shown in Fig. 5.32. In practice it is not possible to reduce ϵ to zero by adjusting the potentiometers since there are always harmonics and pickup in the circuit. Hence the record is always a rectangular hyperbola.

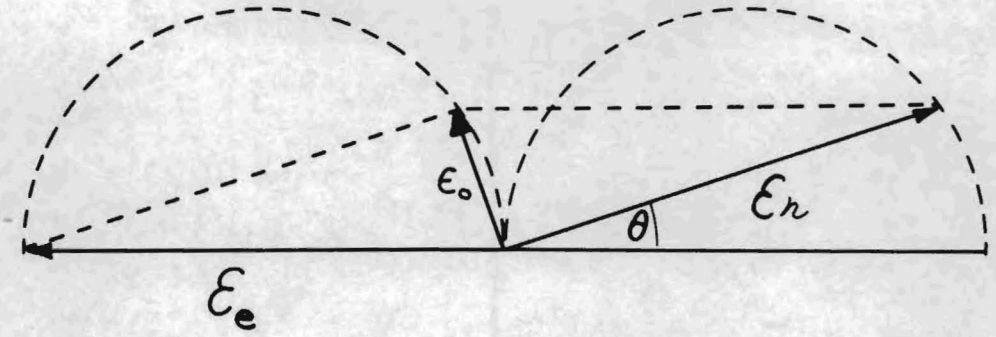

Fig. 5.31

VECTOR DIAGRAM FOR BALANCING EXTENSOMETER WITH REFERENCE LVDT.

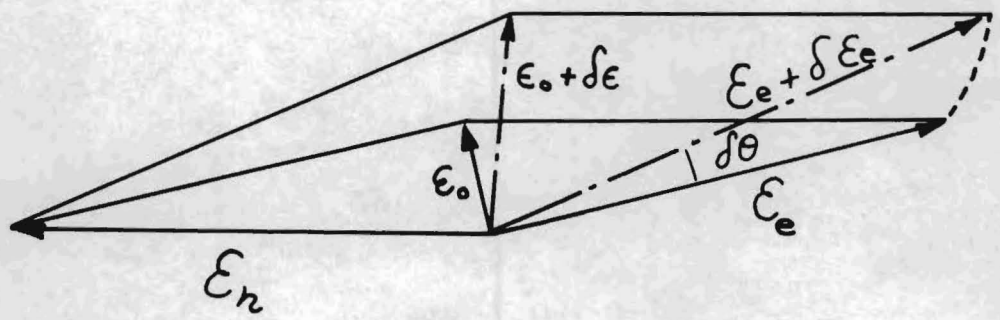

Fig. 5.32

VECTOR DIAGRAM SHOWING THE VOLTAGE RECORDED ON THE MICROMAX.

DWG.-11664
PSI-A-148
NOT CLASSIFIED

Results. A load of 175 to 190 lb at 265°C on a 3-in.-long specimen of extruded crystal bar swaged to 1/8 in. diameter and annealed at 750°C in vacuum* gave a satisfactory creep rate. After the initial set the estimated creep rate was about 6 mils/day. (The absolute value is uncertain because the behavior of the LVDT was not understood at the time. This estimate was made by correcting the reference LVDT readings by the inverse of the ratio of the reference LVDT total extension to the total extension found in the specimen on removal.) After about a week the creep rate decreased to about 0.004 mil/day. After 19 days the specimen had crept about 0.125 in. Increasing the specimen temperature 5°C produced no noticeable change in creep rate (less than 10%).

IRRADIATION OF GRAPHITE-CARBON RODS

R. H. Kernohan

Exploratory investigations on radiation damage to graphite-carbon bars manufactured by Battelle Memorial Institute were begun. Using some of the new remote-control apparatus recently developed for the hot cells, weight, dimensions, electrical resistivity, relative thermal conductivity, and modulus of elasticity were determined for 12 bars formed by six different fabrication techniques. These bars were then irradiated for two weeks in the fast-flux section of the X reactor. Measurements will be repeated after irradiation.

Battelle plans to make graphite-carbon bars containing enriched uranium in the form of UO_2 nodules of size varying from about 20 to 500 μ. These rods will be irradiated in the X reactor, and physical properties before and after irradiation will be compared. It is hoped that from these experiments some idea may be obtained of the optimum size of UO_2 nodule for minimum fission fragment damage to any material.

*We are indebted to S. H. Paine, Jr., Argonne National Laboratory, for the specimens.

6. LIQUID FUELS

RADIATION DAMAGE TO LIQUID FUELS

W. G. Keilholtz H. E. Robertson
J. G. Morgan C. C. Webster

Radiation damage to liquid fuels and their containers is to be studied in the X-10 reactor, the LITR, the Y-12 cyclotron, and the Berkeley 60-in. cyclotron.

Temperature and pressure measurements of liquid fuels under radiation conditions will be started in the X-10 reactor during June. The equipment is now undergoing a period of bench testing without radiation. The ORNL radiation-damage program is expected to become active in the LITR in the near future. The NAA group will undertake a program on fuel stability in July using the Berkeley 60-in. cyclotron.

Liquid fuels in inconel containers are being bombarded in the Y-12 cyclotron. A discussion of the detailed experiment is given under the heading "Y-12 Cyclotron Studies" in Sec. 2. It is anticipated that samples from cyclotron bombardments will be examined by standard metallographic and analytical procedures.

The Mass Spectrographic Group under Dr. C. R. Baldock at Y-12 is making some fundamental studies on the materials evolved from liquid fuels at high temperatures in an attempt to work out a sensitive method for detecting instability of the fuel under radiation.

Analytical methods for the examination of radiation damage and corrosion samples from the cyclotron are being developed by the Analytical Chemistry Division at X-10 and the Isotope Physics Spectrographic Group at Y-12. Analytical methods for hot samples from the X-10 reactor are being developed by the Analytical Chemistry Division at X-10.